UNIVERSITY OF GENOA

Department of Experimental Medicine

Section of General Pathology

PhD Course in Experimental Medicine

Curriculum of Molecular and Cellular Pathology of Aging-related Diseases

XXXIII CYCLE

"Heme oxygenase 1 in BRAF^{V600} melanoma: Evidence for a role in chemoresistance, immune-escape and angiogenesis"

Giulia Loi

Director: Professor Giambattista Bonanno

Tutor: Professor Mariapaola Nitti

Co-tutor: Professor Giovanni E. Mann

Academic year 2020/2021

ABSTRACT

Heme oxygenase 1 (HO-1) is widely recognized as a protective enzyme that counteracts cell damage through the antioxidant, antiapoptotic and anti-inflammatory activity of its metabolic products. By increasing cell resistance to stressors, HO-1 induction has been related with the gain of resistance and progression of different types of cancers and its involvement in favoring immune-escape and angiogenesis has been hypothesized. In this work, HO-1 expression in primary melanoma cells treated with the BRAF-mutated inhibitor Vemurafenib/PLX4032 has been investigated as a factor limiting cell death and recognition by Natural killer cells, that are the first line of defence of natural immune system against melanoma growth and spreading. The initial part of the work was carried out in collaboration with Professor Pietra's research group at the Clinical Immunology Laboratory, Ospedale Policlinico San Martino in Genoa. Different cell lines, isolated in house from melanoma patients, were exposed to 1–10μM PLX4032. In three cell lines (MeOV-1, MeTA and MeMI), PLX4032 reduced melanoma cell viability up to 45%, while HO-1 expression was upregulated. HO-1 silencing/inhibition further significantly reduced melanoma cells viability following PLX4032 treatment. Furthermore, in PLX4032-treated melanoma cells, the expression of B7H6 and ULBP3, ligands of NKp30 and NKG2D activating receptors on NK cells, was downregulated and completely restored by HO-1 silencing/inhibition. This is the first report implicating HO-1 in limiting PLX4032 efficacy and melanoma recognition by NK cells, and these data contributed to a paper published in The International Journal of Cancer at the beginning of 2020.

Further, the molecular mechanisms underlying HO-1 induction in melanoma cells exposed to PLX4032 have been studied. After treatment with 10μM PLX4032, MeOV-1 cells showed an early activation of the redox sensitive transcription factor Nrf2, and a long-lasting HO-1 induction. Notably, the upregulation of HO-1 was Nrf2-dependent, as it was prevented by Nrf2 silencing. Moreover, among the Nrf2-dependent genes, only HO-1 was induced in MeOV-1 exposed to PLX4032 since, under the same experimental conditions, other Nrf2-dependent genes such as GCLM, GCLC and NQO1 were not modulated. Moreover, a stable downregulation of Bach1, a negative regulator of HO-1 induction, was found. The present findings have identified a molecular mechanism, involving stable downregulation of Bach1 and early activation of Nrf2 that drives the induction of HO-1 in response to PLX4032 treatment.

In an ERASMUS Plus collaboration with Professor Giovanni Mann at King's College London, UK, the effects of changes in the ambient oxygen levels on MeOV-1 cell responses to PLX4032 and HO-1 induction were investigated. PLX4032-treated MeOV-1 cells adapted long-term (5 days) to either 5kPa (physiological normoxia) and 1kPa (hypoxia) O_2 showed pERK levels, cell

viability, HO-1, Bach1 and Nrf2-dependent gene expression similar to cells cultured under standard conditions (18kPa O_2). Moreover, HIF-1α expression was induced by cell adaption to 1kPa O_2 but, interestingly, protein levels were already high in untreated cells cultured under 18kPa or 5kPa O_2 due to the constitutive activation of pERK pathway. Furthermore, in MeOV-1 cells adapted to 18kPa and 5kPa O_2, HIF-1α expression was almost completely abolished after 10μM PLX4032 treatment, while HIF-1α protein expression was only partially decreased in 1kPa O_2-adapted MeOV-1 cells. Thus, no substantial differences in MeOV-1 cell response to PLX4032 were observed under altered O_2 levels in cell culture, resulting most likely from the high basal expression of HIF-1α in this cell line.

In order to evaluate the role of HO-1 in favouring melanoma angiogenesis, endothelial tube formation was examined in cultured bovine and human endothelial cells. Under standard culture conditions (18kPa O_2), conditioned media (CM) derived from PLX4032-treated MeOV-1 cells increased the formation of tubes in bovine aortic endothelial cells (BAEC) seeded on Matrigel, while CM derived from HO-1 silenced MeOV-1 cells treated with PLX4032 significantly prevented tube formation. To verify the proangiogenic ability of CM derived from cells adapted to normoxia (5kPa O_2) or hypoxia (1kPa O_2), and the role played by HO-1 downregulation, additional experiments were conducted with human cerebral microvascular cells (hCMEC/D3) and human endothelial cells from vein (HECV) adapted to 5kPa O_2. These endothelial cells were adapted at 5kPa O_2, seeded on Matrigel with CM derived from PLX4032-treated MeOV-1 adapted to 5kPa and 1kPa O_2. Some samples were co-treated with HO-1 inhibitor SnMP-IX.

Unfortunately, due to the COVID-19 pandemic, these experiments have been performed only few times in the London laboratories, and thus only preliminary results are included in the thesis. HO-1 inhibition in MeOV-1 cells adapted at 5kPa and 1kPa O_2 completely prevented the ability to form tubes. In these experimental conditions, no significant modulation of VEGF-A expression was observed suggesting that HO-1 dependent proangiogenic effects may not be related to the modulation of VEGF-A.

In conclusion, the present results highlight the specific involvement of HO-1 in limiting the efficacy of Vemurafenib/PLX4032 on melanomas carrying on $BRAF^{V600}$ mutation, by the combined modulation of Nrf2 and Bach1, and in favouring immune-escape by the downregulation of NK cell ligands B7H6 and ULBP3. Indeed, not only HO-1 silencing but also the use of HO-1 enzymatic inhibitor, already in clinical use, has been shown to increase PLX4032 efficacy and to improve NK recognition and killing. Furthermore, preliminary data highlight that HO-1 silencing/inhibition decreased the angiogenic potential of MeOV-1 cells in a VEGF-independent manner, even though the molecular mechanisms have yet to be investigated. Further

studies of heme oxygenase 1, Nrf2 and Bach1 are warranted to confirm their potential as target co-treatment with Vemurafenib for the treatment of BRAF mutated melanoma.

ACKNOWLEDGEMENTS

I would like deeply to thank my tutor, Professor Mariapaola Nitti, for her invaluable supervision, support and tutelage during the course of my PhD degree.
She continuously provided encouragement and was always willing, patient and enthusiastic to assist me in any way she could throughout the PhD project.
I would also thank Doctor AnnaLisa Furfaro for her treasured teachings and support which were really influential in shaping my experiment methods and that were fundamental during my experience abroad.
Their guide, started from my bachelor's degree until this PhD project,
made me the better person who I am now.
Also, I thank Caterina Ivaldo, with whom I had the pleasure of starting the PhD study,
for her support and friendship.
I would like to express my thanks to Professor Giambattista Bonanno, Professor Ernesto Fedele and Professor Cinzia Domenicotti who give me the opportunity to work on this project
in the laboratory at the Experimental Medicine Department in Genoa and,
by the Erasmus Plus program, at the King's College of London.
My deep gratitude extends to Professor Giovanni E. Mann, from the King's College of London, for his invaluable advice, continuous support, enthusiasm and patience towards me.
Under his supervision, I had the opportunity to grow and to improve myself in an international dynamic environment.
Far from home, he and his collaborators and students make me feel accepted and encouraged me for all the time that I spent in London.
Finally, I would like to thank all the members of the Vascular Biology, in particular Doctor Sarah Chapple, Doctor Gabriela Warpsinski, Doctor Matthew Smith, Doctor Maria Paraskevi Psefteli, Miss Emily Boorman and Miss Fan Yang.
Their kind help and support have made my study and life in the UK a wonderful time,
that I will never forget.

LIST OF PUBLICATIONS AND MEETINGS

Articles

Anna L. Furfaro, Selene Ottonello, Giulia Loi, Irene Cossu, Sabrina Piras, Francesco Spagnolo, Paola Queirolo, Umberto M. Marinari, Lorenzo Moretta, Maria A. Pronzato, Maria C. Mingari, Gabriella Pietra and Mariapaola Nitti. "**HO-1 downregulation favors BRAFV600 melanoma cell death induced by Vemurafenib/PLX4032 and increases NK recognition**". *International Journal of Cancer*, 2020. DOI: 10.1002/ijc.32611

Abstracts

Giulia Loi, AnnaLisa Furfaro, Maria Adelaide Pronzato, Gabriella Pietra, Giovanni E. Mann, Mariapaola Nitti. "**HO-1 induction limits the efficacy of Vemurafenib in human melanoma cells cultured in physiological normoxia and hypoxia favoring angiogenesis**". *Free Radical Biology and Medicine*, 2019. DOI: 10.1016/j.freeradbiomed.2019.05.021

G. Loi, A. Furfaro, G. Pietra, G.E. Mann and M. Nitti. "**Role of HO-1 in melanoma resistance to BRAF inhibitor vemurafenib in MeOV-1 cells cultured under hyperoxia, physiological normoxia and hypoxia**". *The Physiological Society: Future Physiology 2019 – Liverpool*.

Anna Lisa Furfaro, Irene Cossu, Giulia Loi, Sabrina Piras, Selene Ottonello, Umberto Maria Marinari, Lorenzo Moretta 4, Maria Adelaide Pronzato, Maria Cristina Mingari, Gabriella Pietra, Mariapaola Nitti. "**Natural killer recognition of primary melanoma cells treated with BRAFV600E inhibitor is favored by heme oxygenase 1 down-regulation**". *Free Radical Biology and Medicine*, 2018. DOI: 10.1016/j.freeradbiomed.2018.04.343.

Meetings, Congress and Courses

Ferrara, 19-21 Giu 2019 International Society for Free Radical Reserch - Europe Congress
Liverpool, 17-18 Dic 2019 Meeting of The Physiological Society
Londra, 9 Ott 2019 64th London Vascular Biology Forum Christmas Poster Meeting
Londra, 9 Ott 2019 63th London Vascular Biology Forum Meeting
Londra, 17 Lug 2019 62th London Vascular Biology Forum Meeting
Londra, 1 Mag 2019 61th London Vascular Biology Forum Meeting
Londra, 7 Dic 2018 Fellowship of Postgraduate Medicine - Centenary Conference
Londra, 5 Dic 2018 60th London Vascular Biology Forum Meeting
Genova, 19-20 Set 2018 Animal Models for perinatal stress and metabolism
Lisbona, 4-7 Giu 2018 International Society for Free Radical Reserch - International Biennal Meeting
Novara, 17-18 Nov 2017 Scientific meeting "Scuola Dianzani"
Genova, 18-20 Apr 2016 Alternative predictive models in Toxicology Course

LIST OF ABBREVIATIONS

ABCB6	ATP-binding cassette B6
AKT	Serine/threonine-specific protein kinase
ALL	Acute lymphoblastic leukemia
APS	Ammonium pyrosulphate
ATP	Adenosine triphosphate
BAEC	Bovine aortic endothelial cells
BCC	Basal cell carcinoma
BRAF	V-Raf murine sarcoma viral oncogene homolog B1
BSA	Bovine serum albumin
BVR	Biliverdin reductase
CM	Conditioned medium
CO	Carbon monoxide
CO_2	Carbon dioxide
dd H_2O	double distilled water
DEPC H_2O	Diethyl pyrocarbonate water
DMSO	Dimethyl sulfoxide
ERK	Extracellular signal–regulated kinases
GCLC	Glutamate-Cysteine Ligase Catalytic Subunit
GCLM	Glutamate-Cysteine Ligase Modifier Subunit
Glut-1	Glucose transporter 1
GSH	Glutathione
GSK-3beta	Glycogen synthase kinase 3 beta
hCMEC/D3	human cerebral microvascular endothelial cell line
HIF-1α	Hypoxia inducible factor 1α
HO-1	Heme oxygenase-1
HO-2	Heme oxygenase-2
HECV	Human endothelial cells from vein
MAPK	Mitogen-activated protein kinase
MW	Molecular Weight
NAD(P)H	Nicotinamide adenine dinucleotide phosphate
NMSC	Non-melanoma skin cancer
NQO1	NAD(P)H quinone dehydrogenase 1
Nrf2	Nuclear factor (erythroid-derived 2)-like 2

p-AKT	Phospho-AKT
PBS	Phosphatase Buffered Saline
PCR	Polymerase chain reaction
p-ERK 1/2	Phospho extracellular signal regulated kinase
p-FAK	Phospho-Focal adhesion kinase
PKAα	Protein kinase A
PLX	Vemurafenib / PLX4032
p-STAT	Phospho-Signal Transducer and Activator of Transcription
RT	Reverse transcriptase
SCC	Squamous cell carcinoma
SCF	Skp, Cullin, F-box containing complex
SDS-PAGE	Sodium dodecyl sulphate – polyacrylamide gel electrophoresis
SnMP-IX	Tin Mesoporphyrin IX
STR	Short tandem repeat
TEMED	Tetramethylethylenediamine
UM	Uveal Melanoma
β-ME	β-mercaptoethanol
β-TrCP	β-transduction repeat-containing protein

INDEX

Abstract.....

Acknowledgements.....

List of Publications and meetings.....

List of Abbreviations.....

1 Introduction.....1

1.1 Nrf2.....1

1.1.1 Structure of Nrf2.....3

1.1.2 Keap1-dependent Nrf2 regulation.....4

1.1.3 Keap1-independent Nrf2 regulation.....6

1.1.4 Nrf2 and tumors.....6

1.2 Heme Oxygenase -1.....8

1.2.1 Discovery of heme oxygenase.....8

1.2.2 Heme Oxygenase 1 and its physiological role in cells.....8

1.2.3 Heme oxygenase 1 and its pathological role in tumors.....10

1.3 Melanoma.....12

1.3.1 Melanocytes.....12

1.3.2 Epidemiology and frequently of melanoma in the word.....12

1.3.3 Genetic Classification of Cutaneous Melanoma.....13

1.3.4 Therapeutic approaches.....15

1.3.5 Vemurafenib/PLX4032.....16

1.3.6 Resistance to the PLX4032 treatment.....17

1.3.7 Tumor microenvironment.....17

1.3.8 Tumor Angiogenesis.....19

1.4 Relevance of physiological oxygen levels.....22

2 Aims.....25

3 Materials and Methods.....26

3.1 Cell culture and treatments 26
3.1.1 Melanoma cell lines and treatments 26
3.1.2 Endothelial cell lines 26
3.1.3 Culturing cells under physiologic and hypoxic environments: The Sci-tive® in vitro workstation 27
3.2 siRNA for Nrf2 and HO-1 28
3.3 Viability Assay 29
3.4 Proliferation assay 30
3.5 RT-PCR 31
3.5.1 RNA extraction 31
3.5.2 Quantification of the extracted RNA 32
3.5.3 Reverse transcriptase reaction (RT) 32
3.5.4 PCR 32
3.6 Immunoblotting 34
3.6.1 Protein extraction and quantification 34
3.6.2 Samples preparation 34
3.6.3 Gel preparation and SDS-PAGE electrophoresis 34
3.6.4 Blotting 35
3.7 Immunofluorescence 36
3.8 Tube formation assay 37
3.9 Statistical analysis 39
4 Results 40
4.1 HO-1 upregulation reduces PLX4032 efficacy and NK recognition 40
4.1.1 PLX4032 abolishes ERK phosphorylation and decreases viability of melanoma cells bearing $BRAF^{V600}$ mutation 41
4.1.2 HO-1 protein levels in melanoma cell lines increases after PLX4032 treatment 42
4.1.3 HO-1 silencing enhances the efficacy of PLX4032 and further reduces cell viability 43
4.1.4 Melanoma viability is further reduced by co-treating cells with HO-1 inhibitor and PLX4032 45

4.1.5 PLX4032 treatment of MeOV-1 reduces the expression of B7H6 and ULBP3, ligands for NK cells; their expression were restored by HO-1 silencing 46

4.1.6 PLX4032/SnMP-IX co-treatment restores the expression of B7H6 and ULBP3 48

4.2 HO-1 induction in PLX4032-treated cells is dependent on Nrf2 activation and Bach1 downregulation. 49

4.2.1 24h PLX4032 treatment does not modulate other Nrf2-dependent genes 49

4.2.2 Short time PLX4032 treatments highlight a Nrf2 translocation into the nucleus 51

4.2.3 HO-1 is up-regulated after 3 and 6 hours of PLX4032 treatment 53

4.2.4 Bach1 expression is downregulated after PLX4032 treatment 55

4.2.5 Nrf2 silencing decreases HO-1 expression in MeOV-1 treated with PLX4032 . 56

4.3 Lowering oxygen tension does not modify MeOV-1 cell response to PLX4032 57

4.3.1 MeOV-1 cells adapted to 1kPa O_2 appear more elongated in comparison to MeOV-1 cells cultured under 18kPa O_2 and 5kPa O_2 58

4.3.2 MeOV-1 growth rate under physiological normoxia and hypoxia is lower than under standard hyperoxic culture conditions 59

4.3.3 Different oxygen tensions do not affects the ability of PLX4032 treatment to inhibit ERK phosphorylation 60

4.3.4 HO-1 is upregulated by PLX4032 in cells cultured in all oxygen tensions 61

4.3.5 GCLC, GCLM and NQO1 genes are not affected by PLX4032 treatment in MeOV-1 cells regardless different oxygen tensions 62

4.3.6 Bach1 expression is downregulated after 24h PLX4032 treatment regardless of oxygen tension 63

4.3.7 Different oxygen tensions do not affect the efficacy of PLX4032 treatment and HO-1 inhibition further improves it 64

4.3.8 HIF-1α levels are abolished after PLX4032 treatment in MeOV-1 cells adapted to 18kPa and 5kPa O_2 but still present in cells adapted at 1kPa O_2 65

4.3.9 Conditioned medium from MeOV-1 cells treated with PLX4032 increases endothelial tube formation 66

4.3.10 CM from MeOV-1 treated with HO-1 inhibitor and exposed to PLX4032 reveals a decreased ability to form endothelial tubes 67

4.3.11 CM from MeOV-1 adapted to 5kPa and 1kPa O_2 and co-treated with PLX4032/SnMP-IX reduces tube formation in HECV and hCMEC/D3 adapted to 5kPa O_2 68

4.3.12 VEGF mRNA expression is not modified by PLX4032 treatment in MeOV-1 cells cultured under different oxygen tensions 70

5 Discussion 71

6 Conclusions and future research perspectives 78

7 References 80

8 Appendixes 104

1 INTRODUCTION

1.1 Nrf2

The redox sensitive transcription factor Nrf2 (Nuclear factor (erythroid-derived 2)-like 2) plays a key role in controlling cell response to stressors. By interacting with the specific Antioxidant Response Element (ARE) target sequences in the promoter regions of target genes, Nrf2 is involved in the regulation of antioxidant, detoxifying and anti-inflammatory proteins. Indeed, with a core of 5'-RTGACNNNGC-3', ARE sequence is a cis-acting DNA regulatory element that mediates the transcriptional activation of several genes encoding protection against electrophiles and reactive oxygen species (ROS) and enzymes involved in phase II metabolism (Motohashi et al., 2004; Rushmore et al., 1991; Yamamoto et al., 2018) Thus, Nrf2 activates a wide range of genes with antioxidant and detoxifying activity (Zgheib et al., 2018).

Moreover, several anti-inflammatory molecules and enzymes involved in the metabolism are regulated by Nrf2. Based in their functions, in Table 1-1 Nrf2 target genes are divided into five groups.

Table 1.1: Example of gene products regulated by Nrf2 and their biological function.

	Function	Gene Products	Refs
Group 1	Enzymes involved in synthesis and regeneration of glutathione	GCLM, GCLC, γ-glutamylcysteine (GLG), peroxiredoxin (Prx), enzymes that produce NADPH, Glucose-6-phosphate dehydrogenase (G6PD)	(Agyeman et al., 2012; Chorley et al., 2012; Macleod et al., 2009; Malhotra et al., 2010; McBean et al., 2015)
Group 2	Enzymes characterized by detoxifying activity towards drugs, xenobiotic substances and aldehydes	NAD(P)H quinone oxidoreductase (NQO1), glutathione S-transferase (GST), Cystine/Glutamate Antiporter system (xCT)	(Agyeman et al., 2012; Higgins et al., 2011; Macleod et al., 2009)
Group 3	Enzymes involved in heme group metabolism and free iron chelation	HO-1, Ferrochelatase (FECH), ATP-binding cassette B6 (ABCB6)	(Chorley et al., 2012; Menegon et al., 2016)
Group 4	Enzymes involved in protein degradation	Sequestrosome 1 (SQSTM1)	(Chorley et al., 2012)
Group 5	Enzymes involved in lipid metabolism and glycogen homeostasis	Glycogen branching enzyme (GBE), Lipase H (LIPH)	(Paek et al., 2012; Paladino et al., 2018)

1.1.1 *Structure of Nrf2*

Human Nrf2 consists of 605 amino acids and is divided into seven distinct regions called Nrf2-ECH homology (Neh) domains with different functions (Canning et al., 2015; Itoh et al., 1995) (see Fig. 1-1).

- **Neh1** domain presents a Cap'n'Collar sequence (CNC) of 43 amino acids. The CNC sequence contains the basic leucine zip (bZIP) domain (Moi et al., 1994). This region is essential for Nrf2 activity and heterodimerization with other bZIP proteins, for example with nuclear protein small Maf (sMaf) (Hirotsu et al., 2012);
- **Neh2** domain is the main region for the negative control of Nrf2 operated by Kelch-like ECH-associated protein 1 (Keap1) as detailed later. In this region there are two highly conserved sequences needed for the binding to Keap1 : the first is the high-affinity ETGE motif and the second is the lower-affinity DLG motif (Kobayashi et al., 2002; McMahon et al., 2003; McMahon et al., 2006; Tong et al., 2006);
- **Neh3** domain is involved in the transcriptional activation of Nrf2 by the interaction with the chromodomain helicase DNA-binding protein 6 (CHD6) (Hayes et al., 2009);
- **Neh4** and **Neh5** are the transactivation domains for increasing the rate of gene transcription (Katoh et al., 2001); they bind to the coactivators cAMP Response Element Binding Protein (CREB-protein and/or the receptor-associated coactivator-RAC) (Kim et al., 2013);
- **Neh6** domain regulates the degradation of Nrf2 in a Keap1-independent manner. This domain contains two conserved motifs, DSGIS and DSAPGS recognized by β-transducin repeat-containing protein (β-TrCP). The DSGIS motif contains the glycogen synthase kinase-3 (GSK-3) phosphorylation site that enhances the ability of beta-TrCP to repress Nrf2 (Rada et al., 2011);
- **Neh7** domain can engage in a direct protein-protein interaction between and Nrf2 and the DNA-binding domain of retinoid X receptor alpha (RXRα): this interaction causes the suppression of Nrf2 activity by preventing the recruitment of the coactivator to Neh4 and Neh5 domains (Wang et al., 2013).

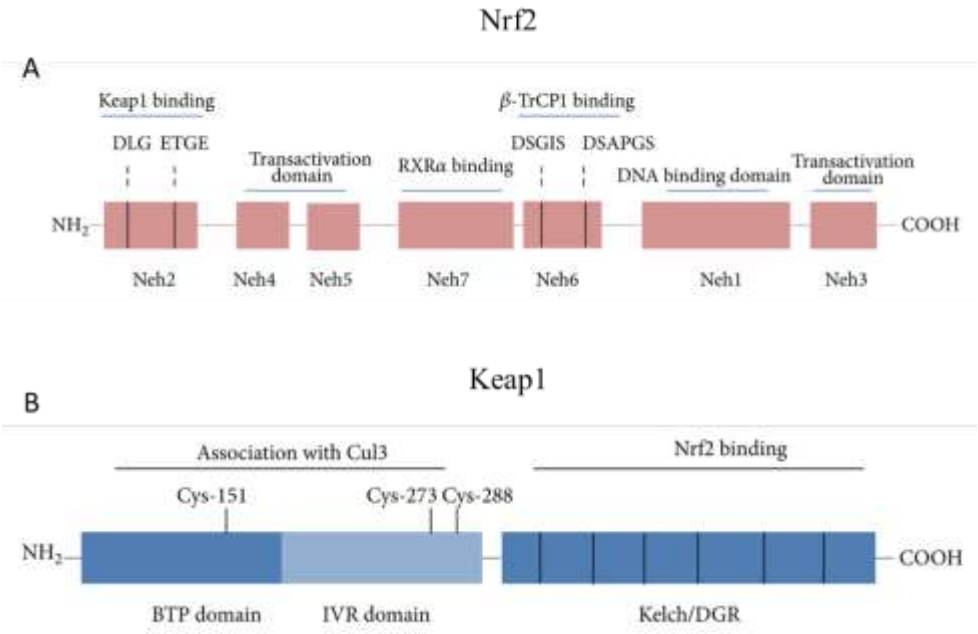

Figure 1-1: Schematic representation of Nrf2 and Keap1 protein domains. (**A**) Nrf2 has seven different domains, Neh1-Neh7. Neh1 contains the basic region leucine zipper motif, important for DNA stability and binding and for the heterodimerization with Mafs proteins. In the Neh2 domain there are two binding regions, DLG and ETGE, responsible for the interaction with Keap1. Neh3, Neh4 and Neh5 motifs are involved in the transactivation activity of Nrf2. Neh6 is a serine-rich region that regulates the stability of Nrf2. Neh7 is the region for binding RXRα. (**B**) In Keap1 structure are present three major domains. The BTB domain mediates Keap1 homodimerisation; the IVR domain contains critical cysteine residues and together they associate with Cul3. The Kelch/DGR domain mediates the binding with the Neh2 domain of Nrf2 (Furfaro et al., 2016).

1.1.2 *Keap1-dependent Nrf2 regulation*

Under basal conditions, Nrf2 is localized in the cytosol and binds to its negative regulator Keap1 via the Cullin 3-based ubiquitin E3 ligase complex (Cul3). Keap1 promotes the continuous ubiquitination and subsequent degradation of Nrf2 via the 26S proteasome, thereby maintaining low basal cytosolic levels (Kobayashi et al., 2006); the turnover of Nrf2 is less than 20 min under basal condition (McMahon et al., 2004)

When cells are exposed to oxidative or electrophilic stimuli, cysteine residues in Keap1 are modified and the enzymatic activity of E3 ubiquitin ligase is inhibited. Subsequently, Nrf2 accumulation in the nucleus (Taguchi et al., 2011) enables the binding with Mafs proteins to create an heterodimer, which in turn binds to the ARE-sequences and promotes transcription of target genes (Kobayashi et al., 2006; Osburn et al., 2008).

Keap1 acts as an oxidative stress sensor through the modification of some cysteine residues (Holland et al., 2010). In the structure of Keap1, showed in Fig. 1-1, three main residues have been identified as crucial regulator of Nrf2 activity:

- Cys151 in BTB domain
- Cys273 and Cys288 in IVR domain

Indeed, it has been shown that a mutation in these three cysteine residues can significantly modify the antioxidant responses mediated by Nrf2 (Kobayashi et al., 2009; McMahon et al., 2010; Takaya et al., 2012; Bryan et al., 2013).
The schematic interaction between Nrf2 and Keap1 is depicted in Fig. 1-2.

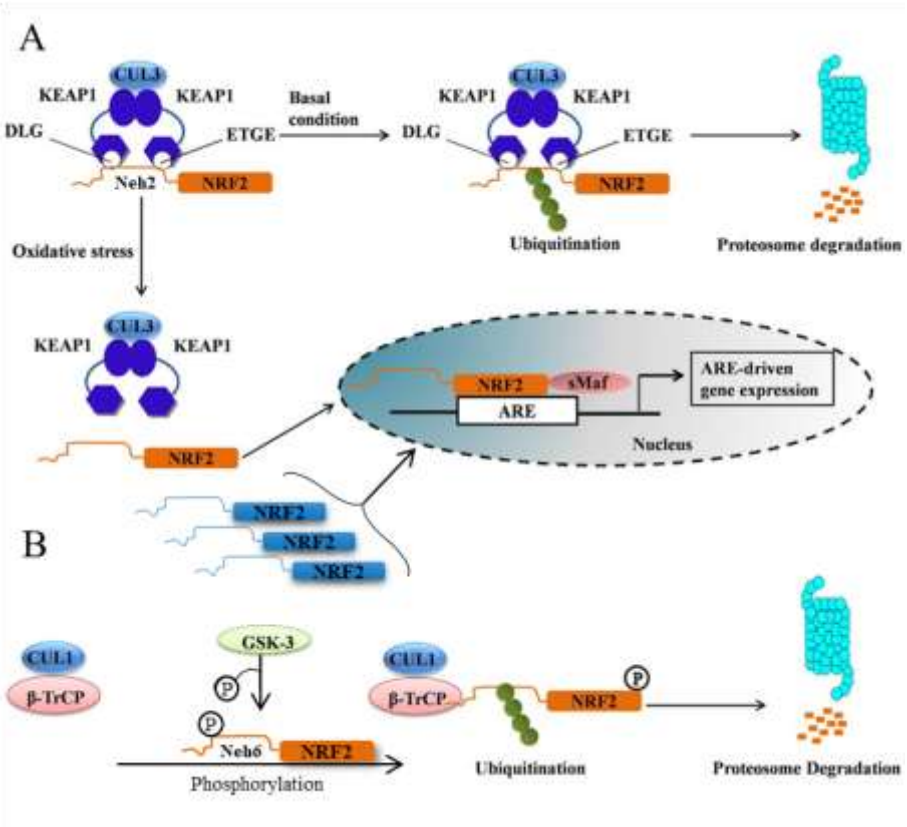

Figure 1-2: Regulation of redox signalling by the Keap1/Nrf2 pathway. **(A)** Under basal conditions, interaction of Nrf2 with its cytosolic binding protein Keap1 leads to ubiquitination of the transcription factor and degradation via the 26S proteasome. Following oxidation of cysteine residues performed by electrophilic or other stress agents, Keap-1 dissociates from Nrf2 (orange) that can translocate into the nucleus together with newly synthesized Nrf2 (blue). **(B)** GSK-3 phosphorylates the Ser residues presents in Neh6 domain and this leads Nrf2 to the proteasome degradation (Adapted from Ahmed et al. 2017).

Nrf2 can be also regulated via autophagic degradation of Keap1. The autophagic scaffold protein p62/SQSTM1 (sequestrome-1 protein) can compete with Nrf2 for binding to Keap1. Indeed, p62/SQSTM1 contains a conserved Keap1-interacting region with a STGE binding motif very similar to ETGE motif. This structure enables competitive binding to the DGR domain of Keap1 (Ichimura et al., 2013; Jain et al., 2010; Komatsu et al., 2010; Lau et al., 2010; Taguchi et al., 2012; Tebay et al., 2016) and the formation of a p62/SQSTM1-Keap1 complex that promotes the autophagic degradation of Keap1, activating Nrf2.

1.1.3 *Keap1-independent Nrf2 regulation*

Many studies have suggested that Nrf2 can be also regulated by protein phosphorylation of glycogen synthase kinase 3 (GSK-3) (Cullinan et al., 2003), which is directly involved in the ubiquitination and proteasomal degradation of other proteins like Snail (Zhang et al., 2004; Zhou et al., 2004), prolactin receptor (Taguchi et al., 2011) and β-catenin (Rada et al., 2011).
GSK-3 works by phosphorylating a cluster of Ser/Thr residues presents in the sequences DSGIS and DSAPGS in the Neh6 domain of Nrf2, generating a phosphorylated destruction motif, named phosphodegron (Ahmed et al., 2017; Chowdhry et al., 2013; Rada et al., 2011). This phosphorylated motif is recognized by the SCF/ β-TrCP complex, a multi-protein E3 ubiquitin ligase complex, that catalyses Nrf2 ubiquitination and proteasomal degradation.

1.1.4 *Nrf2 and tumors*

In a healthy cell, the activity of Nrf2 favors cell survival by affording protection from oxidative stress induced damage. However, the upregulation of Nrf2 in tumor cells can favor cell growth as well, by protecting cancer cells against chemotherapeutic agents (Rojo de la Vega et al., 2018; Wang et al., 2008). It has been shown that a high and prolonged activation of Nrf2 is associated with progression, angiogenesis, metastatic invasion, chemoresistance and radioresistance, and thus considered as a poor prognostic factor (Furfaro et al., 2016; Moon et al., 2015; Na et al, 2014)
There are two main mutations involved the constitutive activation of Nrf2 in tumor cells, gain-of-function mutations of Nrf2 or loss-of-function mutations of Keap1. Nrf2 gain-of-function mutations determine stabilization of Nrf2 and result in a continuous activation of its target genes. A stable Nrf2 overexpression is founded in different types of tumors such as lung (Shibata et al., 2008), breast (Nioi et al., 2007), neck (Stacy et al., 2006) and ovarian cancers (van der Wijst et al., 2014). Loss-of-function mutations of Keap1, mainly located in the Kelch/DRG domain, do not enable the binding to Nrf2 and its subsequent proteasomal degradation (Jaramillo et al., 2013;

Mitsuishi et al., 2012; Shibata et al., 2010). The alteration of Keap1 is founded in malignant glioma (Muscarella et al., 2011) and colorectal cancers (Hanada et al., 2012).

Non-genomic alterations can also lead to an increase in the activity of Nrf2. For example, p21 acting as positive regulator of Nrf2, interferes with Keap1-dependent ubiquitination leading to Nrf2 stabilization and overexpression (Chen et al., 2009). DJ-1 is another protein able to reduce the association of Nrf2 with Keap1 leading to its stabilization (Gan et al., 2010). Indeed, it has been shown in human neuroblastoma SH-SY5Y that DJ-1 expression is enhanced and favored the expression of detoxification enzymes such as NQO1 (Taira et al., 2004). In general, all the proteins that contain an ETGE motif could interfere with the binding between Keap1 and Nrf2 and thereby lead to a decrease proteasomal degradation of Nrf2.

A large body of literature confirms that tumor cells have high levels of Nrf2, which renders them less sensitive to different chemotherapy and radiotherapy agents (Furfaro et al., 2016; Jeong et al., 2018; Li et al., 2017). Human ovarian cell lines SKOV3, OV90 and MCF-7/DOX, resistant to the chemotherapeutic agent doxorubicin, have a high activity of Nrf2 in comparison to the chemosensitive cell lines A2780 and MCF-7 (Zhong et al., 2013). Our own studies demonstrate that Nrf2 activation plays a key role in the resistance of neuroblastoma cells to GSH depletion or to proteasome inhibition induced by therapeutic agent Bortezomib (Furfaro et al., 2012, 2014).

It has also been shown that in the prostate tumor cell line DU145, the transcription factor Nrf2 and its target genes play a key role in radioresistance (Jayakumar et al., 2014). Indeed, these cells exhibit a higher GSH/GSSG ratio in comparison to radiosensitive cell lines. Furthermore, cell treatment with all-trans retinoic acid, that inhibits Nrf2 activity, increases the efficacy of radiotherapy (Lee et al., 2012).

Thus, Nrf2, in different types of cancers, is recognized as a potent target to improve tumor therapies reducing cancer progression.

1.2 Heme Oxygenase -1

1.2.1 *Discovery of heme oxygenase*

The first researcher who isolated and identified the enzyme that catabolizes hemoglobin was Raimo Tenhunen who, in 1968 named the enzyme as "heme oxygenase" (HO) (Tenhunen et al., 1968). He showed that HO activity was mainly localized in the microsomal fraction of liver cells and demonstrated that HO absolutely requires a stechiometric amount of NADPH and molecular oxygen to generate carbon monoxide (CO), an equivalent of biliverdin/bilirubin (Tenhunen et al., 1969) and iron (Tenhunen et al., 1972). In a coupled reaction, biliverdin reductase converts biliverdin into bilirubin (Yoshida et al., 1977).

In 1971, a study by Pimstone and co-workers showed that HO is highly expressed in tissues normally involved in haemoglobin degradation such as spleen, liver, bone marrow and kidney. In particular, Pimstone showed that, in kidney, HO could be upregulated during haemoglobinuria, in order to counteract the excess of haemoglobin (Pimstone et al., 1971). Moreover, studies from the Yoshida and Maines groups contributed to a better understanding of the degradation reaction performed by heme oxygenase. Yoshida compared the activity of rat heme oxygenase to human heme oxygenase in macrophages and discovered an homology of 80% (Yoshida et al., 1988). Maines described for the first time the presence of two isoforms of heme oxygenase in the microsomal fraction of rat liver and noted that heme oxygenase 1 (HO-1) was increased up to 100-fold in response to exogenous agents such as cobalt or hematin, whereas heme oxygenase 2 (HO-2) was fully refractory to these agents (Maines et al., 1986).

1.2.2 *Heme Oxygenase 1 and its physiological role in cells*

There are different isoforms of heme oxygenase, an inducible form called heme oxygenase 1 (HO-1) and a constitutive isoform called heme oxygenase 2 (HO-2) (Maines et al., 1986). HO-1 is a 32kDa protein present at low levels in most mammalian tissues (Maines et al., 1986). A large variety of stress stimuli can induce its expression including heme, its substrate, heavy metals (Alam et al., 1989), UV irradiation, ROS (Keyse et al., 1989), nitric oxide (NO) (Foresti et al., 1997), and inflammatory cytokines (Terry et al., 1998). HO-2 is a 36kDa protein and is mainly expressed in the brain, testis, spleen, neurons, and endothelial and glial cells.

Thus, HO-1 is the first rate-limiting enzyme in the degradation of heme group into biliverdin (BV), carbon monoxide (CO), and free iron (Maines, 1988). The biological proprieties of HO-1 are mainly determinates by its metabolites and they are all involved in the maintenance of cellular

homeostasis and plays a key role in the adaptive response to oxidative stress (Hayes et al., 2014). BV is converted by biliverdin reductase (BVR) into bilirubin (BR) which exerts a strong antioxidant (Stocker et al., 1987), antiapoptotic (Loboda et al., 2015), and anti-inflammatory activity (Loboda et al., 2016). It is widely known that BR can prevents the peroxidation of proteins and lipids by scavenging different oxygen radicals like singlet oxygen, superoxide anions and hydroxyl radical (Tsai et al., 2019). Furthermore, BR is able to decrease the protein expression of P- and E- selectin. In this way, bilirubin exerts an anti-inflammatory action by preventing leucocyte rolling and inhibiting the complement cascade (Loboda et al., 2016; Nitti et al., 2020).

The potential harmful effects of free iron generation are generally prevented by the parallel induction of the heavy chain of ferritin and the activation of the membrane transporter Fe-ATPase, so that the generation of ROS, through the Fenton reaction, can be prevented by increasing the efflux and chelation of free iron (Balla et al., 1992).

Then, CO exerts antiapoptotic and anti-inflammatory effects by the regulation of different mechanisms. It can modulate soluble guanylyl cyclase (sGC), increasing the production of cGMP and modulating the mitogen-activated protein kinase pathway (MAPK) (Dennery, 2014; Gozzelino et al., 2010). Thus, CO production due to the upregulation of HO-1 stimulates blood vessel formation (Loboda et al., 2008) though the VEGF synthesis (Dulak et al., 2002) and favours the proliferation of endothelial cells (Jözkowicz et al., 2003) crucially involved in wound healing (Grochot-Przeczek et al., 2009). A schematic illustration of HO-1 enzymatic activity is depicted in Fig 1-3.

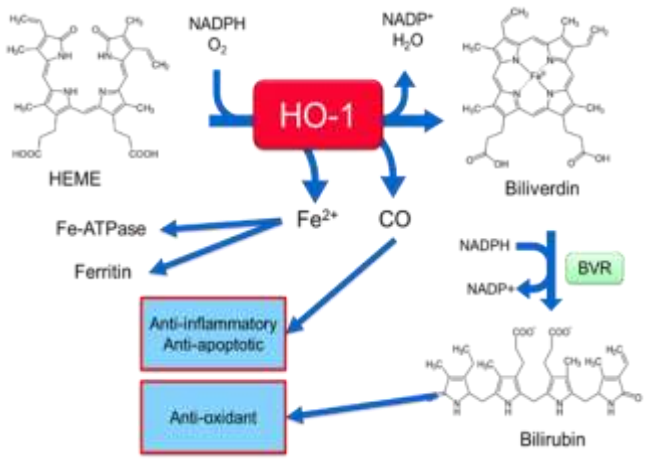

Figure 1-3: Schematic illustration of HO-1 enzymatic activity and functions. Microsomal heme is metabolized by HO-1, using NADPH and oxygen, to generate free iron, carbon monoxide (CO) and bilirubin that, together, have anti-inflammatory, anti-apoptotic and antioxidant effects (Adapted from Nitti et al., 2017).

Thus, HO-1 is highly induced in oxidative stress conditions and its synthesis is regulated mainly at a transcriptional level (Dennery, 2014). In the promoter region of HO-1, in fact, are present several binding sites for different transcription factors activated in oxidative stress conditions, like AP-1, HIF-1, NF-kB, and Nrf2 (Alam et al., 2007). Among these, Nrf2 is considered a key regulator of HO-1 gene transcription (Dennery, 2014).

1.2.3 *Heme oxygenase 1 and its pathological role in tumors*

It has been widely demonstrated that the upregulation of HO-1 plays an important role for cell protection. This implies that HO-1 protects healthy cells from neoplastic transformation by counteracting ROS formation and oxidative stress, but when upregulated in cancer cells can improve their survival (Berberat et al., 2005; Jozkowicz et al., 2007; Nitti et al., 2017). Cancer cells show a massive ROS production caused by their metabolism (Weinberg et al., 2009) and they take advantage from the overactivation of antioxidant defences, in particular those dependent from Nrf2 activation (Traverso et al., 2013). In addition, in the promotor region of HO-1 there are specific sequences for other transcription factors such as NF-kB and AP-1 (Lavrovsky et al., 1994), so that HO-1 can be activated by different signalling pathways (Cheng et al., 2006; D. Ma et al., 2015).

However, the strong association between Nrf2 and HO-1 activation and their correlation with tumour aggressiveness and poor clinical outcomes has been well documented (Wang et al., 2010), and reported in different tumours like non-small lung cancer, cervical cancer, hepatoma (Do et al., 2013), oesophageal squamous carcinoma (Shen et al., 2014), and multiple myeloma (Barrera et al., 2012). It has been demonstrated the malignant transformations with Nrf2-dependent HO-1 activation in B-lymphocytes exposed to prostaglandin J2 (Bancos et al., 2010). High level of heme oxygenase 1 have been observed in different human solid tumors and linked to the resistance to the anti-cancer therapies and the gain of a resistant phenotype (Furfaro et al., 2012; Nuhn et al., 2009). It has been demonstrated that in high-risk neuroblastoma the Nrf2 activation and the overexpression of HO-1 played a crucial role in the resistance to the proteasome inhibitor therapy (Furfaro et al., 2016)**.** Moreover, the upregulation of HO-1 positively correlates to higher microvessel density, metastasis and poor prognosis in different human tumors like NSCLC, colon and breast cancers (Bronckaers et al., 2009). This has been well documented in vitro and in vivo (Bussolati et al., 2004; Grochot-Przeczek et al., 2012; Jozkowicz et al., 2007; Lin et al., 2015; Loboda et al., 2008; Miyake et al., 2011). Importantly, Shang and co-workers treated gastric tumor in mice with an enzymatic inhibitor of HO-1 called zinc protoporphyrin-IX (ZnPP-IX) preventing the peritoneal metastasis (Shang et al., 2015).

Furthermore, many studies demonstrated the role of HO-1 in the regulation of immune system reaction to the tumors (Chauveau et al., 2005). Seo et al. reported that the overexpression of heme oxygenase 1 reduced the protein expression of ICAM-1 and CXCL10 which in turns inhibited the recruitment of T effector cells and cell-mediated cytotoxicity in colorectal cancer cells (Seo et al., 2015). Moreover, it has been highlighted the involvement of HO-1 in macrophage polarization leading to the inhibition of immune response (Arnold et al., 2014). Moreover, tumor recognition from Natural Killer (NK) cells seems to be linked to HO-1 expression. In studies performed in different cervical cancer cell lines, heme oxygenase 1 inhibition increases the expression of INF-γ and TNK-α and, consequently, restores the expression of some markers of NK activation (Gómez-Lomelí et al., 2014).

However, some contrasting evidence has been reported. Many studies have highlighted that the overexpression of heme oxygenase 1 prevents cell proliferation in breast cancer (Hill et al., 2005) and angiogenesis in prostate cancer (Ferrando et al., 2011) mediates the anticancer activity drugs by reducing the matrix metallopeptidase 9 (MMP-9) expression in breast cancer cells (Chao et al., 2013).

HO-1 can also act independently of its enzymatic function. HO-1 has been localized as an integral type I membrane protein in the smooth endoplasmic reticulum (sER) and mainly oriented into the cytoplasm (Yoshinaga et al., 1982). A study has shown that HO-1 undergoes proteolytic cleavage that results in the release of a soluble 27-28kDa HO-1, which lacks of the C-terminal part of the protein, capable of nuclear translocation, and able to promote tumor growth and resistance to therapy regardless of its enzymatic function (Chau, 2015; Q. Lin et al., 2007). Several stimuli can induce the translocation of HO-1 into the nucleus. For example Birrane and co-workers demonstrated that cigarette smoking induces HO-1 nuclear translocation and promotes VEGF secretion in prostate cancer (Birrane et al., 2013). Furthermore, HO-1 nuclear translocation has been shown to correlate with therapeutic resistance with imatinib in chronic myeloid leukaemia cells (Tibullo et al., 2013).

1.3 Melanoma

Melanoma is the most aggressive type of skin cancer characterized by a high ability to metastasize. Thus, although melanoma is the less common skin tumor, it has the higher mortality rate, up to 75% (Chan et al., 2017), and only with an early diagnosis, the patient can have a good outcome.

1.3.1 *Melanocytes*

Melanocytes represent about 1-2% of the epidermal skin cells and are located in the basal layer of the skin (Garibyan et al., 2010). Melanocytes also are present in hair follicles, where they contribute to pigment the hair (Albert et al., 2002), in the uveal tract of eyes and, at lower density, in tissues such as meninges and the anogenital tract (Young, 2009). Melanocytes contains melanosomes, the organelles where the melanin is produced under the control of keratinocytes (Shain et al., 2016). Melanin is a brown pigment that protects the skin from UV radiation injure (Brenner et al., 2008) and the ability of keratinocytes to stimulate melanin production is a consequence of p53 stabilization due to UV-induced DNA damage. P53, in fact, stimulates the expression and release of melanocyte-stimulating hormone (MSH) by keratinocytes (Cui et al., 2007). The receptor of this hormone is the melanocortin 1 receptor (MC1R) expressed on melanocytes and the binding with its ligand activates the signalling pathway involved in the production of melanin (Garibyan et al., 2010). The melanin synthesized in melanosomes is transported via dendrites to adjacent keratinocytes located in the upper layer of the skin for the accumulation.

1.3.2 *Epidemiology and frequently of melanoma in the word*

Melanoma remains a potentially fatal malignancy to date (Rastrelli et al., 2014). The incidence of cutaneous melanoma increased since the early 1970s in predominantly fair-skinned populations until 1990 (MacKie et al., 2009), with a parallel enhancement also of melanoma related-mortality, albeit to a lower degree (Rigel, 2010). Age-cohort period analyses of melanoma incidence in Australia, New Zealand, Norway, Sweden, the UK, and the white population of the USA from 1982 to 2011 revealed that the incidence increased about 3% annually, and will further increase at least until 2022 in Norway, Sweden, the UK, and the USA. (Schadendorf et al., 2018; Whiteman et al., 2016).

In 2012, the estimated age-standardised mortality rates of cutaneous melanoma ranged from 0.1 per 100000 person-year in South-East Asia to 1.5 per 100000 person-year in the EU. The highest mortality rates were observed in New Zealand (4.7 per 100000 person-year) and Australia (4.0 per 100000 person-year) (International Agency for Research on Cancer, 2013). In 2017, the estimated percentage of deaths due to cutaneous melanoma among all skin-cancer deaths (excluding basal-cell and squamous-cell carcinoma of the skin) in the USA was 72% (Siegel et al., 2017). The 5-year age-standardised relative survival for cutaneous melanoma diagnosed in 2000−2007 in Europe ranged from 74.3% (Eastern Europe) to 87.7% (Northern Europe) (Crocetti et al., 2015).

1.3.3 *Genetic Classification of Cutaneous Melanoma*

Melanoma can be classified based on specific mutations reported in specific oncogenes or tumor suppressors.

BRAF Mutations

V-Raf murine sarcoma viral oncogene homolog B1 (BRAF) is a human proto-oncogene. BRAF is a member of the rapidly growing fibrosarcoma (RAS) family of serine-threonine kinases that includes also ARAF and CRAF. They are part of the RAS/RAF/MEK/ERK mitogen activated protein kinase (MAPK) signal pathway (Fedorenko et al., 2011; Schreck et al., 2006).

The structure of RAF harbours the typical C-terminal lobe (C-lobe) and N-terminal lobe (N-lobe) connected by a flexible hinge. There are 3 major active sites of RAF: the nucleotide (ATP or ADP)-binding site, the magnesium-binding site (DFG [Asp–Phe–Gly] motif), and the phospho-acceptor site, called activation segment (AS) (Kornev et al., 2016). In the inactive status, RAF proteins have close and monomeric conformation and the activation segment present a helical conformation that induces the αC helix in the "OUT" position in the N-terminal. In the active status of BRAF, the activation segment is extended allowing the activation segment to move in "IN" position (Pan et al., 2018).

Mutations in BRAF gene are present in 5-10% of all human malignancies with higher incidence in malignant melanoma (59%), thyroid papillary cancers (35,8%) and colorectal cancers (10-20%) (Lochhead et al., 2013). Melanoma bearing BRAF mutation is usually detected in young patients and correlates with sun light exposure (Reddy et al., 2017).

The discovery of the gain-of-function mutation of BRAF in melanoma represents a landmark event in the study of melanoma biology (Fedorenko et al., 2011). Many BRAF mutations have been described, but 40-70% of malignant melanoma harbour a point mutation that determines a substitution of the amino acid valine with the glutamic acid at codon 600 (named V600E), located

in the activation loop of BRAF protein (Bollag et al., 2012). This point mutation results in a conformational modification and leads to a constitutive activation of MAPK pathway. In this way, cells are continuously stimulated to proliferate (Fedorenko et al., 2011). Furthermore, other mutations have been identified in $BRAF^{V600}$ such as valine-to-lysin mutation called $BRAF^{V600K}$ (20%) and valine-to-arginine mutation called $BRAF^{V600R}$ (7%). Interesting, 70-80% of melanoma harbour the $BRAF^{V600E}$ mutation, highlighting the tumorigenic role played by this protein (Reddy et al., 2017).

RAS Mutations

The second common genetic alteration found in melanoma, with almost 20% of the total cases, is the mutation of NRAS gene, at codons 12, 13, 61. NRAS mutation increases melanoma aggressiveness and correlates with poor outcome (Reddy et al., 2017). It has been demonstrated that BRAF and NRAS mutations are mutually exclusive (The Cancer Genome Atlas Network). Moreover, NRAS mutated melanoma is usually diagnosed in older patients or due to a chronic UV exposure in middle-age patients (Muñoz-Couselo et al., 2017).

NF1 Mutation

Neurofibromin 1 (NF1) was identified in 1990 by Wallas and co-workers (Wallace et al., 1990) as a GTPase-activating protein that works as RAS inhibitor. NF1 mutated determinates an uncontrolled activity of RAS/MEK signalling pathway (Kiuru et al., 2017). NF1 mutation is present in 12-18% of all melanoma and is also common in other types of tumors such as neurofibromas and myeloid leukemia (Kiuru et al., 2017). Similar to NRAS, NF1 mutation occurs in older patients or as a consequence of chronic sun light exposure.

Triple Wild-Type Melanoma

Triple Wild-Type (WT) melanoma is a heterogeneous group of melanoma characterized by the absence of BRAF, N/K/H RAS or NF1 mutations (The Cancer Genome Atlas Network, 2015). It has been shown that triple WT melanoma have a significant copy number of gene amplifications containing KIT (containing v-kit Hardy-Zuckerman 4 feline sarcoma viral oncogene homolog), PDGFRA (platelet derived growth factor receptor alpha), kinase insert domain receptor (KDR, also known as VEGFR2), TERT (telomerase reverse transcriptase), CDK4 (cyclin dependent kinase 4) and CCND1 (cyclin D1).

1.3.4 *Therapeutic approaches*

Melanoma therapeutic options depend on location and stage of the tumor and on the type of mutation. The *surgical resection* is the first approach for early stage melanoma patients (Domingues et al., 2018) and it is usually associated with a good outcome (Roberts et al., 2002). For advanced stage of melanoma, surgery is insufficient, and systemic treatment is needed to limit tumor spreading (Roberts et al., 2002).

Radiotherapy is used to treat locoregional melanoma, frequently associated to the surgery of primary melanoma in order to reduce relapses. It is also used as a palliative treatment for advance stage melanoma or as the main therapy if the patient refuses the surgical excision (Strojan, 2010).

Photodynamic therapy is based on the ability to generate ROS to damage the tumor, its vascular system, also by increasing the activity of the immune system (Gollnick et al., 2006). Patients are treated with photosensitizers dyes, such as hypericin, benzoporphyrin derivatives, protoporphyrin IX and associated with activating irradiation to produced ROS.

Immune therapy is based on the possibility to increase the activity of immune cells against the tumor. In mid 90s FDA approved the interferon α2-β (IFN-α) (Rafique et al., 2015) as the first immunotherapy drug. In melanoma, IFN-α is a dose-dependent immunomodulatory and it exerts its anti-proliferative effect by the stimulation of the major histocompatibility complex class I (MHC class I) expression (Domingues et al., 2018). Moreover, cytokine interleukin-2 (IL-2) is used as adjuvant therapy for metastatic melanoma in combination with chemotherapy, radiotherapy or target therapy. IL-2 acts increasing the effector T-cells and regulatory T-cells in order to inhibit melanoma proliferations (Torres-Collado et al., 2018). Ipilimumab is a human monoclonal anti-CTLA-4 antibody that first showed survival benefit for metastatic melanoma patients (Taube et al., 2018; Trinh et al., 2013). CTLA-1 is an inhibitory checkpoint receptor that determinates inactivation and, subsequently, immune tolerance of T-cell (Domingues et al., 2018). Ipilimumab therapy is able to inhibit CTLA-4 and increase T-cell response by higher production of pro-inflammatory cytokines. In this way, the therapy increases the expansion and infiltration of T-cell population (Graziani et al., 2012).

Targeted therapies. The identification of oncogenic driver mutations (such as BRAF, NRAS, etc) in tumors has determined the development of targeted therapies. This is a new approach for counteracting malignancies by targeting a mutated protein that is usually involved in survival, adaptation and proliferation. The targeted therapy includes the use of small molecule inhibitors and antibodies that exert their action only on the mutated proteins so that it is possible to choose the best therapy for the patient based on the tumor mutation profile (Domingues et al., 2018).

1.3.5 *Vemurafenib/PLX4032*

After the discovery of the $BRAF^{V600}$ mutation, the interest to discover a kinase inhibitor of this protein with potential therapeutic benefits notably increased. By using a structure-guided discovery approach, a potent and selective inhibitor of active BRAF has been discovered and called PLX4720 (Tsai et al., 2008).

After more studies, PLX4032 was developed as a compound with a selectivity for $BRAF^{V600}$ over wild-type BRAF that preferentially binds to BRAF in the active conformation (Zhang et al., 2017). Indeed, it can bound the ATP-binding site of BRAF protein and lead to its inactivation: the molecule creates a bridge between Glu600 and Lys507 causing inhibition of the target protein (Bollag et al., 2010).

The chemical name of PLX4032 is *propane-1-sulfonic acid {3-[5-(4-chlorophenyl1)-1H-pyrrolo[2,3-b]pyridine-3-carbonil]-2,4-difluorophenyl}-amide* with a molecular weight of 489,93 Da (Zhang et al., 2017, Fig 1-4).

PLX4032, was rapidly driven through clinical development under collaboration between Roche and Plexxikon laboratories and received the commercial name of Vemurafenib. Phase I trial established that the maximum dose tolerated was 960mg twice a day and highlighted an antitumor activity in 26 of 32 PLX4032-treated patients. Finally, in phase III study compared Vemurafenib with Dacarbazine chemotherapy in patients with metastatic or unresectable melanoma. The study confirmed that Vemurafenib significatively improved the outcome of the patients and after a long follow-up, Vemurafenib was approved as a melanoma monotherapy in more than 90 countries (Chapman et al., 2011; Zelboraf, 2016) .

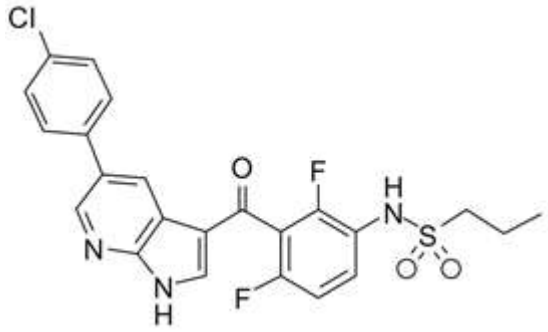

Figure 1-4 Chemical structure of PLX4032. (Zhang et al., 2017)

In general, PLX4032 treatment is well tolerated by patients with manageable side effects, all correlated to a dose and exposure treatment (Garbe et al., 2018). Unfortunately, it has been shown

that, after an initial good response, melanoma can reoccur with higher aggressiveness leading to fatal progression (Stones et al., 2013; Wagle et al., 2011).

1.3.6 *Resistance to the PLX4032 treatment*

The first documented case of Vemurafenib resistance was described by Wagle and co-workers (Wagle et al., 2011) in a 38-year-old melanoma patient. Initial PLX4032 treatment led to a total regression of all subcutaneous tumor nodules within 15 weeks. Unfortunately, melanoma reoccurred with a faster progression and the patient died after a few months.
As resistance mechanisms to the therapy, two hypotheses were formulated:

- MAPK pathway reactivation through secondary mutations, amplifications or other kinases reactivation;
- generation of alternative signals pathways.

Based on these hypotheses, PLX4032 resistance can be upstream or downstream of BRAF protein in an ERK-dependent or independent manner (Nazarian et al., 2011; Wagle et al., 2011; Wang et al., 2013). In ERK-dependent PLX4032 resistance, it has been hypothesized that the upstream activator protein of BRAF is mutated. In this way, the PLX4032-inhibited BRAF (BRAFi) is bypassed by ARAF and CRAF and consequently MAPK signalling pathway is reactivated. In ERK-independent resistance, platelet-derived growth factor receptor β (PDGFRβ) is overexpressed in BRAFi-resistant melanoma cells and this leads to tumor proliferation and growth (Johnson et al., 2015; Wang et al., 2013). It has been demonstrated that PDGFRβ silencing in melanoma cells is associated with anti-apoptotic effects. This evidence suggests that the increase of this receptor is not the only mechanism involved in the resistance (Johnson et al., 2015). Moreover, the increased activation of insulin-like growth factor 1 receptor (IGF1R) by IGF-1can activate RAF-MEK-ERK or PI3K-AKT pathways and may play a role in the development of resistance to the therapy (Villanueva et al., 2013; Wang et al., 2013).

1.3.7 *Tumor microenvironment*

The development and progression of cancer depends not only on cancer cells but also on other elements in the surrounding area of tumors. Indeed, in the area around the tumor mass, a unique involvement of stromal cells, immune cells, endothelial cells and other components, named tumor microenvironment (TME), crucially drives tumor progression. TME involves many types of resident and non-resident constituents (Buhrmann et al., 2014; Ding et al., 2012). Stromal cells compose the residential components of the TME. The non-residential components are

represented by different kind of immune system cells that are also the major factor that determinates the fate of malignancies modulating the development, invasion, metastasis and angiogenesis (Mao et al., 2013). Moreover, every TME is different in composition and characteristics. It depends on the type of cancer and on other intrinsic features.

As mentioned before, the immune system cells play different roles to counteract or support the tumor development and progression. Of interest for cancer therapies, there are:

Macrophages, or *tumor-associated macrophage* (TAMs) are among the most abundant innate immune system cells in the TME. A large body of evidence demonstrates that macrophages (Fidler, 1988) adopt a pro-tumoral phenotype *in vivo* both in the primary and in metastatic sites (Biswas et al., 2013). Indeed, macrophages promote many important features of tumor progression including angiogenesis, tumor cell invasion, motility and intravasation as well as at the metastatic site, stimulation of tumor cell extravasation and persistent growth. Each of these activities are delivered by identifiable sub-populations of macrophages (Qian et al., 2010). These data together with experimental studies showing inhibition of tumor progression and metastasis by inhibition of macrophages, highlighted that immune cell engagement by tumors is essential for the acquisition of a malignant phenotype. Consequently, this cell type might represent an important therapeutic target for cancer treatment (Hinshaw et al., 2019).

T-lymphocytes are present in the TME, recognised as *tumor-infiltrating lymphocytes* (Kiraz et al., 2015). The prevalent lymphocyte population present in the immune microenvironment is made up of CD8+ and CD4+. Those cells are both responsible for the performance of anticancer activity. The initial innate immune sensing of tumors results in recruitment, activation, and clonal expansion of tumor antigen specific CD8+ T cells, which have the potential to kill tumor cells. In fact, tumor-infiltrating CD8+ T cells have been detected in subsets of patients with various cancers such as melanoma and carcinomas of the head and neck, breast, lung, prostate, bladder, kidney, colon, ovary, and esophagus. Importantly, T cell-phenotype infiltration correlates with positive treatment outcomes in these cancers and has been proposed as a prognostic biomarker (Azimi et al., 2012; Corrales et al., 2017; Mahmoud et al., 2011; Pagès et al., 2010).

Natural killer cells (NK) constitute a small subpopulation of lymphocytes belonging to innate immunity with cytotoxic capacity. These cells play an important role in defence against some pathogens and are capable to destroying many types of cancer cells without prior sensitization. They can be the first line of defence against cancer. It has been demonstrated that low NK-cell activity is correlated to an increasing cancer risk (Imai et al., 2000). Upon their activation, NK cells are able to kill numerous human tumors including many apparently non-immunogenic T cell tumors. Therefore, it appears that CTLs and NKs provide complementary anticancer mechanisms (Woo et al., 2015).

NK cells and melanoma

It has been demonstrated from the study of McKay and co-workers that NK cell infiltration in melanoma positively correlates with tumor regression. Indeed, NK cells produce many cytokines and chemokines, including tumor necrosis factor–α (TNF-α), interleukin (IL)–10, CCL2 (MCP-1), CCL3 (MIP1-α) that are all synergically involved in the recruitment of other cells in the inflammation area (Moretta et al., 2005). The activation of NK cells is highly regulated and depends on the balance between activating and inhibiting signals mediated by cell surface receptors (Vivier et al., 2011).

Human leukocyte antigen (HLA) class I-binding receptors represent the mainly inhibitory receptors, including killer immunoglobulin–like receptors (KIR) and CD94/NKG2A.

Among the activating cytotoxicity receptors there are: NKp30 (which binds to B7H6 ligand on tumor cell), NKp46, NKp44 (which binds to mixed-lineage leukaemia protein 5), induced after stimulation by cytokines, and NKG2D, expressed by peripheral NK cells. NKG2D receptor binds MHC I polypeptide-related chains A and B (MICA/B) and UL16-binding proteins (ULBP1-6). NKG2D ligands are induced on the membrane of stressed cells and thus promote many of NK functions in vitro (Bryceson et al., 2006; Lakshmikanth et al., 2009).

Moreover, NK cells can also exert their activity by detecting tumors that are resistant to T-cell action due to loss or downregulation of MHC class I antigens. It has been demonstrated that melanoma treated with PLX4032 increase the expression of HLA class I and HLA-E molecules that inhibit the lysis by NK cells through NKG2A receptors (Frazao et al., 2017).

1.3.8 *Tumor Angiogenesis*

Angiogenesis plays a fundamental role in the survival and proliferation of tumors and their metastases (Emmett et al., 2011). Indeed, angiogenesis is essential in order to satisfy the increased nutritional requirements of the tumor considering that oxygen and nutrients freely diffuse into tissues only up to a distance of 100-200μm from the closest capillary (Levenberg et al., 2005).

Angiogenesis begins with the germination of new capillaries from pre-existing quiescent vessels in presence of pro-angiogenic factors, among which, the most important is vascular endothelial grown factor-A (VEGF-A) (Cho et al., 2019).

Therefore, within the tumor microenvironment, it is necessary that the balance between pro-angiogenic and anti-angiogenic factors favors angiogenesis to promote all the mechanisms involved in cell migration and formation of new capillaries associated with the tumor. This modification within the tumor is called the “angiogenic switch” and plays a fundamental role in

the acquisition of an aggressive tumor phenotype in many tumors, including melanoma (Bergers et al., 2003).

The first evidence of angiogenesis in melanoma was described by Warren and Shubik (Warren & Shubik, 1966). Among the stages of melanoma progression, the vertical growth phase (Mahabeleshwar et al., 2007) is characterized by the invasion of cancer cells into the deeper layers of the dermis to the blood and lymphatic vessels. The vertical growth phase is characterized by rapid proliferation and consequently a greater consumption of nutrients. When tumor progression exceeds the angiogenesis capacity of the entire tumor mass, hypoxia areas can be formed. Hypoxia induces activation of hypoxia inducible factor-1α (HIF-1α) which in turn stimulates the production of VEGF-A, increasing the permeability and migration of endothelial cells. Furthermore, in this phase, melanoma cells have the ability to trans-differentiate into an endothelial-like phenotype. This ability is called “vascular mimicry” and allows melanoma cells to express VEGF-A receptors and generate endothelial-like responses to further enhance the angiogenic stimulus. The creation of new vessels is also followed by the remodelling of the extracellular matrix (ECM), carried out by the integrins and the metalloproteases of the matrix (MMP). The modification of the ECM therefore determines the invasion of the connective layer of the dermis and the release of angiogenic factors from the matrix (Mahabeleshwar et al., 2007; Maniotis et al., 1999). A schematic illustration of melanoma progression is depicted in Fig 1-5.

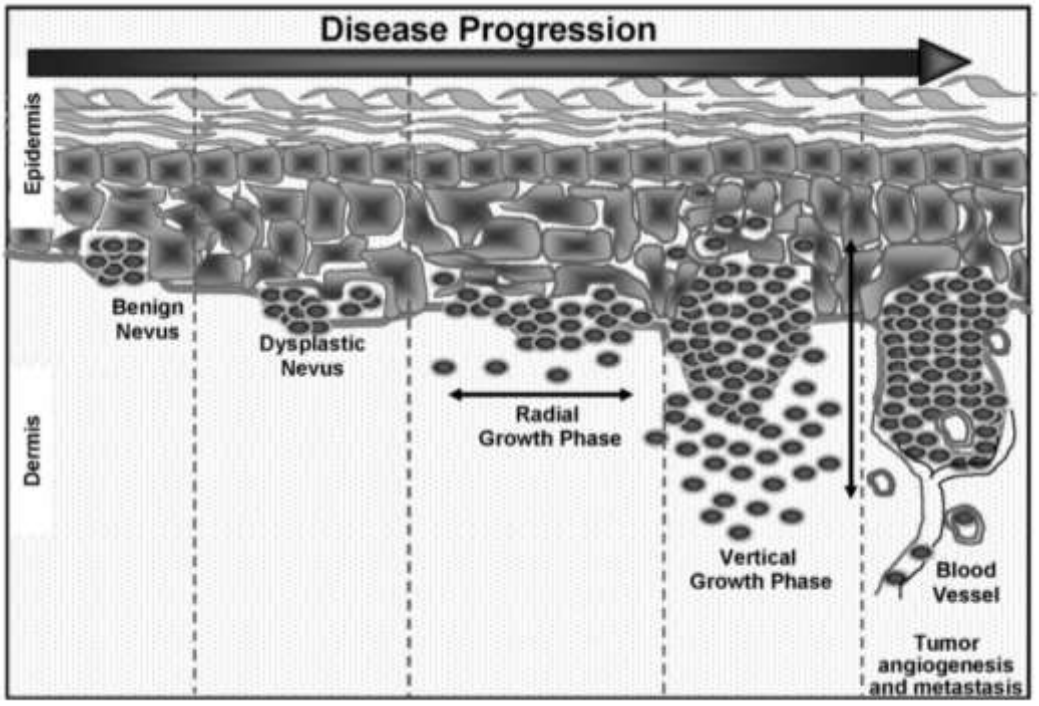

Figure 1-5: Schematic representation of melanoma progression. Uncontrolled proliferation of melanocytes leads to formation of benign nevus and subsequently into dysplastic nevi. This is followed by a rapid radial growth phase, which is characterized by intraepidermal growth. The vertical growth phase is the last step for the melanoma developing (Mahabeleshwar et al., 2007).

It was shown that treatment of $BRAF^{V600E}$ melanoma with the antidiabetic drug metformin accelerates tumor growth through upregulation of VEGF-A (Martin et al., 2012). Furthermore, a recent study has shown the involvement of VEGFR-1 upregulation in the acquisition of resistance in melanoma treated with PLX4032 (Atzori et al., 2020). Moreover, Comunanza and co-workers highlighted that the inhibition of mutated BRAF with PLX4720 (the mouse BRAF inhibitor of PLX4032) and VEGF leads to a suppression of tumor growth and a reduction of colonization in BRAF-mutant mouse model (Comunanza et al., 2017).

1.4 Relevance of physiological oxygen levels

The mechanisms of the oxygen utilization by cells and the consequences associated with their dysfunction have been studied and linked with the generation of reactive oxygen species (ROS). Moreover, the concept of hypoxia as the pathological reduction of oxygen has been recognized as a distinctive sign of disease (Semenza, 2014). Moreover, in order to recapitulate in cell cultures the oxygen levels experienced by cells and tissues in an organism *in vivo*, it becomes of crucial importance to maintain the correct levels of normoxia and hypoxia in cells in culture.
In fact, cell cultures are usually carried out in atmospheric O_2 conditions that are hyperoxic conditions in comparison to levels encountered by tissues *in vivo*. Many studies have highlighted this gap (Pinder et al., 2009), but only in the last few years researchers have addressed this problem.

A workstation for maintaining physiologically relevant O_2 during in vitro cell culture

Technological development has enabled cells to be cultured in vitro under well-defined O_2 levels in order to reproduce a physiological oxygen setting (Keeley et al, 2019).
Today, there are three main instruments enabling researchers to conduct cell cultures under a reduced oxygen environment:

1. An airtight gassed chamber
2. A tri-gas incubator
3. A dedicated O_2-regulated workstation

The airtight chamber is a widely used tool because it is relatively easy to use, and it can be inserted inside the standard 5% CO_2 incubators. Although equipped with dividers, these chambers can be used by a limited number of operators.
The second option is a variant of the classic incubator, called Tri-gas incubator, where it is possible to regulate the oxygen tension using nitrogen gassing. For the manipulation and treatment, cells have to be moved outside the incubator and then maintained in Tri-gas incubator. These procedures subject cells to significant O_2 changes in the culture media (Weinmann et al., 2004) and cells are re-exposed to the ambient oxygen tension during treatments in a laminar flow hood. Although the exposure to ambient O_2 is about 5 min, the media takes hours to equilibrate with a lower oxygen tension again (Mondragon-Teran et al., 2009).
Lastly, a dedicated oxygen workstation is an airtight work area, where it is possible to control every single parameter such as O_2 and CO_2 levels, temperature and also humidity. In this

workstation, cells can be maintained and treated without being re-exposed to different ambient oxygen levels (Keeley et al., 2019).

Work in low oxygen tension: cells behaviour

In a physiological context, when cells are exposed to a lower oxygen tension some adaptive mechanisms are activated to ensure cell survival (Alami et al., 2014; Kumar et al., 2016).
In vitro, these mechanisms are also activated in cells when they are brought from an environmental O_2 level of approximately 18kPa (hyperoxia) to a physiological oxygen level of ~5kPa (normoxia). For example, HIF-1α reaches its peak of expression after 12-16 hours and it takes at least 24 hours to reach a new normalization point, while HIF-2α takes much longer, about 72 hours (Holmquist-Mengelbier et al., 2006). For these reasons, cells have to adapt to the new oxygen tension to achieve a new adapted status. Furthermore, the transition from ambient air to 5kPa O_2 can cause a change in the cellular phenotype, and long-term (~5 days) adaptation is required for human endothelial cells (Chapple et al., 2016) and other cells types such as lung epithelial cells (Kumar et al., 2016) and dental pulp stem cells (Alami et al., 2014).

Work in low oxygen tension: cell media behaviour

The amount of oxygen dissolved in fluids is measured as partial pressure (PO_2) in mmHg or in kilo Pascals (kPa), as the concentration of a gas is directly proportional to the partial pressure that the gas exerts in the solution (Henry's law). Partial pressure best expresses the chemical potential of physiological gases which, in fact, diffuse towards low pressure gradients, not concentration (Henry, 1803).
Oxygen, therefore, is available in the media based on its solubility determined by Henry's law (Henry, 1803). In a standard incubator at 37°C with an environmental PO_2 of about 18kPa, the oxygen solubility is about 77%. Furthermore, the environmental PO_2 will be in equilibrium with the PO_2 of the culture medium because oxygen will diffuse from the environment to the medium following the Fick's second law (Flick, 1855). Therefore, when cells are grown in an environment with reduced oxygen tension, for example 5kPa O_2, it is easy to assume that the PO_2 in the medium has to decrease. Based on Fick's second law is possible to determine how long the media takes to reach the new oxygen equilibrium. As a practical example, in a 90mm Petri dish with 20ml of culture medium placed in an airtight chamber at a 5kPa O_2, it will take approximately 2h to reach the new equilibrium (Keeley et al., 2019). This is because, as we stated before, if the environmental O_2 decreases, the diffusion time increased.
Importantly, Fick's law of oxygen diffusion and its subsequent equilibrium in solution does not include the influence of cells on the medium. Indeed, the consumption of oxygen by cultured

cells and the poor solubility of oxygen in the media generates an oxygen gradient from the atmospheric surface towards the pericellular zone. This oxygen gradient is proportional to the rate of cell oxygen consumption (Mimura et al., 2010). It has been calculated and subsequently experimentally verified that some cell types exhibit such a high rate of oxygen consumption so that cells overexpress the classic hypoxia markers when cultured under physiologically relevant oxygen levels in the absence of blood flow (Flick, 1855).

Furthermore, some studies have shown that cells cultured under normoxia respond differently from cells maintained in hyperoxia. A study conducted on U-87 cells, a glioblastoma multiforme cell line, documented increase in HIF-1α, stimulated migration and increased resistance to therapy in cells exposed to 9kPa O_2 (Albert et al., 2014). In addition, a collection of clinical evidence shows that the state of hypoxia in a tumor can compromise the efficacy of the treatment (Martin et al., 2019; Vaupel et al., 2007). This highlights how the best reproduction of the physiological/pathological environment determines a result closer to the real condition.

2 AIMS

The novel oncogene-targeted therapies, especially Vemurafenib/PLX4032, developed in the last years have been proven to be very effective in $BRAF^{V600}$ positive metastatic melanoma. Unfortunately, in many patients, the disease relapses in less than 12 months. Thus, it is critically important to identify new molecular targets to be modulated in order to improve the efficacy of therapies.

HO-1 induction has been highlighted as a mechanism involved in cancer progression, playing a role in cancer growth, resistance to therapies, invasiveness, angiogenesis and metastatic potential, with different evidence in many kinds of tumor (Nitti et al., 2017). Thus, in this thesis we investigated the involvement of HO-1 in reducing the efficacy of PLX4032 in $BRAF^{V600}$ positive melanoma cells. We further analysed HO-1 involvement in reducing immune recognition. Indeed, HO-1 has a well recognized ability to modulate immune-responses (Naito et al., 2014), but the role played in immune-recognition of cancer cells is still poorly investigated. Moreover, the involvement of HO-1 modulation in regulating the pro-angiogenic ability of melanoma cells is poorly understood and has been investigated.

Finally, the role played by lowering oxygen tensions in cell cultures has been also considered.

3 MATERIALS AND METHODS

3.1 Cell culture and treatments

3.1.1 *Melanoma cell lines and treatments*

Primary $BRAF^{V600}$ melanoma cell lines (MeOV-1/$BRAF^{V600E}$, MeTA/$BRAF^{V600D}$, MeMI/$BRAF^{V600E}$) derived from metastatic lesions were obtained in accordance with consent procedures (nOMA09.001) approved by the International Ethics Board of the National Cancer Institute (IRCCS Policlinico San Martino Hospital, Genoa, Italy). MeWo (RRID: CVCL_0445), a BRAF- wt cell line, was purchased from ECACC.

All the cell lines were authenticated by short tandem repeat (STR) profile analysis (cell IDTM system, Promega, Madison, WI), used within 6 months of resuscitation of original cultures, and tested for mycoplasma contamination.

Melanoma cell lines were routinely cultured in RPMI 1640 medium (Gibco) supplemented with 10% fetal bovine serum (FBS, Euroclone, Italy), 2mM glutamine (Sigma, UK) and 1% penicillin/streptomycin (Sigma, UK), subcultured every 5 days at 1:5, and maintained in 5% CO_2, humid atmosphere and different oxygen conditions.

Cells were treated with 1-10µM PLX4032 (Selleckchem, Houston, TX) for different time point. Pure DMSO was used to dissolved PLX4032. Samples were co-treated for 24h with 10µM Tin mesoporphyrin IX (SnMP-IX, Cayman Chemical Company, Ann Arbor, MI) and 1-10µM PLX4032.

3.1.2 *Endothelial cell lines*

Bovine aortic endothelial cells line (BAEC) were isolated from aortae obtained from a local abattoir (He et al., 2015). An immortalized cell line of human endothelial cell from vein (HECV) derived from human umbilical vein endothelial cells (HUVEC) was kindly provided from Dr Anna Maria Bassi. BAEC and HECV were routinely cultured in DMEM Low Glucose (Sigma, see Appendix 2) supplemented with 10% FBS (Euroclone, Italy), 2mM glutamine (Sigma, UK) and 1% penicillin/streptomycin (Sigma, UK). BAEC were defrosted and were used before passage 6 to prevent phenotype changes.

Human cerebral microvascular endothelial cell line (hCMEC/D3 cell line) was kindly provided by Dr Richard Siow and Dr Melissa Barber (King's College London, UK). hCMEC/D3 (D3)

cells were originally isolated from the temporal lobe of a female patient with intractable epilepsy and immortalised by transduction with lentiviral vectors carrying the SV40 T antigen and human telomerase reverse transcriptase (hTERT) (Vu et al., 2009). D3 cells were cultured in phenol-red free endothelial cell basal medium-2 (EGM-2) (Lonza) supplemented with the following factors as specified by the supplier: 0.025% rhEGF, 0.025% VEGF, 0.025% IGF, 0.1% rhFGF, 0.1% gentamycin, 0.1% ascorbic acid, 0.04% hydrocortisone and 2.5% FBS, and culture media sterilised by filtration. hCMEC/D3 cells were grown to confluence (~1 × 105 cells/cm^2) on tissue culture flasks coated with rat tail collagen (0.01%) (Sigma, USA; Fig. 3-1).

3.1.3 *Culturing cells under physiologic and hypoxic environments: The Sci-tive® in vitro workstation*

In order to obtain results closer to the physiological environment, MeOV-1, BAEC, HECV and hCMEC/D3 cells were cultured in an O_2-regulated workstation (Sci-tive, Baker-Ruskinn Company, USA, Fig. 3-1) set at:

- 5% O_2 - 5% CO_2-balanced N_2 and 75% humidity to reproduce the normoxia,
- and at 1% O_2 - 5% CO_2-balanced N_2 and 75% humidity to reproduce the hypoxia.

Furthermore, all solutions and media were equilibrated for 1-2h under defined O_2 levels before being used. Indeed, molecular O_2 has a very low solubility in water compared to CO_2. Based on the second law of Fick (Fick, 1855) and previously study (Keeley et al., 2019), 20ml of solution takes 82 min to reach 5% O_2 from room air.

Figure 3-1: Workstation for the creation and maintenance of a physiological oxygen environment. Baker-Ruskin Sci-tive workstations provide accurate, stable and defined oxygen, carbon dioxide, temperature and humidity control to replicate the physiological system.

3.2 siRNA for Nrf2 and HO-1

Small interfering RNA was performed by using specific pool of oligonucleotides against human HO-1 (On-TargetPlus SMART pool human HO-1; Dharmacon, Lafayette, CO), to silence MeOV-1, MeTA and MeMI cell lines, and Nrf2 (On-TargetPlus SMART pool human Nrf2; Dharmacon, Lafayette, CO) to silence MeOV-1 cell line. All cell lines seeded in 6-well plates, were transfected with 120pmol/well of siRNA for 24h by using Lipofectamine 2000 (Life Technologies, Carlsbad, CA) according to the manufacturer's instruction.

In our work, melanoma cells were seeded at a density to achieve 70-90% confluence at the moment of the transfection. At the day of the transfection, solution A containing diluted Lipofectamine and solution B containing diluted siRNA were prepared and incubated for 5 min. To create the silencing liposome, solution B was added into solution A and incubated for 20 min. The final volume was achieved by adding complete melanoma medium without antibiotics. Melanoma cell lines were incubated with siRNA for 6h and then the medium was changed with fresh medium.

Cells were then exposed to treatments as described in Section 3.1.1. At the end of the treatment, mRNA or proteins were extract (see Sections 3.5.1 and 3.6.1). The level of mRNA and protein expression of HO-1 and Nrf2 were checked to verify the efficiency of silencing. The specificity was proved by using as a negative control a non-targeting (NoT) silencing pool of oligonucleotides (On-TargetPlus siControl nontargeting pool Dharmacon) at the same concentration used for the target silencing.

3.3 Viability Assay

The efficacy of PLX4032 treatment in decreasing cell viability was assessed using the tetrazolium salt 3-(4,5-dimethylthiazol-2-yl)-2,5-diphenyltetrazolium bromide (MTT) assay (Sigma, UK). Following the interaction with mitochondrial dehydrogenase, the yellow MTT salt is cleaved to form an insoluble purple formazan crystal (Fig. 3-2). MTT cleavage only occurs in metabolically active cells and decreases according to mitochondrial activity (Mosmann, 1983). Melanoma cells were seeded into 96-well plates and treated with 10µM PLX4032 in complete melanoma medium for 24h at 37°C and 5% CO_2 under specified ambient oxygen levels.

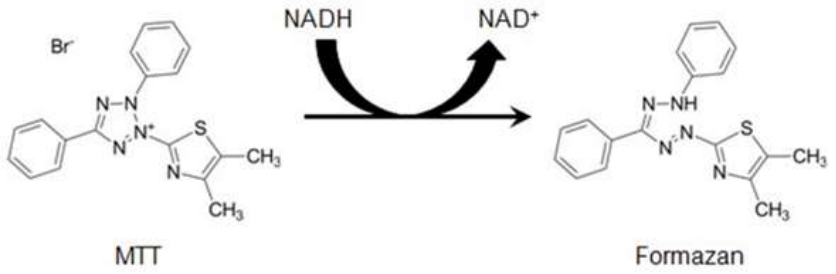

Figure 3-2: MTT assay reaction. 3-(4,5-dimethylthiazol-2-yl)-2,5-diphenyltetrazolium bromide is reduced to formazan and creates dark purple insoluble crystal inside the cells. For the MTT assay, it is necessary to solubilize the formazan crystal through pure DMSO. Data are expressed as a percentage change in absorbance units compared to untreated cells.

At the end of the treatments, MeOV-1 cells were incubated with 100µl of 10% MTT stock solution (5mg/ml) in serum free medium without phenol red for 3h. 50µl of pure DMSO were added to each well and the plate was gently shaken for 20 min to ensure complete lysis of the cells and solubilization of the crystal of formazan. Absorbance (560nm) was measured using a microplate reader spectrophotometer (CLARIOstar, BMG Labtech, UK and Biorad iMark™ microplate reader, software: microplate Manager 6).

3.4 Proliferation assay

To measure the proliferation rate of cells cultured in different oxygen tensions, MeOV-1 cells were seeded in 24-well plates in triplicate at a density of 50000 cells/well. Cells were counted over the following five days using a haemocytometer.

A parallel analysis of protein content was also performed. Cells were lysed using 0,5M NaOH and stored at -20°C. Protein content was determined using the BCA assay as described in Section 3.6.1.

3.5 RT-PCR

Total RNA was extracted using TRIzol reagent (Invitrogen, U.S.A.), a guanidine-isothiocyanate/phenol solution that allows isolation of RNA or using RNeasy® Mini Kit (Qiagen, Germany).

3.5.1 *RNA extraction*

Total RNA extraction by TRIzol reagent

At the end of the treatments, melanoma cells were washed with warm PBS and TRIzol solution was added to each sample. Samples were incubated for 5 min at room temperature to enable the complete association of nucleoprotein complexes. Chloroform was added to each tube, and after a centrifugation at 12000g for 15 min at 4°C. Three phases were formed:

1) aqueous phase, containing RNA;
2) intermediate phase, containing DNA and
3) organic phase, containing proteins.

For the isolation of the RNA, the aqueous phase was transferred into a new tube with an equal volume of isopropanol. Samples were incubated for 10 min at room temperature and centrifuged at 12000g for 10 min at 4°C in order to enable RNA precipitation. After removing the supernatant, the pellet was washed with 70% ethanol, dried and resuspended in DEPC water.

Total RNA extraction by RNeasy Mini Kit

Total RNA was also extracted using a RNeasy® Mini Kit. Cells were washed with 1ml warm PBS and lysed using lysis buffer with 1:100 β-mercaptoethanol (β-ME) which contains guanidine salt, and RNAase inhibitor. An equal volume of ethanol 70% in RNase free water was added to samples and the lysates were transferred into a RNeasy Mini spin column placed in a 2ml collection tube and centrifuged at 8000g for 15 sec at room temperature. After discarding the flow-through, wash buffer was added to the column and centrifuged at 8000g for 15 sec at room temperature. Following, the RNA was washed twice with wash buffer plus ethanol. Finally, RNase-free water was added directly on top of the membrane and after centrifugation at 8000g for 1 min at 4°C, RNA was eluted.

3.5.2 *Quantification of the extracted RNA*

RNA concentration and purity were measured by NanoDrop DN-100 spectrophotometer (NanoDrop Technologies, USA) immediately after the RNA elution. 2µl per sample were used for the measurement. The purity of the RNA was assessed by the ratio of absorbance 260/280 (an indicator of DNA contaminations, between 1.8-2.0) and 260/230 (an indicator of other contaminators, for example salts, between 1.8-2.2).

3.5.3 *Reverse transcriptase reaction (RT)*

To compare mRNA expression in different samples, complementary DNA (cDNA) was reverse transcribed using SuperScriptTM II Reverse Transcriptase (Life Technologies, U.S.A.). Reverse transcriptase reaction (RT) enables the conversion of RNA into cDNA and subsequent amplification of the gene segment of interest via polymerase chain reaction (PCR).
The following protocol was used:

- 500 ng of extracted RNA;
- 10mM deoxyribonucleotides triphosphates (dNTPs);
- 100ng random hexameric primes, oligonucleotide sequences of 6 nitrogen bases that randomly bind the RNA molecules
- Firts ST 5x, a magnesium buffer solution
- SuperScriptTM II Reverse Transcriptase (Life Technologies, U.S.A.)

Reaction was performed using Mastercycler nexux (Eppendorf, UK) and the following program: 10 min at 25°C, 50 min at 42°C, 10 min at 72°C and maintaining at 4°C. cDNA was stored at -80°C to prevent degradation and used for the polymerase chain reaction (PCR).

3.5.4 *PCR*

This reaction allows the amplification of a target gene sequence by using suitable primers (see appendix 14) and Taq polymerase enzyme, a DNA polymerase that works at high temperature. PCR consists of the cyclical repetition of three phases, denaturation, annealing and elongation, through different temperatures. Briefly, in the denaturation phase, the DNA double helix was melted into separate strands (Ramesh et al., 1992). Subsequently, in the annealing phase, the reaction reached the appropriate temperature to allow the primers to bind the target cDNA sequences (64-68°C). Finally, at the temperature of 72°C, Taq polymerase enzyme generates the complementary sequences. These phases were repeated in cycles from 20 to 30 times per assay.

PCR products were separated by electrophoresis using a 2% agarose gel with ethidium bromide, to allow DNA to emit fluorescence after UV exposure. The expression of target genes was compared to the housekeeping gene 18S ribosomal RNA. For densitometric analysis, the GelDoc (BIO-RAD, Italy) was used.

3.6 Immunoblotting

3.6.1 *Protein extraction and quantification*

At the end of treatments, cells were washed with PBS and lysed in SDS buffer or Ripa Buffer (see appendix 14 and 15) with incubation for 5 min in ice. Cells lysates were mechanically collected in new tubes. Each sample was sonicated in ice 4 times for 10 sec with a 10 sec pause between each cycle to further break cell membranes and release the proteins.

To determine protein concentration of total cell lysates, bicinchoninic acid assay (Pierce™ BCA Protein Assay) was used. The method is based on the biuret reaction which allows, in an alkaline environment, the $–NH_2$ groups of proteins to react with Cu^{2+} generating a purple colour with strong absorbance at 562 nm (Mallia et al., 1985).

A standard curve was constructed in duplicate with bovine serum albumin (BSA). Standard curve and samples were incubated with BCA reagents composed of reagent A and reagent B diluted 1:50 at 37°C for 20 min. Absorbance was measuring at 562nm using microplate readers (Tecan Sunrise microplates reader, by Lab Made, software: Magellan 6 and Biorad iMark™ microplate reader, software: microplate Manager 6).

3.6.2 *Samples preparation*

Samples, normalized according to protein content, were prepared to immunoblot by adding loading buffer containing 0.02% bromophenol blue and 1% 2-mercaptoethanol and boiled for 5 min in order to complete protein denaturation.

3.6.3 *Gel preparation and SDS-PAGE electrophoresis*

Sodium Dodecyl Sulphate – PolyAcrylamide Gel electrophoresis (SDS-PAGE) is based on two important features of the proteins (Laemmli, 1970): dimension and intrinsic charge of proteins. Due to the electric current, proteins can be separated through the gels.

Proteins were separated by using precast gels (SDS-poliacrylamide, BioRAD) or home-made acrylamide gels. Acrylamide and bisAcrylamide (Acr/bis) create a molecular sieve that allows to separate proteins through their molecular weight. In order to separate proteins with high molecular weight, low-percentage acrylamide gels are needed, whereas proteins with low molecular weight need high-percentage acrylamide gels.

Acr/bis gels are composed of two parts:

- resolving gel: to separate proteins according to the concentration of Acr/bis (usually 10-15%)
- stacking gel: to easy load the samples for the analysis (usually 4%).

Gels were made in Tris-SDS buffer (appendices 3 and 4), added with ammonium pyrosulphate (APS) and tetramethyl ethylenediamine (TEMED, Sigma, UK): APS is an oxidizing agent that is used with TEMED to catalyse gel polymerization. As reference, molecular weight indicators were run in each gel. When possible, precast gels were used (Bio-Rad, U.S.A.). Thus, samples loaded into gels were subjected to electrophoresis performed for 50 min at 200 volts for precast gels and for 1 h and 30 min at 100 volts for home-made gels.

3.6.4 *Blotting*

At the end of the electrophoresis, proteins were transferred using a semi-dry transfer system (20 volts, 120-180 min) or wet blotting system (100 volts, 50 min) on a polyvinylidene fluoride membrane (PVDF, GE Healthcare, DE), previously activated with 100% methanol for 1 min and equilibrated in transfer buffer (see appendix 8). To minimize the background staining due to non-specific membrane-binding of the antibodies, membranes were saturated with 5% low-fat dry milk in phosphate buffered saline with 0.1% TWEEN solution (Sigma , UK, PBST, see appendix 9) or tris-buffered saline with TWEEN solution (TBST, see Appendix 10), for 1h at room temperature.

Membranes were then incubated with primary antibodies targeted against proteins of interest (see appendix 11) overnight at 4°C. Subsequently, membranes were incubated with a species-specific secondary antibody conjugated with horseradish peroxidase (HPR) for 1h at room temperature, followed by 30min of washing with PBST or TBST. Membranes were then developed using enhanced chemiluminescence (ECL) like Luminata™ Classico Western HRP Substrate (Millipore, U.S.A., No.WBLUC0500), Luminata™ Crescendo Western HRP Substrate (Millipore, U.S.A. No.WBLUR0500) and ECL Plus (Pierce Thermo Fisher, UK). The expression of target proteins was determined relative to the expression of housekeeping protein β-actin. For analysis of immunoblotting data, a densitometric analysis was conducted using Image J (National Institute of Health) or Quantity One® (BioRad, USA).

3.7 Immunofluorescence

Immunofluorescence (IF) has been used to determine the localization of Nrf2. Melanoma cells were seeded on 8-well chamber slides at 150000 cells per well and subsequently treated as described in Section 3.1.1. At the end of treatments, cells were fixed and permeabilized with cold 100% methanol for 5 min on ice. After washing with PBS, cells were incubated with Nrf2 primary antibody (Santa Cruz, USA) at 4°C O/N. The next day, ALEXA fluor antibody 488 (Thermo Fisher, U.S.A.), the fluorophore-labelled secondary antibody, was added to the cells for 1h. After a PBS wash, cells were incubated with the nucleus dye To-Pro (Thermo Fisher, U.S.A.). After the last wash with PBS, the slide was mounted using Mowiol and the images were acquired using a 3-channel TCS SP2 laser-scanning confocal microscope (Leica Mycrosystem, Germany).

3.8 Tube formation assay

The tube formation assay (Speyer et al., 2014) is one of the most widely used *in vitro* methods that measures the ability of endothelial cell to form tubes. In our work, the tube formation assay was used for determining the angiogenic ability of conditioned media (CM) from melanoma cells by analysing endothelial cell tube formation.

Endothelial cells were grown to 80-90% confluence, trypsinized with trypsin-EDTA, centrifuged at 300g for 5 min, washed with warm sterile PBS. Endothelial cells were resuspended in conditioned media collected from melanoma cells and centrifuged at 600g for 5 min to remove floating cells.

Endothelial cells were seeded on an extracellular matrix (ECMs, Matrigel® Matrix, Corning, U.S.A.), a basement membrane-like material composed by laminin, collagen IV, heparan sulphate proteoglycans, entactin/nidogen and growth factors.

A schematic representation of the experimental protocol is shown in Fig. 3-3. The same protocol was used also for silencing HO-1. Photos were taken every 2h for a maximum of 10h to have an overview of the rate of tube formation. Selected photos were quantified using Wimasis Image Analysis Software.

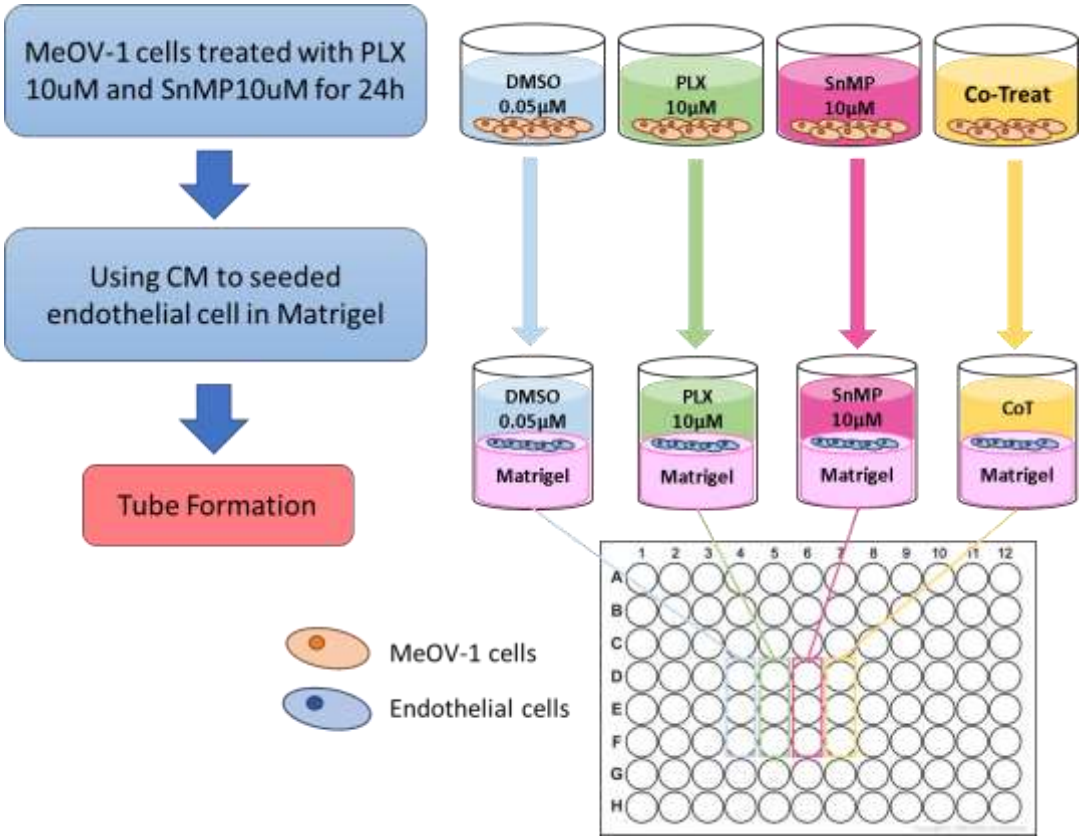

Figure 3-3: Schematic representation of tube formation experiment. MeOV-1 cells were treated with 10µM PLX4032 and 10µM SnMP-IX for 24h. At the end of treatment, medium derived from melanoma cells was transferred to endothelial cells seeded on Matrigel. Photos of growing tubes were taken every 2h using Leica IM500 software (Leica Image Manager); 5x magnification.

3.9 Statistical analysis

All data denote the mean ± S.E.M. of measurements in *n* different cultures, unless stated otherwise. Statistical analyses were performed using Prism software package (GraphPad Software, CA). One-way analysis of variance (ANOVA) and Dunnett's multiple comparison tests were applied when comparing more than three groups, with $p < 0.05$ considered significant.

4 RESULTS

4.1 HO-1 upregulation reduces PLX4032 efficacy and NK recognition

The first part of this work was conducted in collaboration with the Laboratory of Clinical Immunology at Ospedale Policlinico San Martino Genova (Professor Gabriella Pietra).
Primary tumor cell lines were isolated in-house from metastatic tissue samples by Prof. Pietra's group and characterized by STR profile at the local cell Biobank (Biobank and cell factory - Ospedale Policlinico San Martino Genova). $BRAF^{V600}$ mutation determinates constitutive activation of pERK pathway favouring cell growth and cancer progression. In this part of the work, two lines carrying a $BRAF^{V600E}$ mutation (MeOV-1 and MeMI), one line carrying on $BRAF^{V600D}$ mutation (MeTA) and one BRAF wild type (wt) commercial line (MeWO) were used to evaluate the involvement of HO-1 in limiting the efficacy of PLX4032 (a specific inhibitor of $BRAF^{V600}$) and in modifying the recognition and killing activity of NK cells.

4.1.1 *PLX4032 abolishes ERK phosphorylation and decreases viability of melanoma cells bearing BRAF^{V600} mutation*

Four melanoma cell lines were treated with PLX4032. To verify the specificity of PLX4032 treatment in inhibiting BRAF^{V600}, the protein level of ERK phosphorylation (pERK) was evaluated. After 24h of 1-10μM PLX4032 treatment, MeOV-1, MeTA and MeMI showed a reduction of pERK levels. Instead, the level of p-ERK was not modified by PLX4032 treatment in the MeWO BRAF wt. Moreover, as expected, the expression of total ERK was not modified in all cell lines (Fig. 4-1).

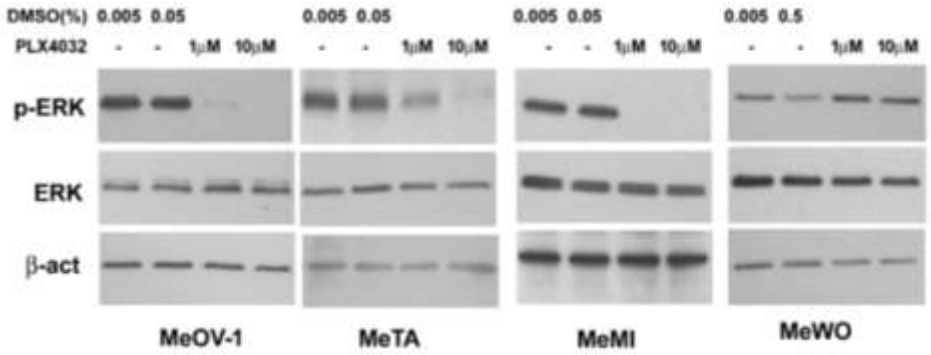

Figure 4-1: Immunoblot analysis of ERK phosphorylation. p-ERK and total ERK were evaluated in melanoma cell lines exposed to increasing concentrations of PLX4032 or DMSO alone. β-actin was used as a loading control. The blots are representative of 4 independent experiments for each cell line.

Moreover, a MTT assay revealed that cell viability was progressively reduced (25% and 45% in MeOV-1, 16% and 43% in MeTA, 25% and 44% in MeMI, at 1μM and 10μM PLX4032, respectively), when compared to cells exposed to DMSO alone. No changes were observed in MeWO cells (Fig. 4-2).

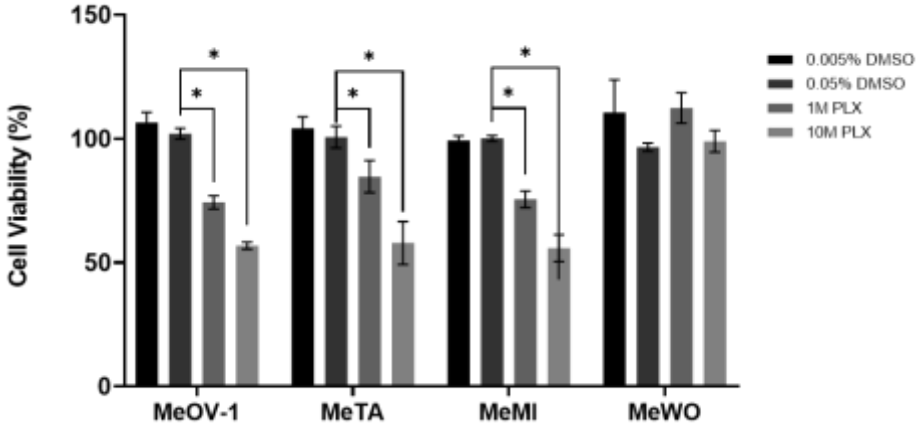

Figure 4-2: Cell viability assessed by MTT assay after 1-10μM PLX4032 treatments. The graphs are representative of 4 independent experiments for each cell line. Data denote mean ± S.E.M, *p < 0.05.

4.1.2 *HO-1 protein levels in melanoma cell lines increases after PLX4032 treatment*

Considering the role played by Nrf2/HO-1 in cancer cell resistance and progression (Furfaro et al., 2016), we started to analyse the modulation of HO-1 expression in our cell context. HO-1 expression was almost undetectable in untreated MeOV-1 and MeTA cells and induced by PLX4032. In MeMI cells, there was a basal expression of HO-1 which was increased by PLX4032 (+52% and +41% at 1μM and 10μM PLX4032 in comparison to DMSO alone). Importantly, neither basal expression nor induction of HO-1 was observed in BRAF wild type MeWO cells in response to PLX4032 treatment. However, MeWO cells were able to induce HO-1 when exposed to a standard HO-1 inducer, hemin (Fig. 4-3).

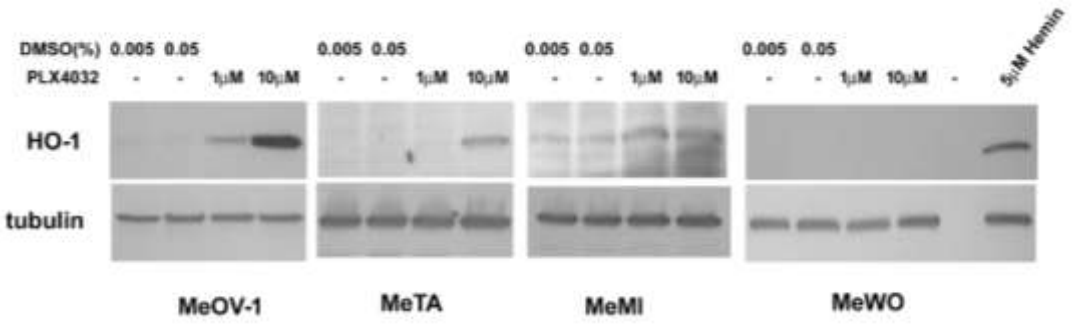

Figure 4-3: Immunoblot analysis of HO-1. HO-1 was analysed in melanoma cells exposed to increasing concentrations of PLX4032 or DMSO alone and β-tubulin used as a loading control. Hemin was used in MeWO cells as positive control of HO-1 induction. The blots are representative of 4 independent experiments for each cell line.

4.1.3 *HO-1 silencing enhances the efficacy of PLX4032 and further reduces cell viability*

Considering the role played by HO-1 induction as key factor in limiting the efficacy of tumor therapies (Cheng et al., 2016; Furfaro et al., 2016; Ma et al., 2015), the effect of HO-1 silencing was evaluated in MeOV-1, MeTA and MeMI cells exposed to PLX4032. The MTT assay showed that in PLX-treated melanoma cell lines and silenced for HO-1 shows a further decreased the number of viable cells in comparison to cells exposed to PLX4032 alone (Fig. 4-4 section A). Under the same experimental conditions, HO-1 silencing efficiently prevented the upregulation of HO-1 induced by 10μM PLX4032 in MeOV-1 and MeTA and by 1μM PLX4032 in MeMI, as shown by protein (Fig. 4-4 section B) and mRNA (Fig. 4-4 section C) analysis.

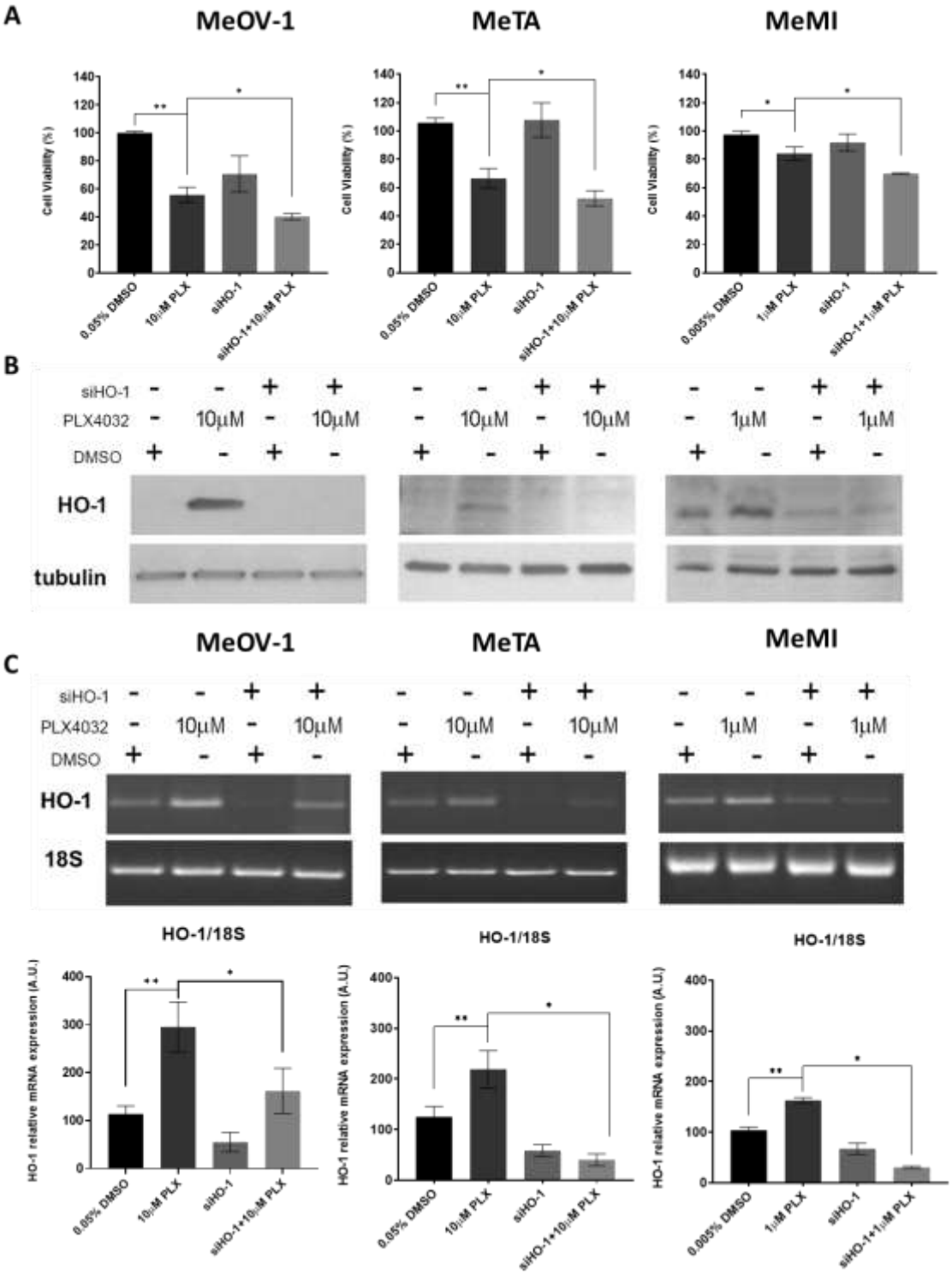

Figure 4-4: Evaluation of cell viability after HO-1 gene silencing. (**A**) MTT assay was used to evaluate cell viability after HO-1 silencing and 24h 1-10μM PLX4032 treatment. The graphs are representative of 4 independent experiments for each cell line. Data denote mean ±S.E.M., *$p < 0.05$; **$p < 0.01$.

Figure 4-4: Evaluation of cell viability after HO-1 gene silencing - continue. (**B**) HO-1 protein levels were detected by immunoblot analysis. β-tubulin expression was used to normalize the results. The blots are representative of 4 independent experiments for each cell line. (**C**) HO-1 mRNA expression was analysed by RT-PCR. 18S mRNA level was used as housekeeping gene. The bands are representative of 3 independent experiments for each cell line. Mean ± S.E.M), *p < 0.05; **p < 0.01.

4.1.4 *Melanoma viability is further reduced by co-treating cells with HO-1 inhibitor and PLX4032*

MeOV-1 and MeMI cell lines co-treated with 1-10μM PLX4032 and 10μM SnMP-IX and MeTA cell line co-treated with 10μM PLX4032 and 10μM SnMP-IX, a specific enzymatic inhibitor of HO-1 activity (Mancuso, 2017; Schwartz et al., 2011), showed a significant reduction in viability compared to cells treated with PLX4032 alone (Fig. 4-5).

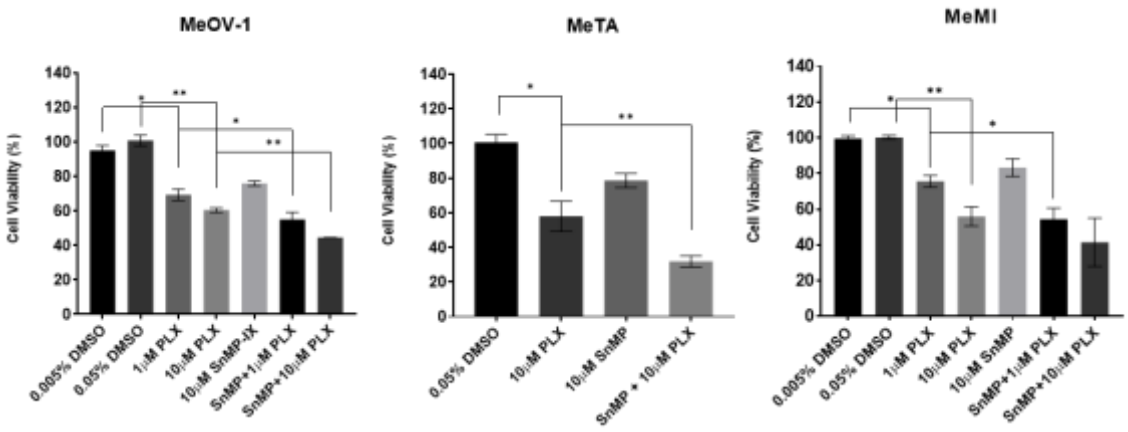

Figure 4-5: Cell viability after 1-10μM PLX4032 and 10μM SnMP-IX treatment. Cell viability was assessed using a MTT assay following co-treatment of cells with 1-10μM PLX4032 and 10μM SnMP-IX in MeOV-1 and MeMI and with 10μM PLX4032 and 10μM SnMP-IX in MeTA cell line for 24h. The graphs are representative of 3 independent experiments for each cell line. Mean ± S.E.M., *p< 0.05; **p< 0.01.

4.1.5 *PLX4032 treatment of MeOV-1 reduces the expression of B7H6 and ULBP3, ligands for NK cells; their expression were restored by HO-1 silencing*

In order to define how the $BRAF^{V600}$ inhibitor treatment interferes with the MeOV-1 phenotype and susceptibility to NK cells, the expression of B7H6 and ULBP3 in both untreated and 1-10μM PLX4032-treated MeOV-1 cells was investigated. The mRNA levels of B7H6 and ULBP3 in PLX-treated MeOV-1 of both B7H6 and ULBP3 showed a significant expression level reduction in MeOV-1 were significantly reduced. Importantly, in MeOV-1 silenced for HO-1 and treated with 1-10μM PLX4032, the expression of B7H6 and ULBP3 were completely restored highlighted the role of HO-1 in reducing the expression of NK activating ligands (Fig. 4-6).

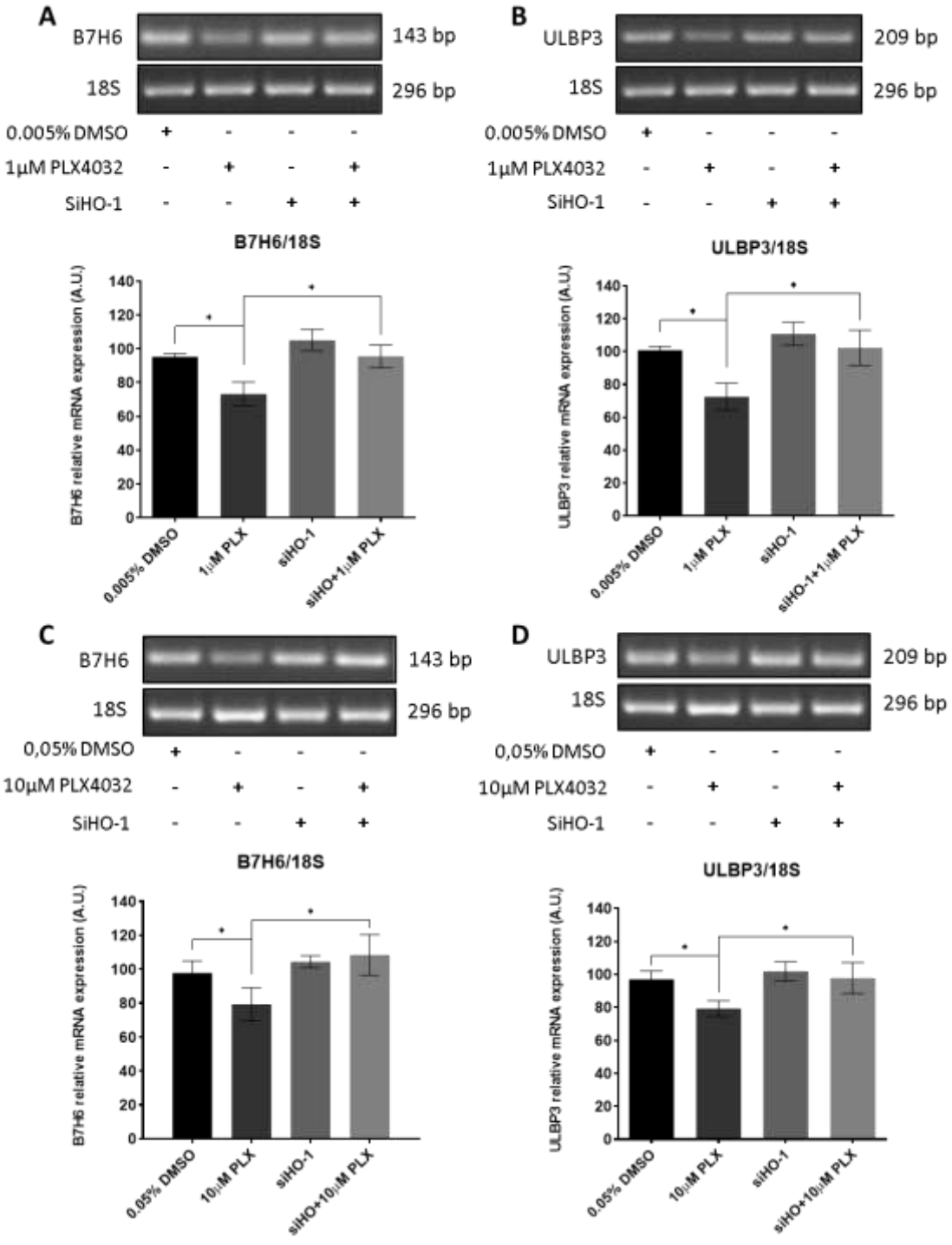

Figure 4-6: mRNA expression of B7H6 and ULBP3 in PLX4032-treated MeOV-1 cells and MeOV-1 cells silenced for HO-1. RT-PCR analysis of B7H6 (panels **A** and **C**) and ULBP3 (panels **B** and **D**) mRNA expression in MeOV-1 cells treated with 1μM (panels **A** and **B**) or 10μM (panels **C** and **D**) PLX4032. Graphs are representative of 4-5 independent experiments. Mean ± S.E.M., *$p < 0.05$; (**A**) n=5; (**B**) n=5; (**C**) n=5; (**D**) n=4.

4.1.6 *PLX4032/SnMP-IX co-treatment restores the expression of B7H6 and ULBP3*

The inhibition of the enzymatic activity of HO-1 increased cell susceptibility to NK cells by restoring the expression of ligands for NKp30 and NKG2D activating NK receptors. Indeed, the combination of 1-10µM PLX4032 and 10µM SnMP-IX restored the expression of B7H6 and ULBP3 in the MeOV-1 melanoma cell line (Fig. 4-7).

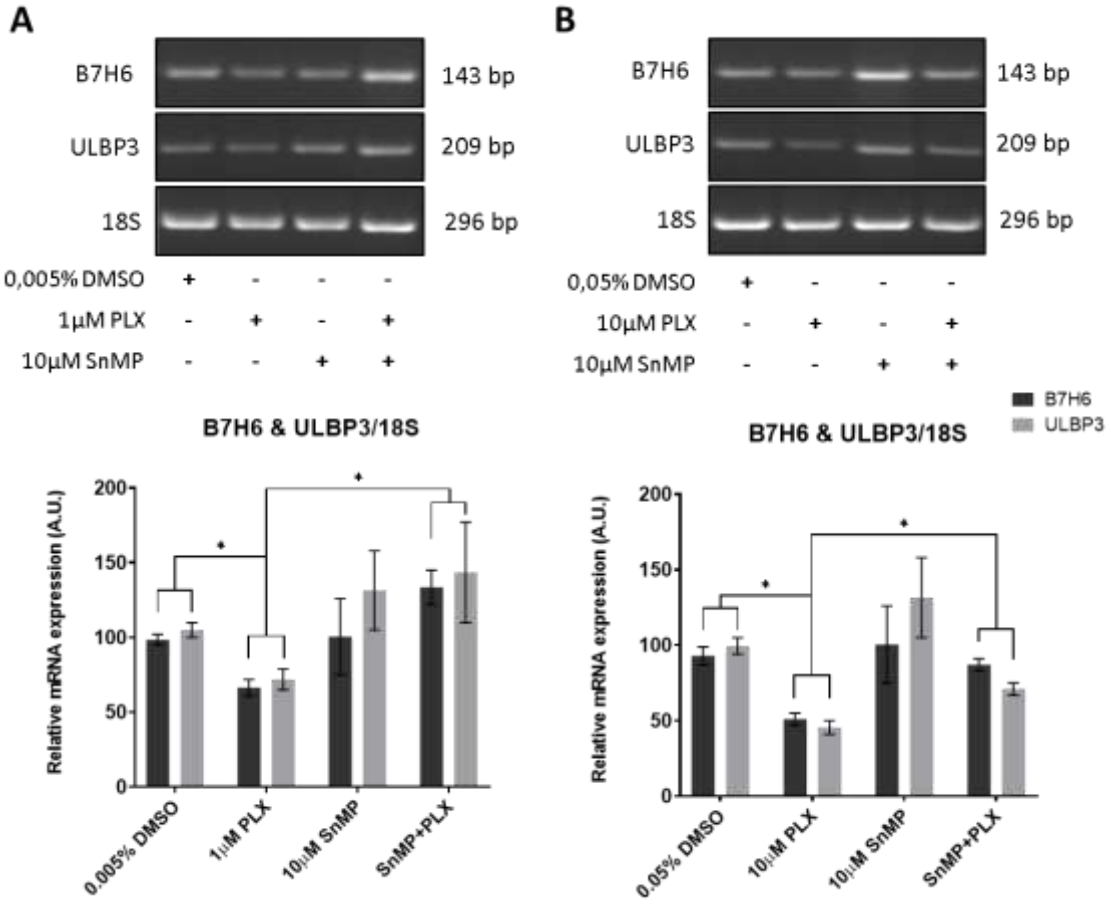

Figure 4-7: mRNA expression of B7H6 and ULBP3 on MeOV-1 co-treated with PLX4032 and SnMP-IX. B7H6 and ULBP3 mRNA expression was assessed by RT-PCR in MeOV-1 cells co-treated with 10µM SnMP-IX and 1µM (**A**) or 10µM PLX4032 (**B**) for 24h. 18S mRNA was used as housekeeping gene. The bands show a representative experiment. Graphs are representative of 4 independent experiments for each cell lines. Mean ± S.E.M., *p < 0.05.

Results shown in section 4.1 are part of a paper published in 2020 which also includes the analysis of the NK phenotype and killing activity in response to $BRAF^{V600}$ melanoma cells exposed to PLX4032 and also treated with SnMP-IX or silenced for HO-1 (Furfaro et al., 2020).

4.2 HO-1 induction in PLX4032-treated cells is dependent on Nrf2 activation and Bach1 downregulation.

From the previous results, we identified an important role for HO-1 induction in reducing efficacy of PLX4032 treatment and limiting NK cell recognition in different BRAF mutated melanoma primary cells. Here, we have further investigated the underlying molecular pathway involved in HO-1 induction following PLX4032 exposure in $BRAF^{V600E}$ MeOV-1 cells.

4.2.1 *24h PLX4032 treatment does not modulate other Nrf2-dependent genes*

In order to define whether Nrf2 is involved in HO-1 upregulation, other Nrf2-dependent genes were evaluated on MeOV-1 cells exposed to 10μM PLX4032 for 24h. As shown in Fig. 4-8 section A, mRNA expression of GCLM, GCLC and NQO1 genes was not modified in the experimental condition tested. Moreover, immunofluorescence analysis of Nrf2 established that Nrf2 was mainly localized in the cytosol in comparison to the nucleus after 24h PLX4032 treatment (Fig. 4-8, section B).

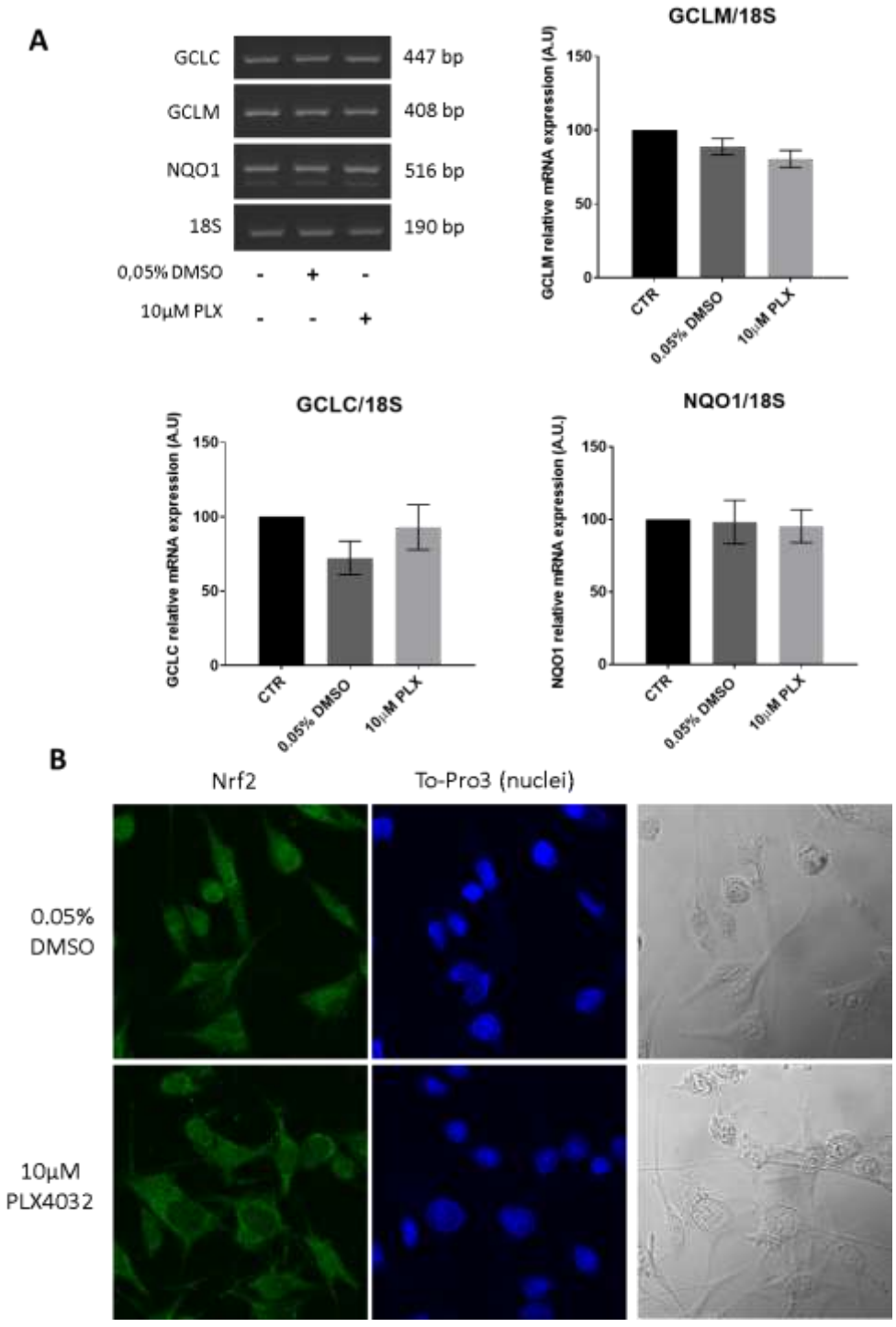

Figure 4-8: Nrf2-dependent gene analysis and Nrf2 subcellular localisation in MeOV-1 exposed to PLX4032. (**A**) GCLM, GCLC and NQO1 mRNA expression was assessed by RT-PCR in MeOV-1 cells treated with 10μM PLX4032 for 24h. 18S mRNA was used as the housekeeping gene. The bands are representative of 4 independent experiments. Mean ± S.E.M. (**B**) Immunofluorescence for Nrf2 of MeOV-1 cells treated with 10μM PLX4032 for 24 h. To-Pro3 was used for staining nuclei. Images are representative of 2 independent experiments. Photo were taken using a 3-channel TCS SP2 laser-scanning confocal microscope (Leica Mycrosystem, Germany). Scale bar 20μm.

4.2.2 *Short time PLX4032 treatments highlight a Nrf2 translocation into the nucleus*

Since Nrf2 is involved in early cell responses to oxidative stress, Nrf2 localization was also monitored after short-time (from 30 min to 3h) PLX4032 treatment. In this experimental condition, immunofluorescence clearly showed Nrf2 translocation into the nucleus (Fig. 4-9).

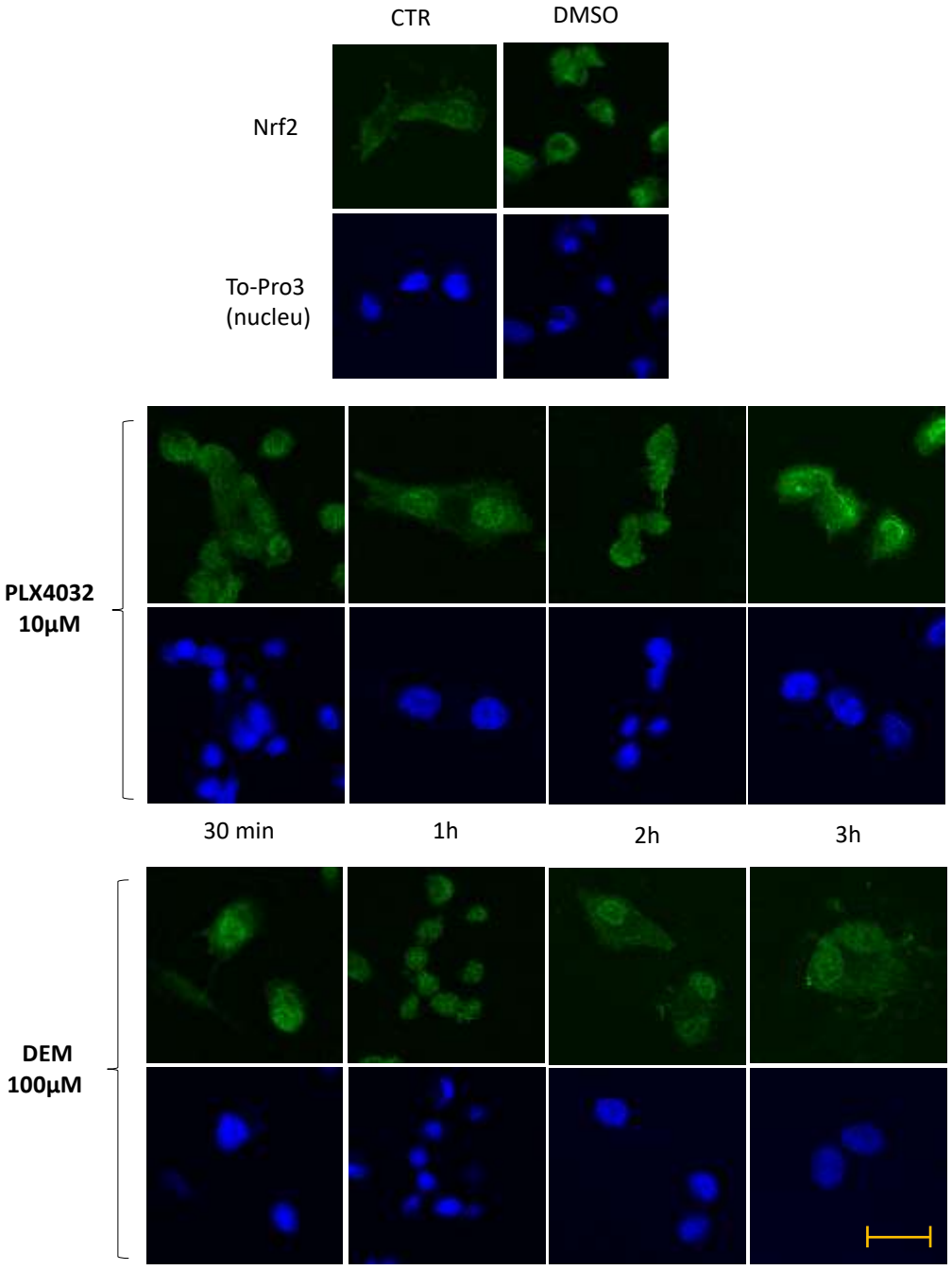

Figure 4-9: Nrf2 subcellular localization after short-time PLX4032 treatment. Immunofluorescence assay for Nrf2 of MeOV-1 cells treated with 10µM PLX4032 for 30 min, 1-, 2- and 3h. Positive control was performed by treating cells with 100µM diethylmaleate (DEM), a Nrf2 inducer. To-Pro3 was used for staining nuclei. The images are representative of 2 independent experiments. Photos were taken using a 3-channel TCS SP2 laser-scanning confocal microscope (Leica Mycrosystem, Germany). Scale bar 10µm.

4.2.3 *HO-1 is up-regulated after 3 and 6 hours of PLX4032 treatment*

Considering the short-term activation of Nrf2 in response to PLX4032 exposure, mRNA expression levels of Nrf2-dependent genes were then analysed at shorter experimental time points. As shown in Fig. 4-10, 10μM PLX4032 treatment induced HO-1 expression starting from 6h, albeit non-significantly but with a clear trend. Interestingly, in the same experimental condition PLX4032 treatment did not change NQO1, GCLC and GCLM expression levels. Interestingly, the Nrf2 inducer DEM was able to increase only the expression of HO-1, whist NQO1, GCLC and GCLM were not affected.

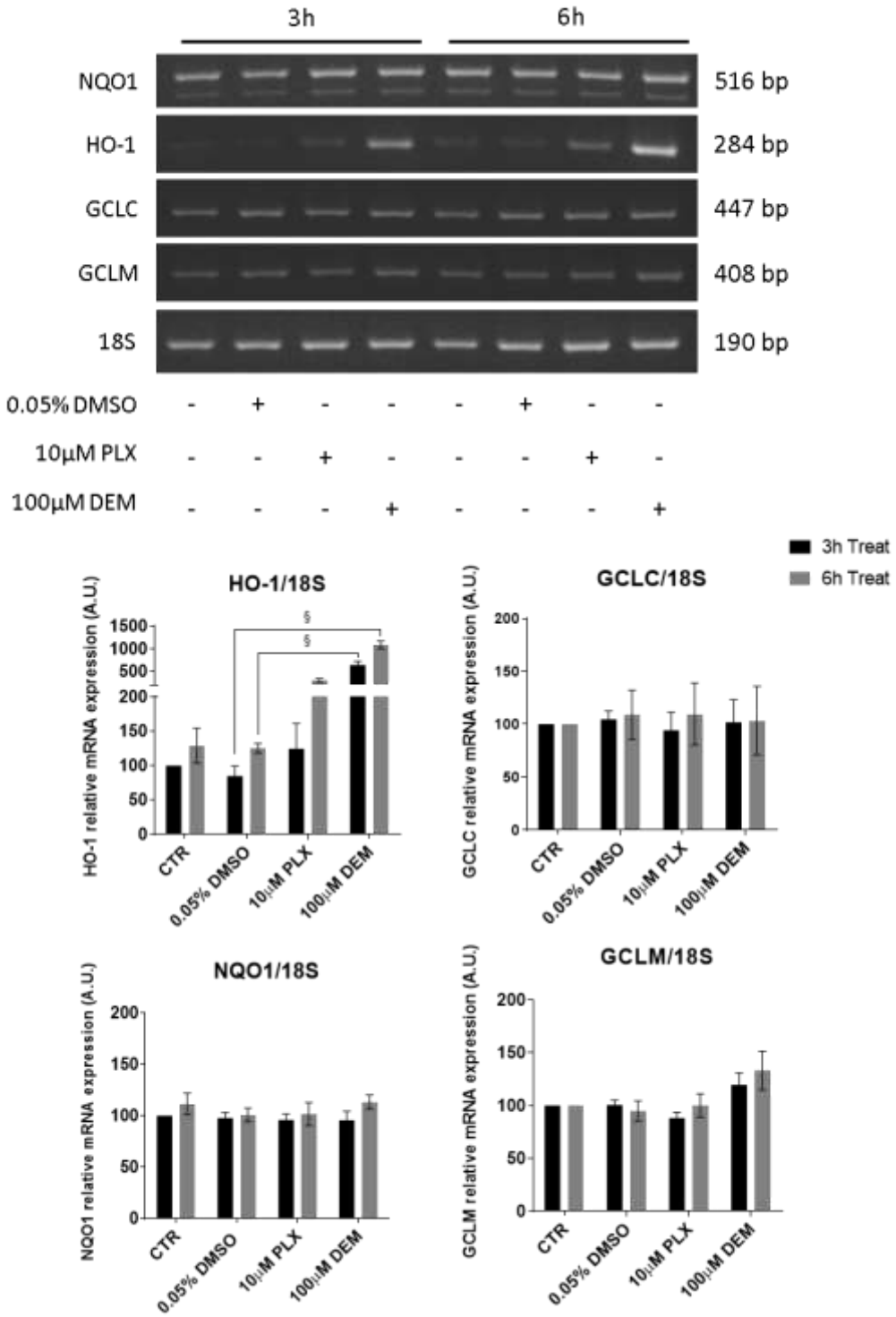

Figure 4-10: Upregulation of Nrf2-dependent genes. HO-1, GCLC, NQO1 and GCLM mRNA expression was assessed by RT-PCR in MeOV-1 cells treated with 10μM PLX4032 for 3h and 6h. Diethylmaleate (100μM DEM), a Nrf2 inducer, was used as a positive control. 18S mRNA was used as a housekeeping gene. The bands are representative of 3 independent experiments. Mean ± S.E.M., §p<0.0001.

4.2.4 *Bach1 expression is downregulated after PLX4032 treatment*

Considering that Bach1 is the negative competitor of Nrf2 binding to the ARE sequence and is specifically related to the induction of HO-1 (Dhakshinamoorthy et al., 2005), the expression level of Bach1 after PLX4032 treatment was evaluated. Fig. 4-11 shows that Bach1 protein levels decreased significantly after 24h PLX4032 treatment (***p<0.005) but a trend of reduction could be observed also at shorter time points.

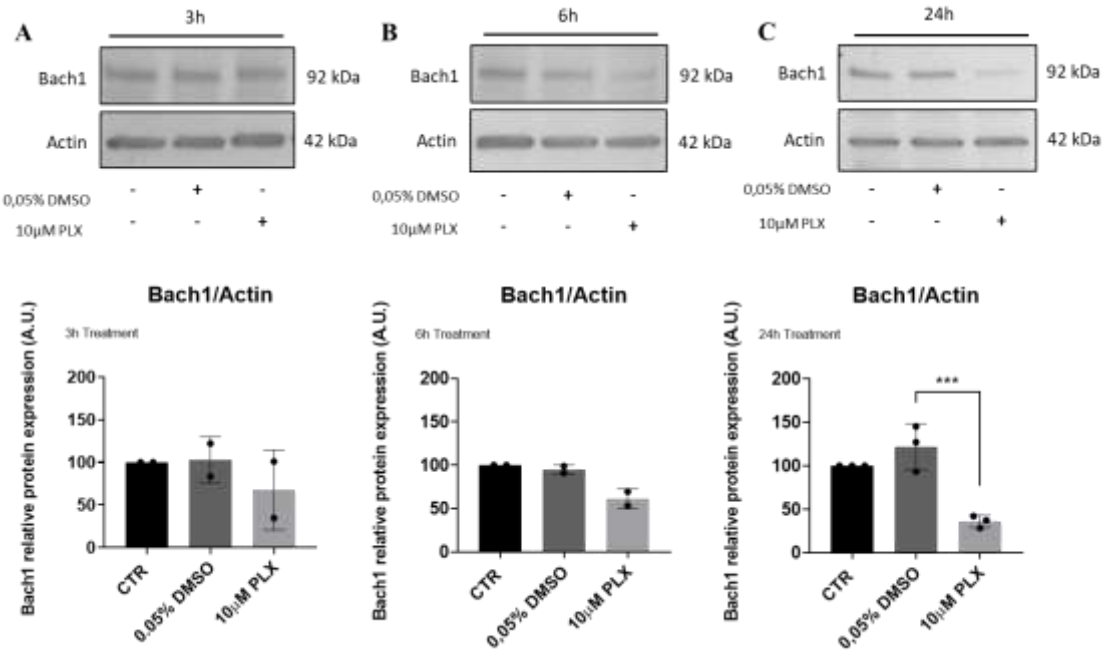

Figure 4-11: Immunoblot of Bach1 after treatment with 10μM PLX4032. (**A-B**) Protein levels of Bach1 were evaluated by immunoblotting whole cell lysates from MeOV-1 cells treated with 10μM PLX4032 for 3-6h. β-actin was used to normalize the results. The blots are representative of 2 independent experiments. (**C**) Protein levels of Bach1 were evaluated by immunoblotting whole cell lysates from MeOV-1 cells treated with 10μM PLX4032 for 24h. β-actin was used to normalize the results. The blots are representative of 3 independent experiments. Mean ± S.E.M., ***p<0.005.

4.2.5 *Nrf2 silencing decreases HO-1 expression in MeOV-1 treated with PLX4032*

Finally, to prove an involvement of Nrf2 in HO-1 induction following PLX4032 exposure, Nrf2 silencing was performed. As shown in Fig. 4-12, Nrf2 silencing prevented the overexpression (both mRNA and protein) of HO-1 due to 10µM PLX4032 treatment in MeOV-1 cells.

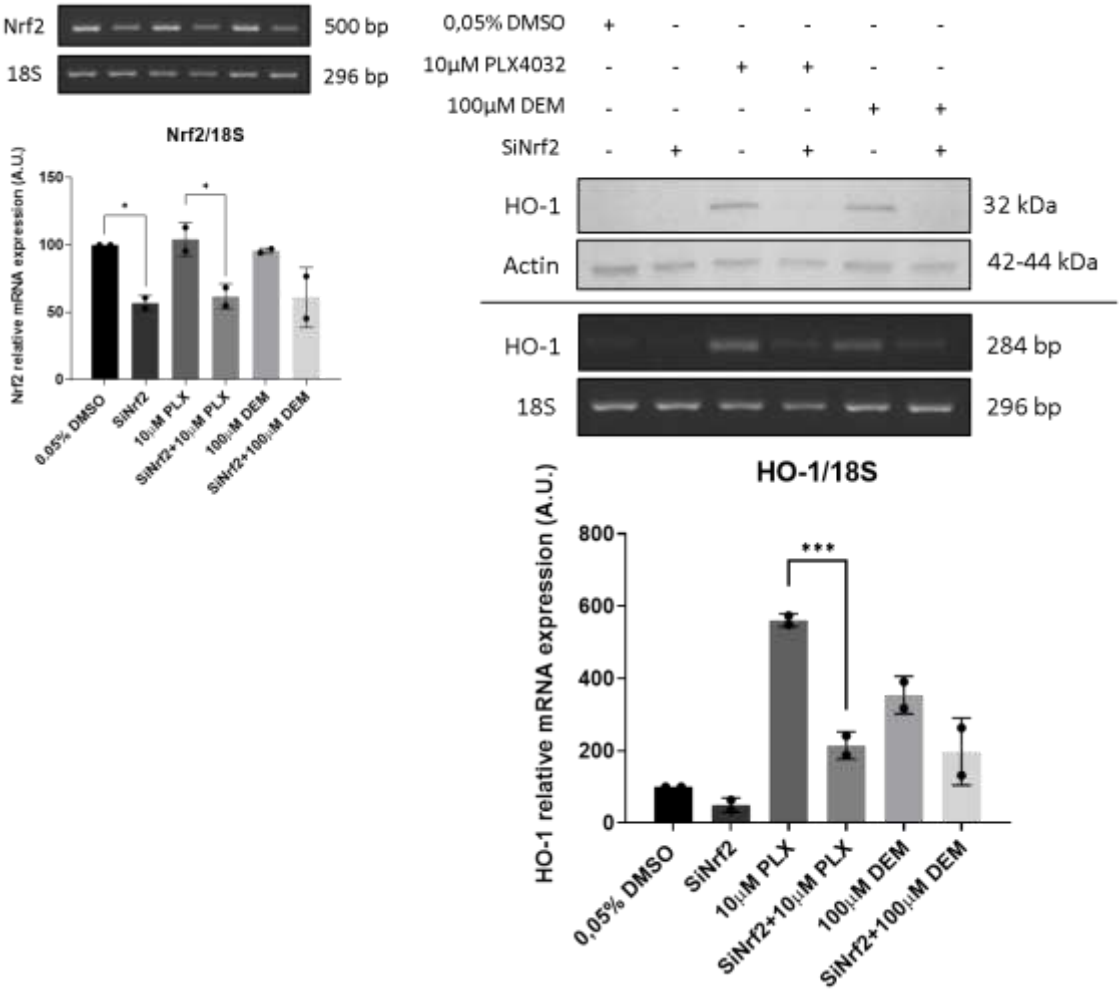

Figure 4-12: Expression levels and immunoblot of HO-1 after Nrf2 silencing. Nrf2 silencing was performed for 24h before 10µM PLX4032 or 100µM Diethylmaleate (DEM) treatments. mRNA level of Nrf2 was evaluated to confirm the efficacy of gene silencing. HO-1 mRNA and protein expression were assessed by immunoblotting and by RT-PCR, and DEM was used as a positive control. 18S mRNA was used as housekeeping gene. Blots are representative of 2 independent experiments. Mean ± S.E.M., *p<0.05. ***p<0.005.

4.3 Lowering oxygen tension does not modify MeOV-1 cell response to PLX4032

As reviewed in Section 1.4, the oxygen tension in cell cultures is an important parameter to be taken into consideration especially when oxygen-sensitive molecular pathways are evaluated, including cellular antioxidant responses. In order to analyse whether reduction of oxygen tension in cell cultures can modify melanoma response to PLX4032, MeOV-1 cells were cultured under normoxia (5kPa O_2). Moreover, in order to evaluate the role played by hypoxia in the activation of HO-1, some experiments were conducted in cells cultured under 1kPa O_2. This part of the work was carried out in Prof. Mann's laboratory at King's College London where a Physiological Oxygen Facility with hoods with adjustable oxygen tension are available. Moreover, in order to evaluate the involvement of HO-1 in melanoma angiogenetic ability, medium collected from all the experimental conditions were used for tube formation assays on endothelial cells.

4.3.1 *MeOV-1 cells adapted to 1kPa O_2 appear more elongated in comparison to MeOV-1 cells cultured under 18kPa O_2 and 5kPa O_2*

MeOV-1 cells cultured for 5 days under 18kPa O_2 or 5kPa O_2 look very similar. However, after 5 days adaptation to 1kPa O_2, cells appear elongated and less dense in comparison to MeOV-1 cells cultured under 18kPa and 5kPa oxygen levels (Fig. 4-13)

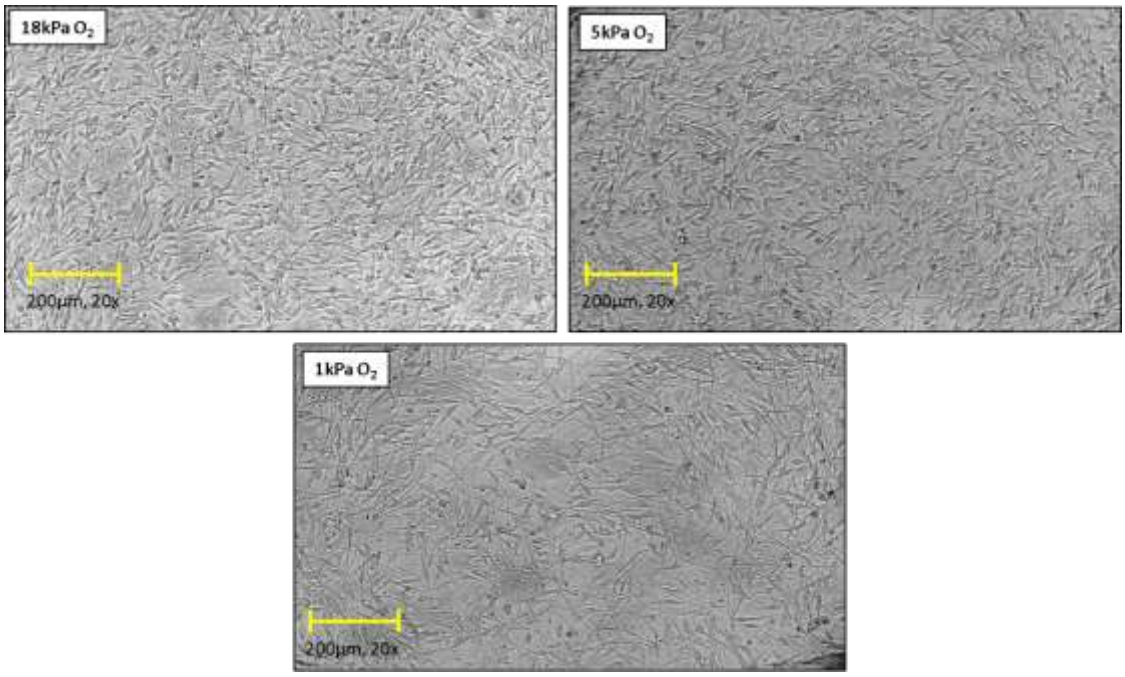

Figure 4-13: Melanoma cells morphology after 5 days of adaptation to different O2 levels. MeOV-1 cell were maintained in different oxygen conditions as indicated. Photos were taken using LumaView software; scale bar 200µm, 20x magnification.

4.3.2 *MeOV-1 growth rate under physiological normoxia and hypoxia is lower than under standard hyperoxic culture conditions*

The MeOV-1 cell line has never been cultured under different oxygen tensions. For this reason, MeOV-1 proliferation was measured to evaluate the impact of oxygen on cell growth. Fig. 4-14 shows that MeOV-1 cells adapted for 5 days to 5kPa and 1kPa O_2 exhibited a similar trend in growth rate. Whereas, MeOV-1 cell line adapted for 5 days under standard hyperoxic culture conditions (18kPa O_2) showed a higher growth rate in comparison to melanoma cells adapted to either 5kPa or 1kPa O_2 levels. These results were confirmed by measuring cell protein content.

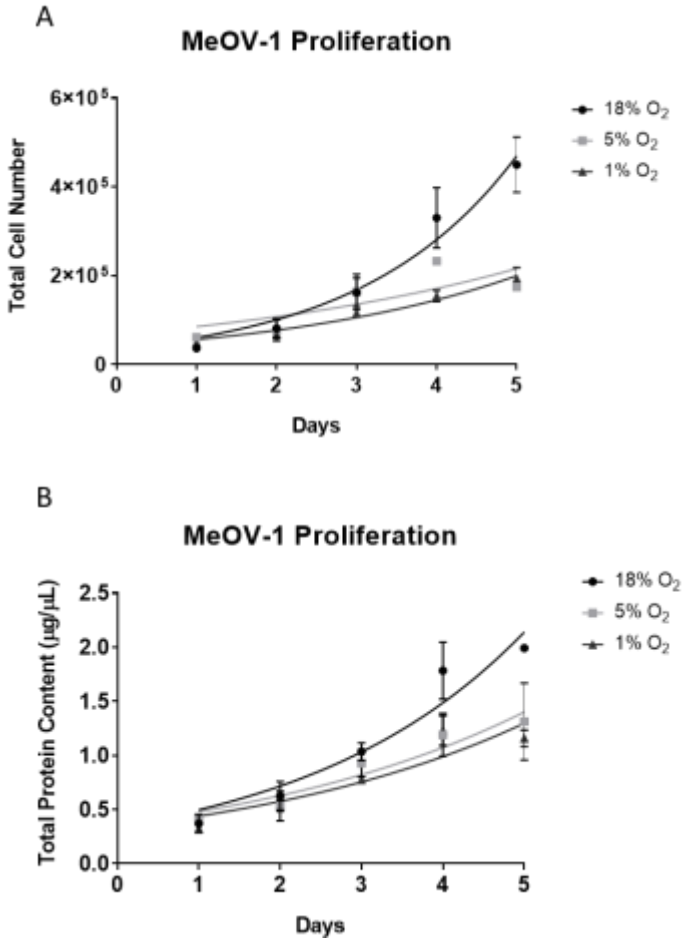

Figure 4-14: MeOV-1 proliferation and protein content after 5 days of adaptation to different O_2 levels. (**A**) Proliferation rates is determined by cell counting in cells cultured under different oxygen tensions. (**B**) Total protein content was analysed in the same cultures in which cell proliferation was determined by cell counting. The graphs are representative of 2 independent experiments, with data denoting mean ± S.E.M.

4.3.3 *Different oxygen tensions do not affects the ability of PLX4032 treatment to inhibit ERK phosphorylation*

The efficacy of PLX4032 treatment was examined in MeOV-1 cells adapted to the different oxygen tensions. MeOV-1 exposure to PLX4032 for 24h abolished ERK phosphorylation in cells adapted to 5kPa O_2 or 1kPa O_2 (Fig. 4-15).

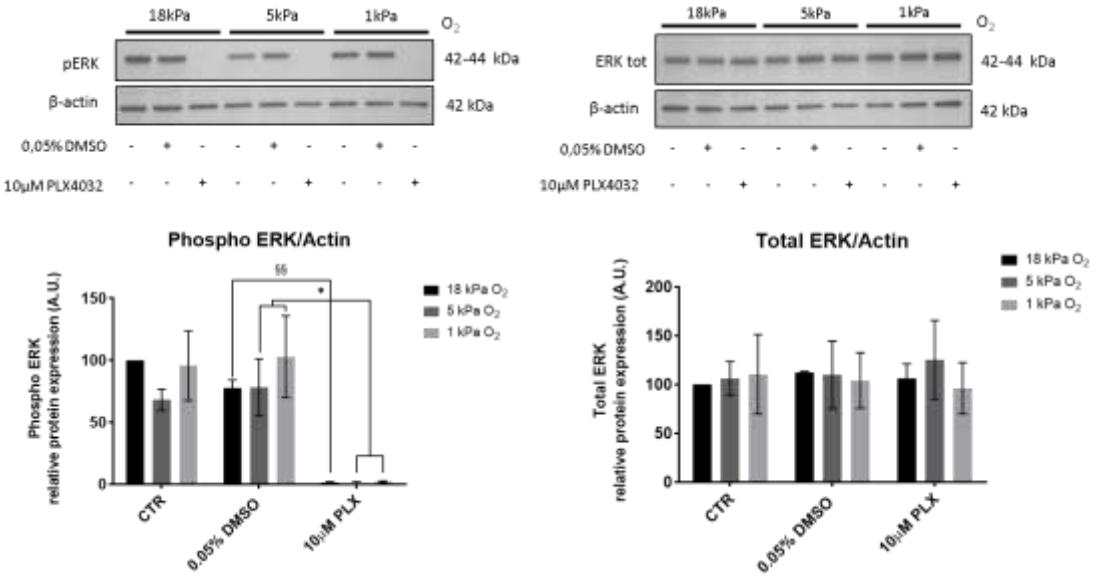

Figure 4-15: Immunoblot analysis of ERK phosphorylation. p-ERK and total ERK were evaluated in MeOV-1 cells cultured at 18kPa or adapted to 5kPa and 1kPa O_2 and then treated with 10μM PLX4032 (or DMSO) for 24h. β-actin was used as a loading control. The blots are representative of 3 independent experiments. Mean ± S.E.M., *p<0.05, §§p<0.0001.

4.3.4 *HO-1 is upregulated by PLX4032 in cells cultured in all oxygen tensions*

HO-1 protein and mRNA levels were evaluated after 24h PLX4032 treatment (10µM). Even though with a less extent compare to cells cultured at 18kPa O_2, HO-1 protein was induced by PLX4032 in cells cultured at 5kPa and 1kPa O_2.

Consistently, PLX4032-dependent mRNA HO-1 induction were observed in all experimental conditions tested (Fig. 4-16).

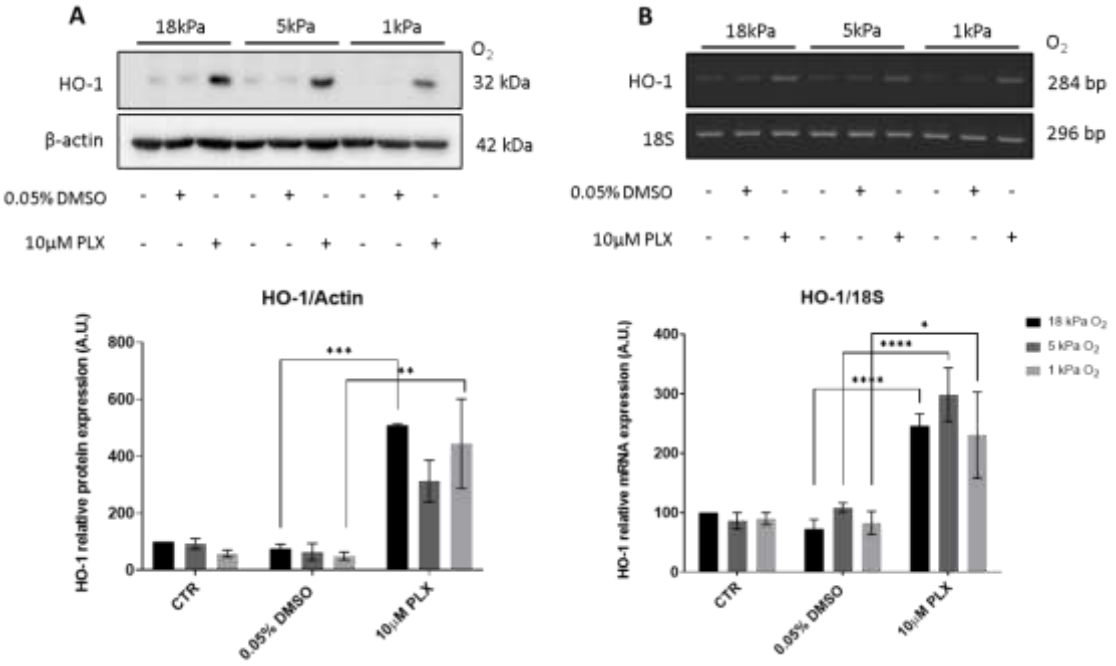

Figure 4-16: Analysis of the effects of adaptation to different ambient oxygen levels on HO-1 protein and mRNA expression. (A) HO-1 protein level was examined in MeOV-1 cells cultured under 18kPa or adapted to 5kPa and 1kPa O_2 and then treated with 10µM PLX4032 (or DMSO) for 24h. β-actin was used as a loading control. The blots are representative of 3-4 independent experiments. Mean ± S.E.M., **p<0.01, ***p<0.005. (**B**) In the same experimental condition, HO-1 mRNA expression was assessed by RT-PCR in MeOV-1 cells. 18S mRNA level was used as housekeeping gene. The bands are representative of 4 independent experiments. Mean ± S.E.M., *p<0.05, ****p<0.001.

4.3.5 *GCLC, GCLM and NQO1 genes are not affected by PLX4032 treatment in MeOV-1 cells regardless different oxygen tensions*

In Sections 4.2.1 and 4.2.3, we showed no changes in the expression of Nrf2-dependent genes GCLC, GCLM and NQO1 after 24h or even short-time PLX4032 treatment. Fig. 4-17 shows that also in MeOV-1 cells adapted to different oxygen tensions, changes in Nrf2-dependent genes were not observed after 10µM PLX4032 exposure at any oxygen tension considered.

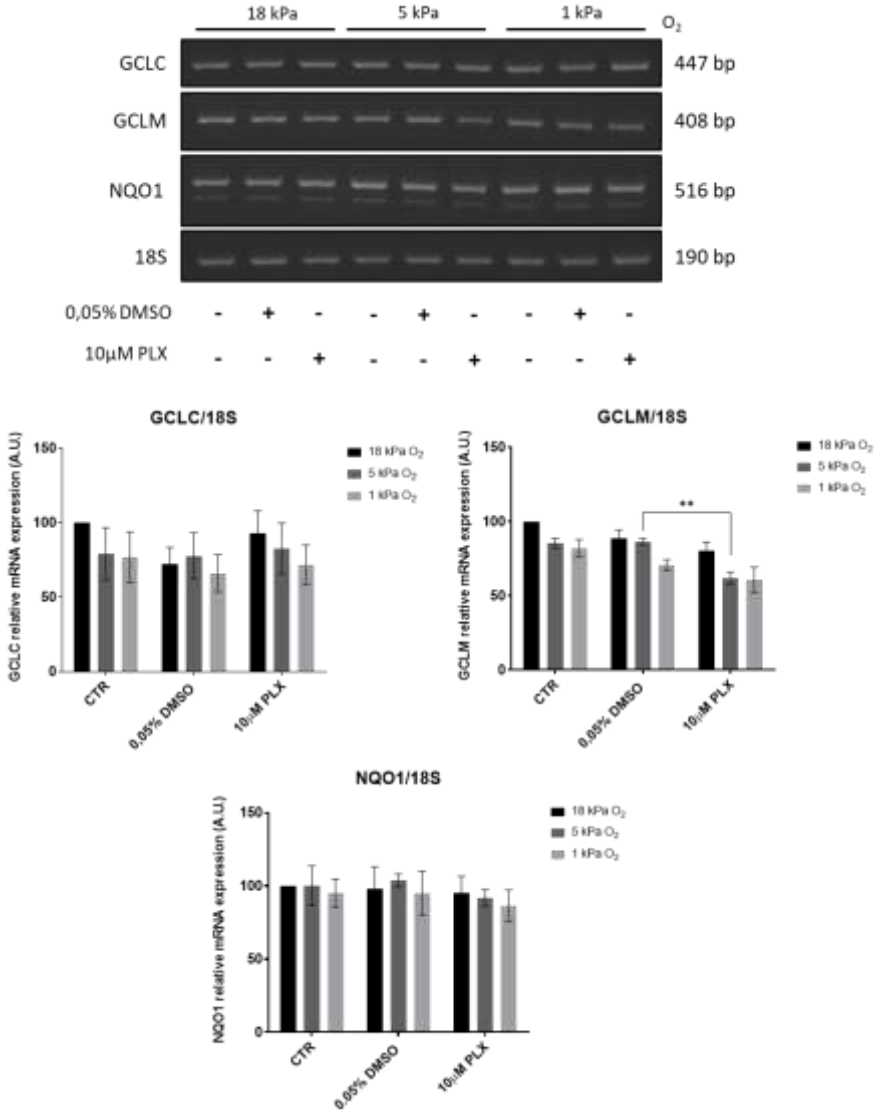

Figure 4-17: Evaluation of mRNA of Nrf2 downstream genes. GCLC, GCLM and NQO1 mRNA expression was assessed by RT-PCR in adapted MeOV-1 cells after 24h PLX4032 treatment (10µM). 18S mRNA level was used as housekeeping gene. The bands are representative of 4 independent experiments. Mean ± S.E.M, **p<0.01.

4.3.6 *Bach1 expression is downregulated after 24h PLX4032 treatment regardless of oxygen tension*

In section 4.2.4 we showed the reduction of Bach1 expression at different time points in MeOV-1 cells exposed to PLX4032. Fig. 4-18 shows that similar result was obtained also in cells adapted to 5kPa and 1kPa O_2 and exposed to PLX4032.

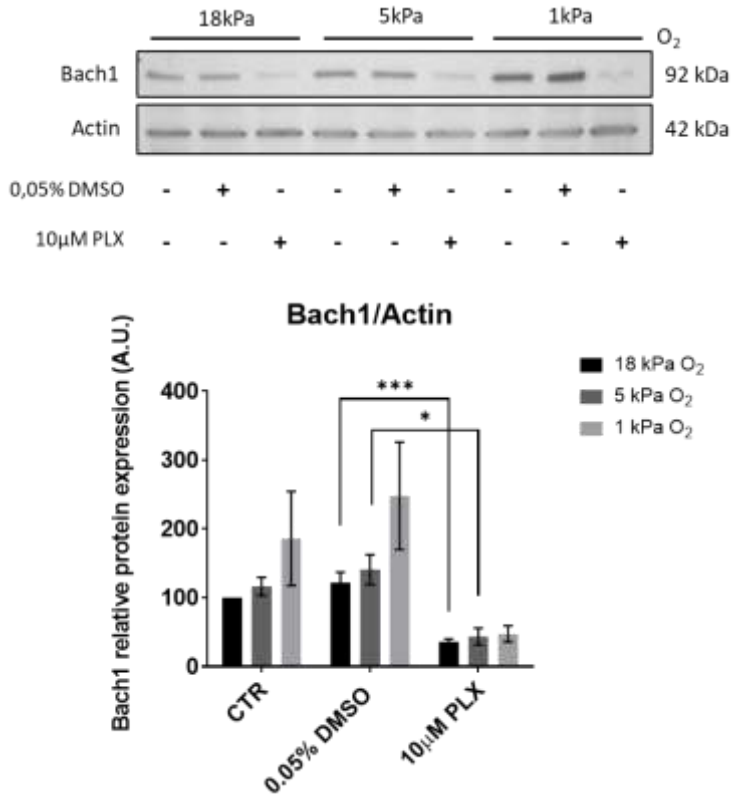

Figure 4-18: Immunoblotting of Bach1 after 24h treatment of 10μM PLX4032. Bach1 protein levels were evaluated in MeOV-1 cells cultured at 18kPa or adapted to 5kPa and 1kPa O_2 and then treated with 10μM PLX4032 (or DMSO) for 24h. β-actin was used as a loading control. The blots are representative of 3 independent experiments. Mean ± S.E.M.,*$p<0.05$, ***$p<0.005$.

4.3.7 *Different oxygen tensions do not affect the efficacy of PLX4032 treatment and HO-1 inhibition further improves it*

Figure 4-19 shows that 10µM PLX4032 treatment was able to significantly reduce cell viability by about 45% in MeOV-1 cells adapted at 18kPa O_2, by about 36% in MeOV-1 cells adapted at 5kPa O_2 and by about 35% in MeOV-1 cells adapted at 1kPa O_2 in comparison to cells treated with the DMSO alone. Moreover, HO-1 inhibition obtained by using SnMP-IX significantly further reduced cell viability of MeOV-1 treated with PLX4032 in all oxygen tensions.

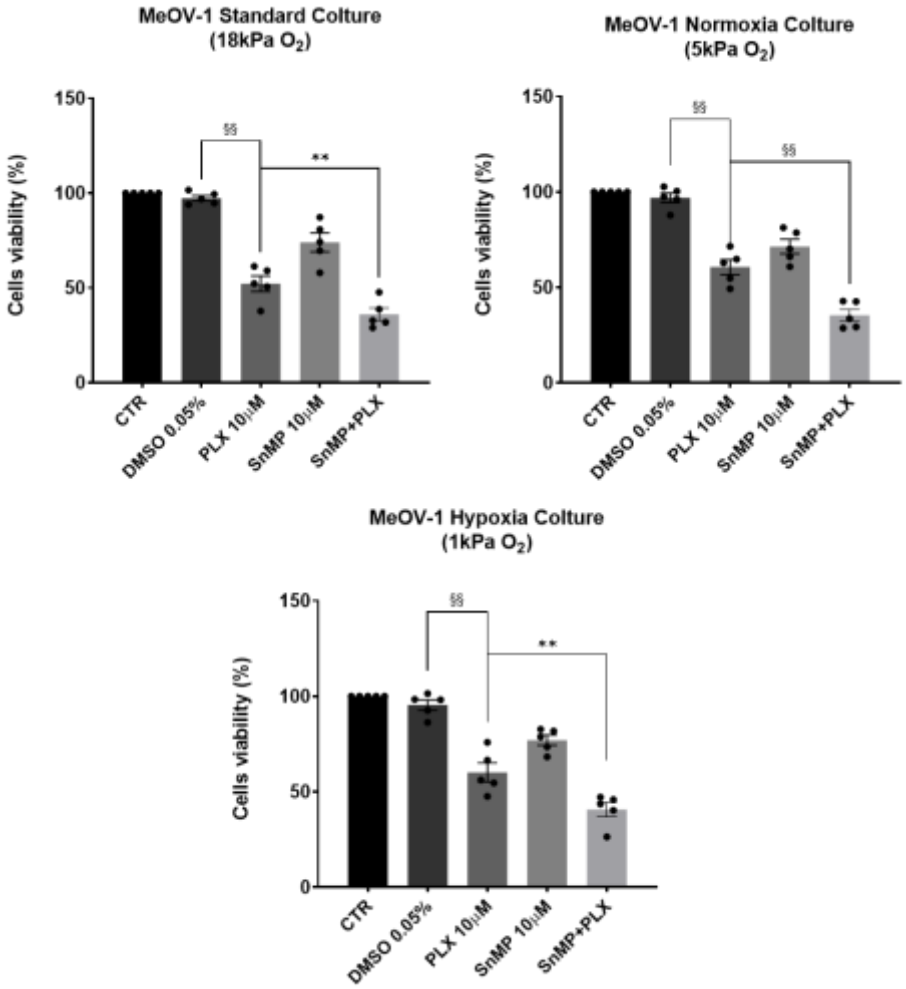

Figure 4-19: Melanoma cell viability after PLX4032 treatment and cotreatment with SnMP-IX. MeOV-1 were seeded in 6-well plates and cultured under 18kPa O_2 or adapted to 5kPa and 1kPa O_2 for 5 days. Cells were then treated with 10µM PLX4032 and 10µM SnMP-IX for 24h. Graphs are representative of 5 independent experiments. Mean ± S.E.M. **p<0.01, §§p<0.0001.

4.3.8 *HIF-1α levels are abolished after PLX4032 treatment in MeOV-1 cells adapted to 18kPa and 5kPa O_2 but still present in cells adapted at 1kPa O_2*

Since experiments were conducted to examine the effects of lowering O_2 tension, it seemed important to check the expression of HIF-1α, a critical transcription factor in the induction of cell responses to hypoxia (Ratcliffe et al., 1998). It is important to note that HIF-1α expression can be already upregulated in melanoma cells under basal conditions due to the $BRAF^{V600}$ mutation, as observed for other $BRAF^{V600}$ mutated melanoma cells (Kumar et al., 2007).

In agreement, we found that HIF-1α is expressed in untreated cells and that basal expression trended to increase in cells adapted to 1kPa O_2. Moreover, exposure of cells to PLX4032 for 24h resulted in a reduction in HIF-1α protein expression in cells cultured under 18kPa or 5kPa O_2. In contrast, the reduction in HIF-1α expression was significant lower in cells cultured under 1kPa O_2. Furthermore, inhibition of HO-1 with SnMP-IX did not modify PLX4032 mediated effects on HIF-1α protein levels.

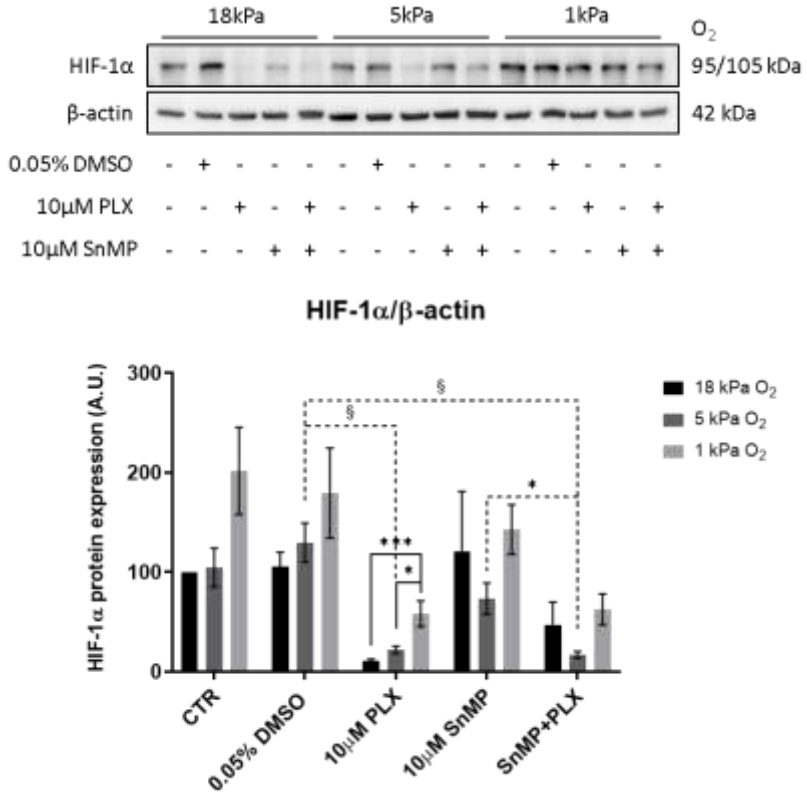

Figure 4-20: HIF-1α protein levels in MeOV-1 cells adapted for 5 days to different O_2 level and treated with PLX4032 and SnMP-IX. HIF-1α protein level was evaluated by immunoblot analysis in MeOV-1 cells cultured at 18kPa or adapted to 5kPa and 1kPa O_2 and then treated with 10μM PLX4032 (or DMSO) and 10μM SnMP for 24h. β-actin was used as a loading control. The blots are representative of 3 different MeOV-1 cultures. Mean ± S.E.M. *p<0.05, ***p<0.005, §p<0.0005.

4.3.9 *Conditioned medium from MeOV-1 cells treated with PLX4032 increases endothelial tube formation*

To evaluate the angiogenic potential mediated by upregulation of HO-1, a tube formation assay was performed using conditioned medium from MeOV-1 cells. Fig. 4-21 shows that BAEC cells seeded with conditioned medium (CM) derived from melanoma cells treated with 10µM PLX4032 increased endothelial tube formation compared to cells seeded with CM derived from DMSO-treated MeOV-1 cells. Interestingly, silencing of HO-1 activity significantly reduced the pro-angiogenic stimulus highlighting a possible role for HO-1 in mediating pro-angiogenic activity of melanoma cells exposed to PLX4032.

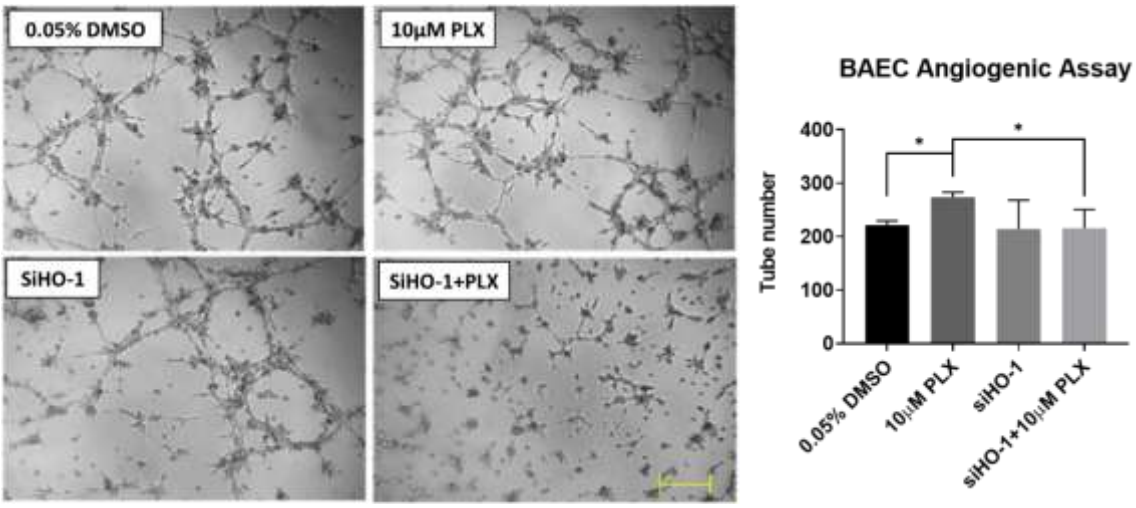

Figure 4-21: Tube formation is increased in BAEC seeded with medium from PLX4032-treated MeOV-1 cells. MeOV-1 cells were silenced for HO-1 and treated as indicated. Tube number was quantified using WIMASIS Image Analysis Software. Images were obtained using Leica IM500 Software; scale bar 200µm. Data denote mean ± S.E.M., n = 4 independent MeOV-1 cultures, *p<0.05.

4.3.10 *CM from MeOV-1 treated with HO-1 inhibitor and exposed to PLX4032 reveals a decreased ability to form endothelial tubes*

Based on the results obtained with HO-1 silencing, the effect of pharmacological inhibition of HO-1 has also been tested. Fig. 4-22 shows, from one preliminary experiment, that when BAEC cells were seeded with CM derived from MeOV-1 treated with HO-1 inhibitor and PLX4032, tube formation was reduced.

Considering the strong effect observed in endothelial cells treated with CM derived from MeOV-1 exposed to SnMP-IX, further experiments will be designed to exclude toxicity of SnMP-IX in endothelial cells.

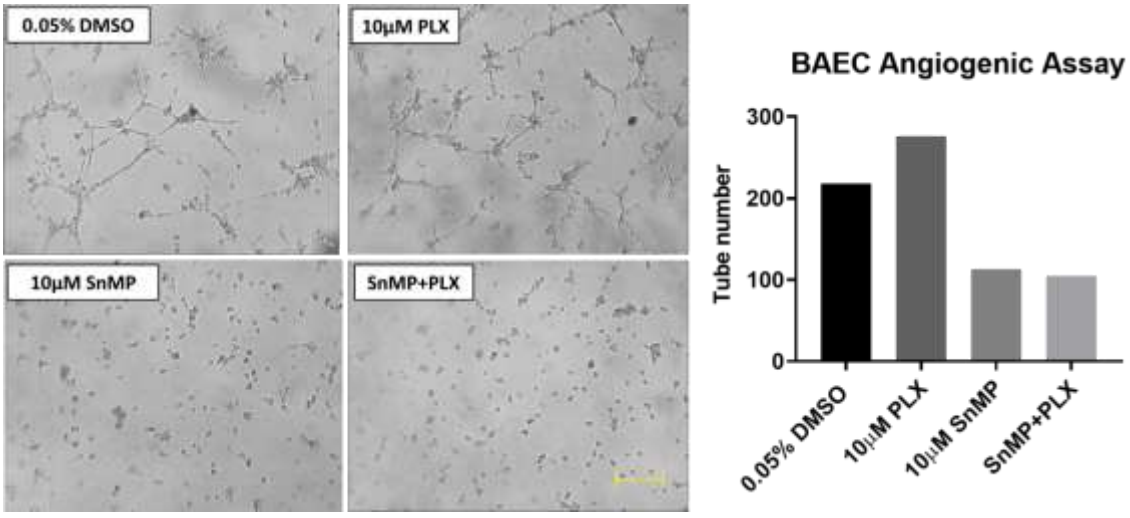

Figure 4-22: Tube formation test using BAEC. BAEC were seeded on Matrigel with CM derived from MeOV-1 cells treated as indicated. Data derived from n = 1 experiment. Tube number was quantified using WIMASIS Image Analysis Software. Images were obtained using LumaView software; scale bar 200µm.

4.3.11 *CM from MeOV-1 adapted to 5kPa and 1kPa O_2 and co-treated with PLX4032/SnMP-IX reduces tube formation in HECV and hCMEC/D3 adapted to 5kPa O_2*

Experiments showed in sections 4.3.9 and 4.3.10 were conducted using MeOV-1 and BAEC cells cultured in standard conditions (18kPa O_2).

Then, the experimental setting was modified in order to mimic the oxygen tensions measured *in vivo* (Keeley et al., 2019). We used MeOV-1 adapted to normoxia (5kPa O_2) or hypoxia (1kPa O_2) and endothelial cells (HECV and hCMEC/D3) adapted to normoxia. HECV are an immortalized cell line derived from HUVEC (Romano et al., 2009). Moreover, since is widely known that the brain is one of the organs where melanoma frequently can metastasize, the hCMEC/D3 cell line derived from the cerebral microvasculature (Weksler et al., 2013) was also used. Fig 4-23 shows that CM derived from melanoma cells adapted to 5kPa or 1kPa O_2 recapitulated in both endothelial cell lines the pro-angiogenetic effects observed using cells cultured in standard 18kPa O_2 conditions. In particular, enzymatic inhibition of HO-1 in MeOV-1 cells always prevented tube formation.

The data shown are still preliminary, deriving from two experiments for cells adapted to 5kPa O_2 and from one experiment for cells adapted to 1kPa O_2.

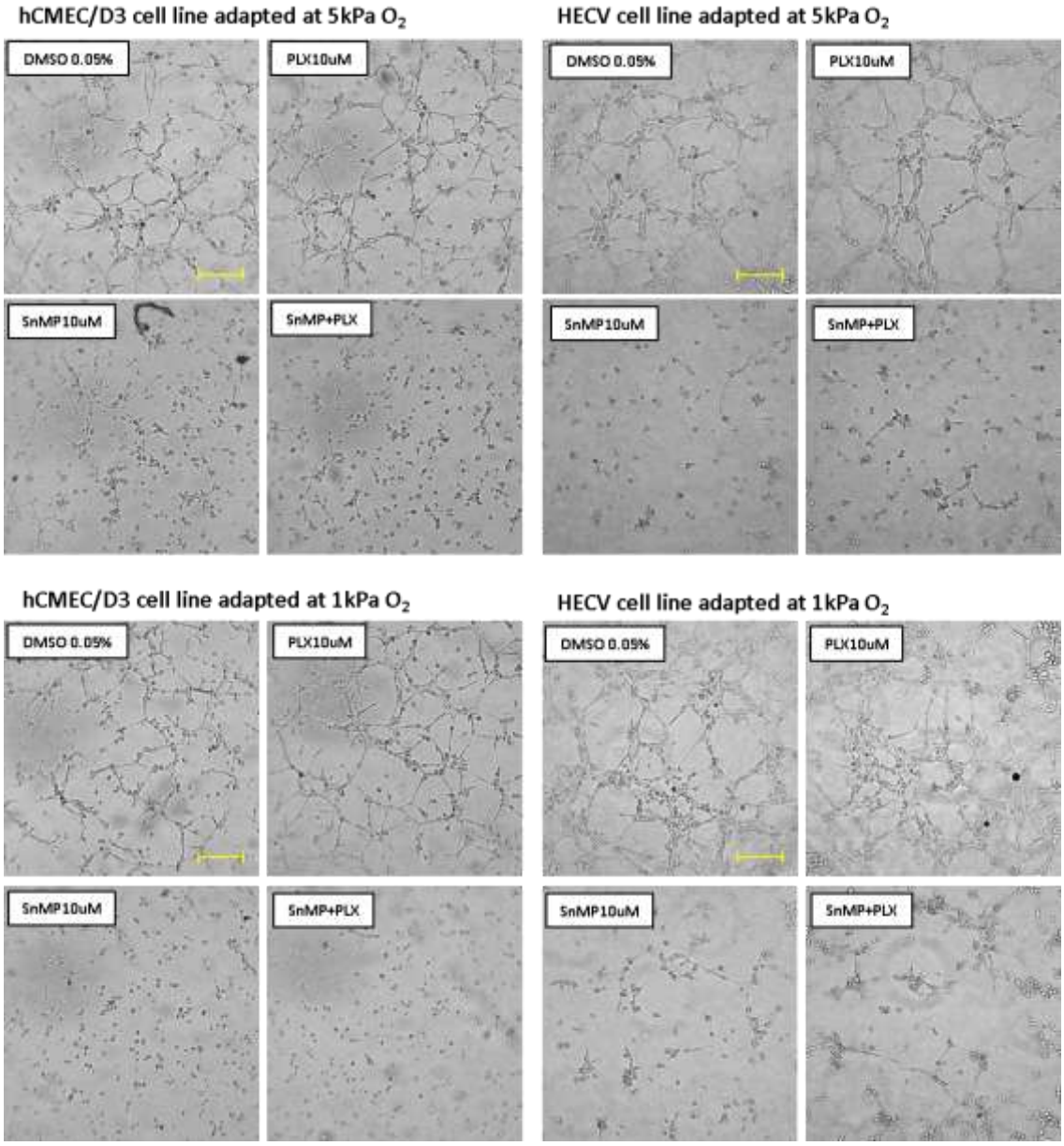

Figure 4-23: HECV and hCMEC/D3 tube formation induced by conditioned medium from MeOV-1 adapted to 5kPa and 1kPa O_2. HECV and hCMEC D3 were adapted for 5 days at 5kPa O_2. Cells were seeded on Matrigel with CM from MeOV-1 cells adapted to 5kPa or 1kPa O_2 and treated with PLX4032 and SnMP-IX, as indicated. n = 2 for 5kPa O_2, n = 1 for 1kPa O_2. Images were obtained using LumaView software; scale bar 200µm.

4.3.12 *VEGF mRNA expression is not modified by PLX4032 treatment in MeOV-1 cells cultured under different oxygen tensions*

Analysis of VEGF showed the increased expression of mRNA basal level in MeOV-1 cells adapted to 1kPa O_2. Moreover, cells treated with PLX4032 and SnMP-IX under different oxygen tensions revealed no significant changes in all experimental conditions tested.

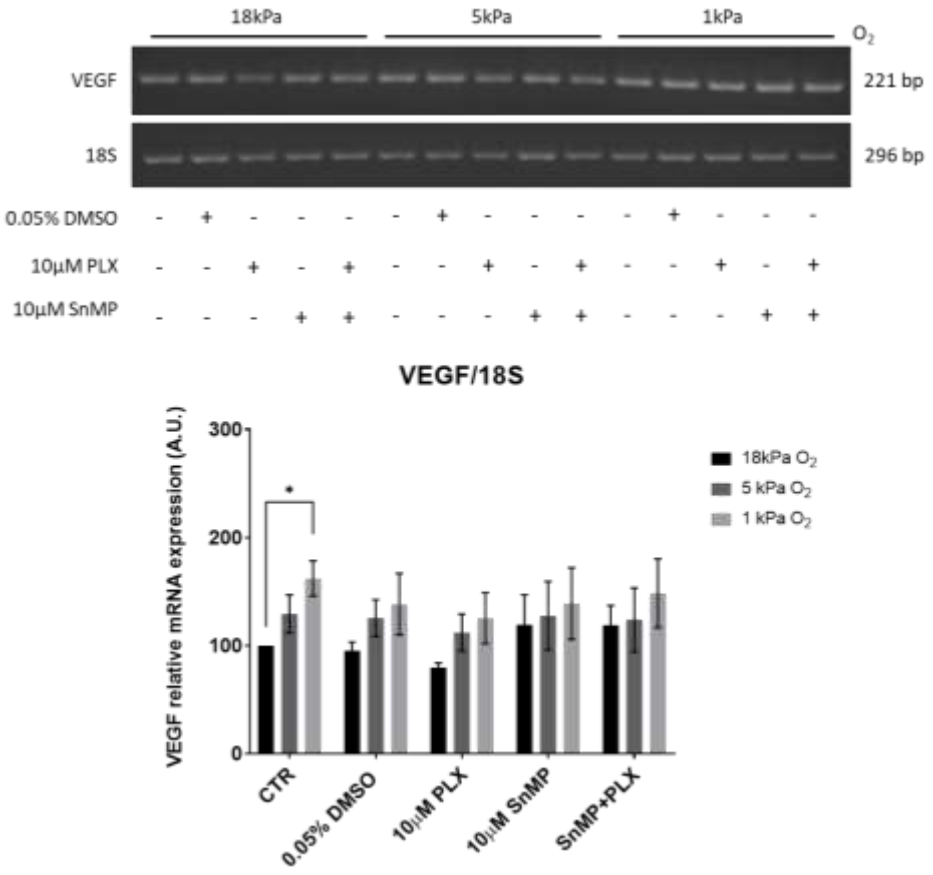

Figure 4-24: mRNA expression of VEGF in PLX4032-treated MeOV-1 cells in different oxygen tensions. VEGF mRNA expression was assessed by RT-PCR in adapted MeOV-1 cells after 24h treatment with 10µM PLX4032 and/or 10µM SnMP-IX. 18S mRNA was used as a housekeeping gene. Data denote mean ± S.E.M. *$p<0.05$, n = 4 independent MeOV-1 cultures.

5 DISCUSSION

In the present study, upregulation of heme oxygenase 1 (HO-1) in primary $BRAF^{V600}$ melanoma cells was shown for the first time to limit the efficacy of Vemurafenib/PLX4032 and to reduce cell recognition by Natural Killer (NK) cells. Moreover, Nrf2 activation and Bach1 inhibition have been shown to be involved in HO-1 upregulation which limits PLX4032 efficacy in cells cultured at under standard (18kPa) and lower (5kPa and 1kPa) oxygen levels. Finally, preliminary data implicate HO-1 downregulation/inhibition in MeOV-1 cells with the reduction of pro-angiogenic activity of conditioned media from melanoma cells treated with PLX4032.

Even with significant improvements achieved with new targeted therapeutic approaches, melanoma still has a highly unfavourable prognosis. Indeed, 50% of patients who present the somatic mutation of BRAF at the codon 600 ($BRAF^{V600}$), responsible for the continuous activation of the MAPK pathway, can be treated with specific inhibitors of BRAF kinase pathway. Indeed, Vemurafenib/PLX4032 has been proved very effective against $BRAF^{V600}$ mutated melanomas, significantly improving the patient survival rate. Unfortunately, in most cases, drug resistance is associated with tumor relapse development (McArthur et al., 2014). Thus, research focused on new potential candidates to improve the efficacy of targeted therapies is pivotal.

The present study postulated a role for HO-1 as a possible limiting factor of PLX4032 efficacy. HO-1 is a powerful stress sensor in cells and is efficiently upregulated increasing cell resistance through the activity of its metabolites, such as CO and bilirubin which display antioxidant, antiapoptotic and immune-regulatory properties (Loboda et al., 2015). The role of HO-1 upregulation in cancer progression has already been highlighted in different types of tumors (Furfaro et al., 2016; Nitti et al., 2017). However, studies on the role of HO-1 in melanoma are rarely reported, and its function in melanoma development and progression is poorly characterized.

In this study, three primary $BRAF^{V600}$ mutated melanoma cell lines (MeOV-1, MeTA and MeMI) isolated in house from patients have been used, thanks to the collaboration with Prof. Pietra from the Laboratory of Clinical Immunology, Ospedale Policlinico San Martino, Genoa. Cells were fully characterized at the local Biobank. Cells have been treated with 1-10μM PLX4032, a range of doses comparable with the ones used in clinic. In all cell lines, HO-1 expression increased after exposure to PLX4032, both in terms of mRNA and protein, limiting the efficacy of PLX4032 in reducing melanoma viability. Indeed, HO-1 silencing, which efficiently prevents HO-1 upregulation, further reduced cell viability in PLX4032-treated cells, as also shown in

combination with the lowest dose of the drug (1μM) in MeOV-1 and MeMI cells. Similar results were also obtained with the highest dose of PLX4032 (10μM) in MeOV-1, MeTA and MeMI cells. Thus, the ability of HO-1 to limit PLX4032 efficacy is not cell specific, as it is shared by different $BRAF^{V600}$ mutated melanoma lines. Importantly, other cell lines carrying the $BRAF^{V600}$ mutation were analysed and showed basal expression of HO-1 but no induction after PLX4032 exposure (data not shown). The potential role of basal HO-1 expression in these cell lines was not investigated further. Interestingly, the BRAF wild type line (MeWO) which is insensitive to PLX4032 exposure, exhibits neither basal expression nor induction of HO-1, even though is able to upregulate HO-1 when exposed to a classical HO-1 inducer (Hemin).

Although there is no reports of expression of HO-1 in MeWO cells, the present findings suggest that the molecular mechanism underlying HO-1 induction in MeOV-1 cells in response to PLX4032 is directly linked to pERK inhibition, which is not achieved in wild type BRAF cells exposed to PLX4032. Consistent with our results, it has been recently reported that BRAF-ERK pathway activation is associated with HO-1 induction, leading to cyclin activation and promoting melanoma proliferation (Liu et al., 2019). In the same work, HO-1 has been reported to be increased in melanoma samples compared with surrounding normal tissues by immunohistological analysis (Liu et al., 2019). Furthermore, other studies have reported stronger HO-1 immunoreactivity in malignant nodules compared to benign nevi (Arena et al., 2015). However, studies conducted on melanoma cell lines generally report a very low (if none) basal expression of HO-1 which is then upregulated by stressors (Keyse et al., 1989; Was et al., 2006). However, other evidence suggests that upregulation of HO-1 may not be related to BRAF mutation. Indeed, suppression of HO-1 has been shown to favor arsenic-induced apoptosis in both BRAF mutated and wild type melanoma cell lines (Ivanov et al., 2011). However, it is important to note that melanoma is a high heterogeneous tumor type, and that basal expression, as well as the induction of HO-1, can be influenced by the activation of many signalling pathways. The role of HO-1 in different types of melanoma and different stages of melanoma progression remain to be investigated.

In MeOV-1, MeTA and MeMI, we also tested the ability of SnMP-IX, a specific pharmacological HO-1 inhibitor, to improve PLX4032 efficacy and found that it improves PLX4032 effects, similar to the effects of HO-1 silencing. SnMP-IX has been already used in the clinic to treat hyperbilirubinemic disease (Valaes et al., 1994) and has been proposed to increase the efficacy of chemotherapy in neuroblastoma (Barbagallo et al., 2019) and melanoma (Barbagallo et al., 2015) and act as check point inhibitor in breast cancer (Muliaditan et al., 2018). Our observations clearly show the efficacy of the combined treatment even at the lowest dose of PLX4032 used.

This opens to the possibility to combine PLX4032 treatment with HO-1 inhibitors, enabling the dose of PLX4032 to be reduced and thereby minimize side effects.

We subsequently analyzed whether BRAF inhibition may interfere with melanoma recognition by NK cells and the involvement of HO-1. NK cells play a pivotal role in the control of tumor growth and metastases and an impaired cytotoxic activity of NK cells has been correlated with melanoma relapse and progression, as shown by the reduced NK infiltration in metastatic nodules from BRAFi resistant patients (López-Cobo et al., 2018). Thus, one of the current therapeutic challenges is to overcome tumor immune escape and restore NK cell recognition ability. To address this challenge, a detailed knowledge of the molecular mechanisms involved in NK killing activity toward tumor cells remains fundamental. Among activating cytotoxicity receptors on NK cells are NKp30, which binds to B7H6 ligand on tumor cell and NKG2D receptor that binds UL16-binding proteins (ULBP1-6).

We evaluated the expression of B7H6 and ULBP3 ligands on melanoma cells. Indeed, even if the pattern of NK cell ligands expression is highly tumor cell-specific and dependent on the oncogenic route activated in the different melanoma cells (Frazao et al., 2017), B7H6 and ULBP3 are the preferential molecular targets for NK cell-mediated recognition and killing of MeOV-1 cells, as shown by our collaborator Prof. Pietra (Pietra et al., 2009, 2012). Analysis of MeOV-1 cells treated with PLX4032 revealed that B7H6 and ULBP3 mRNA expression was significantly downregulated in cells treated with 1μM or 10μM PLX4032, and that HO-1 silencing or HO-1 inhibition restored their expression.

These data shown are part of a study conducted in collaboration with Prof. Pietra's laboratory of Clinical Immunology and were published jointly in 2020 (Furfaro et al., 2020). In addition to the results in this thesis, evidence that NK cells degranulation and killing is reduced towards melanoma cells treated with PLX4032 has been reported as well as the demonstration that HO-1 inhibition or silencing is able to restore NK cells recognition and killing (Furfaro et al., 2020). To our knowledge, this is the first evidence establishing the involvement of HO-1 in regulation of NK ligand expression. Other research groups have recently shown a decrease in the activity of NK cells towards melanoma cells treated with BRAFis, without reference to HO-1 involvement. Indeed, these studies have shown that increasing the expression of ligands for NK receptors through treatment with histone deacetylase inhibitors restores the recognition and killing of melanoma cells by NK (López-Cobo et al., 2018; Wu et al., 2012). Evidence of HO-1 involvement in immune recognition has been provided in other contexts. Indeed, it has been demonstrated that HO-1 is involved in the regulation of programmed death-1 ligand 1 (PD-L1) expression in renal cancer cells and its induction contributes to immune-escape (Balan et al., 2015). Moreover, it has been recently proposed that HO-1 inhibition obtained by SnMP-IX

improves the immunological response to chemotherapy (Muliaditan et al., 2018). Furthermore, Schillingmann and collaborators showed that HO-1 inhibition using SnMP-IX improves T-cells specific function in the treatment of patients with Wilms disease (Schillingmann et al., 2019) and Yong and co-workers demonstrated that HO-1 inhibition in acute myeloid leukaemia (AML) increases immune cell responses (Yong et al., 2020). CO and bilirubin, two metabolites of HO-1 activity, may be possible candidates to explain the immune-regulatory effects. Indeed, even though no evidence has been reported so far in cancer cells, CO plays a pivotal role in reducing immune cell functions (Ryter et al., 2016) and bilirubin is a well-recognised immune modulator (Haga et al., 1996; Sundararaghavan et al., 2018).

Subsequently, in this work we investigated the molecular pathways that determine the up-regulation of HO-1 in the MeOV-1 cell line. The major transcription factor, even if not the only one, involved in the induction of HO-1, is Nrf2 and HO-1 induction observed in MeOV-1 cells exposed to PLX4032 was shown to be dependent from Nrf2 activation. Indeed, Nrf2 silencing prevented PLX4032 induced HO-1 up-regulation. Interestingly, only HO-1 is induced whilst up-regulation of other Nrf2-dependent genes such as GCLC, GCLM and NQO1 was not observed. However, the involvement of other transcription factors in HO-1 induction due to PLX4032 cannot be ruled out. Notably, Nrf2 shows a quick response to PLX4032, moving into the nucleus in the first 2 hours of treatment, whilst HO-1 is still induced 24 hours after PLX4032 treatment. Thus, we cannot exclude that other pathways may synergize with Nrf2 to sustain HO-1 induction. In this context, it is conceivable that AKT/PI3K plays a role. Indeed, PI3K/AKT and MAPK/ERK pathways crosstalk has been crucially highlighted as a mechanism involved in cancer resistance to therapy, since the inhibition of one pathway can activate the other as a compensatory mechanism (Cao et al., 2019). Moreover, it has been recently shown that AKT activation can drive melanoma progression and resistance to PLX4032 of BRAF mutated melanoma (Luebker et al., 2019; Ma et al., 2020). In addition, the AKT/PI3K pathway has been demonstrated to be involved in HO-1 induction in the context of modulation of inflammatory responses (Shi et al., 2019) and in cancer cell responses (Dal-Cim et al., 2012). However, this aspect has not been investigated in the present study.

Moreover, the oxidative state of melanoma cells treated with PLX4032 merits consideration. It has been demonstrated that PLX4032, even following short-term treatment, promotes mitochondrial respiration favoring reactive oxygen species (ROS) production (Hall et al., 2013; Lim et al., 2014; Menon et al., 2015). Moreover, PLX4032-resistant melanoma cells show a high rate of mitochondrial activity and oxidative stress (Corazao-Rozas et al., 2013). Thus, it is possible that Nrf2 acts as sensor of oxidative stress through the degradation of its inhibitor Keap1,

promoting the transcription of HO-1. However, since oxidative stress was not examined in PLX4032 treated cells, we cannot exclude the possible involvement of non-canonical pathways of Nrf2 activation such as GSK3β. Indeed, upregulation of the Wnt/GSK3β pathway has been associated with resistance to BRAF inhibitor therapy (Shi et al., 2019) and correlated with melanoma progression (Da Forno et al., 2008). Further, GSK3β is involved in Keap-1 independent activation of Nrf2 (Chowdhry et al., 2013), and this pathway deserves more investigation in order to complete the analysis of molecular mechanisms involved in HO-1 induction in PLX4032 treated cells.

However, our results strongly highlight the role played by Bach1 in the induction of HO-1. Indeed, it is known that Bach1 is a negative modulator for genes containing ARE sequence and therefore is a competitor for Nrf2 (Dhakshinamoorthy et al., 2005). In particular, Bach1 represses the expression of HO-1 by forming heterodimers with Mafs (Ogawa et al., 2001). Indeed, these Bach1/Mafs complex is specific for the ARE sequences contained in HO-1 promoter and makes AREs inaccessible for the activation by Nrf2 (Raghunath et al., 2018). In this way, Bach1 could play a specific role as a negative regulator of HO-1 more than of other Nrf2-dependent genes. We demonstrated that Bach1 expression after short (3-6h) and long-term (24h) PLX4032 treatments is decreased. We observed similar results in other contexts, providing evidence that HO-1, but not GCLC or GCLM, was induced in response to oxidative stress in neuroblastoma cells (Piras et al., 2017). In addition, it has been shown that the $BRAF^{V600}$ mutation upregulates sMaf and recruiting a set of other repressors among which Bach1 and favours transcriptional repression of genes involved in promoter methylation (Fang et al., 2016).

In the last part of this study, the effect of the oxygen tension on MeOV-1 cells treated with PLX4032 was examined. It is well known that oxygen tension under standard culture conditions is higher than physiological oxygen levels encountered in vivo (Keeley et al., 2019) and this can lead to different cellular responses. In addition, in cancer the complexity of the microenvironment highlights the importance of oxygen tension. Indeed, in tumor growth hypoxia is a driver of tumor progression inducing cell modification in order to survive and proliferate (Ke et al., 2006). For these reasons, we used Baker-Ruskin Sci-tive workstations in order to adapt $BRAF^{V600E}$ MeOV-1 cells to 5kPa and 1kPa O_2 and to determine whether the effects of PLX4032 treatments were affected by alterations in ambient oxygen levels.

Although MeOV-1 cells exhibited a slower growth rate and a modest change of morphology under lower oxygen levels, the efficacy of PLX4032 was not modified. In fact, ERK phosphorylation was abolished by PLX4032 treatment in cells adapted at 5kPa or 1kPa O_2 as well as in cells cultured at 18kPa O_2. This result is in agreement with a publication showing that

PLX4032 maintains its efficacy in inhibiting ERK pathway on BRAF mutated melanoma cells exposed to hypoxia conditions (Pucciarelli et al., 2015).

Moreover, HO-1 was significantly upregulated by PLX4032 at 1kPa O_2, comparable to 18kPa, with a similar trend observed at 5kPa O_2. However, mRNA expression of HO-1 was always significantly increased by PLX4032 treatment under all experimental conditions. Other Nrf2-dependent genes were not modified and Bach1 was always downregulated by PLX4032 both at 5kPa or 1kPa O_2. In agreement with our results, a study of Chapple and co-workers reported that mRNA/protein levels of Bach1 were upregulated in HUVEC adapted to 5kPa O_2 independently on HIF-1α stabilization. In the same experimental condition, Bach1 silencing only restored Nrf2-regulated upregulation of HO-1 (Chapple et al., 2016).

In addition, HO-1 enzymatic inhibition further reduces cell viability in combination with PLX4032 in cells adapted to different oxygen tensions. Thus, our data obtained with cells adapted to 5kPa and 1kPa O_2 essentially recapitulate what observed in standard cultured conditions. In addition, from the analysis of HIF-1α we established that MeOV-1 cells have a high basal expression of HIF-1α. It has been demonstrated that $BRAF^{V600E}$ mutation *per se* increases the expression of HIF-1α (Kumar et al., 2007) leading cell resistance to hypoxic conditions. In agreement, we demonstrated a trend of increased expression of HIF-1α in hypoxia most likely due to protein stabilization as already demonstrated by others (Chang et al., 2005; Ke et al., 2006). Furthermore, Kuphal and co-workers demonstrate that an environment with high ROS levels and inhibition of NF-kB, a pathway already involved in melanoma chemoresistance (Lehraiki et al., 2015), is associated with increased HIF-1α stabilization (Kuphal et al., 2010). The increased stabilisation of HIF-1α may be a reason why PLX4032 is less effective in reducing HIF-1α expression in cells adapted to 1kPa O_2 in comparison to cells adapted to 5kPa or 18kPa O_2. In agreement with our results, a study by Widmer and co-workers shows that invasive melanoma did not increase its invasive potential after hypoxia (Widmer et al., 2013). However, this aspect deserves further investigation.

Finally, the proangiogenic activity of PLX4032-treated cells was investigated. Our data demonstrate that conditioned media from PLX4032-treated MeOV-1 cells are able to increase endothelial tube formation, and interestingly both genetic ablation and enzymatic inhibition of HO-1 reduces this effect. Similar results were obtained using different endothelial cell lines in both standard (18kPa O_2) and lowered oxygen conditions (5kPa and 1kPa O_2). Unfortunately, only preliminary data with endothelial cells adapted to normoxia and melanoma cells treated in normoxia or hypoxia could be obtained. However, the involvement of HO-1 dowregulation/inhibition in preventing the pro-angiogenetic activity of MeOV-1 conditioned

media merits further investigation. Moreover, even though we believed that PLX4032 inevitably dowregulated the expression of VEGF (Beazley-Long et al., 2015), more recent evidence suggests that VEGF expression is not modified by PLX4032 treatment (Osrodek et al., 2019). Moreover, in the latter study, in agreement with our results, the induction of VEGF was demonstrated in cells cultured at lower oxygen tension. Indeed, our data show no modification in the expression level of VEGF in cells exposed to PLX4032 under any of the experimental conditions tested, but an increased expression of VEGF in cells exposed to 1kPa oxygen.

Importantly, similar results concerning VEGF expression and HO-1 expression have been already published. In 2006, Was and co-workers evaluated the role of HO-1 overexpression in melanoma cells. They demonstrated that conditioned medium (CM) derived from HO-1 overexpressing melanoma cells increased the angiogenic potential of HUVEC 5-fold compared to unconditioned medium. Interestingly, in wild type melanoma cells and HO-1 overexpressing melanoma cells, VEGF levels were very similar. Furthermore, the treatment of CM with anti-VEGF antibodies did not modify the ability to form tubes of HUVEC cells, suggesting that VEGF could have a secondary role in the angiogenic potential of HO-1 overexpressing melanoma cells. However, the treatment of CM with anti-VEGF antibodies prevented endothelial cell proliferation induced by CM from wild type melanoma cultured under hypoxic conditions (Was et al., 2006), emphasizing the importance of VEGF in mediating angiogenesis induced by hypoxia. Thus, the role of HO-1 in proangiogenic activity of melanoma cells merits further investigation in order to identify and characterize new targets to potentially modulate and/or prevent melanoma metastases.

6 CONCLUSIONS AND FUTURE RESEARCH PERSPECTIVES

This study has provided the first evidence that in primary melanoma cell lines harbouring the $BRAF^{V600}$ mutation, upregulation of heme oxygenase 1 (HO-1) induced by Vemurafenib/PLX4032 treatment reduces cell recognition of NK cells through the downregulation of specific activation ligands. Moreover, the present work demonstrates that modulation of Nrf2 and Bach1 induced by PLX4032 is involved in the upregulation of HO-1, leading to the reduction of chemotherapic drug efficacy in cells cultured under normoxia or hypoxia. Finally, preliminary data on the role played by HO-1 silencing or inhibition in the reduction of the angiogenic potential of MeOV-1 cells has been provided, further highlighting the potential importance of HO-1 as a target to reduce melanoma progression.

However, the role played by HO-1 in the different types of melanoma remains to be investigated. As discussed, other melanomas can express HO-1 in untreated conditions and the functional meaning of this requires further investigation as well as consideration different types of melanomas. Thus, studies of possible correlations between tumor stage and HO-1 expression could highlight HO-1 as a possible tumor progression marker useful for clinical prognosis.

Furthermore, it is crucial to dissect the role of Nrf2 and Bach1 in HO-1 induction due to PLX4032 and their possible correlation with the modulation of NK ligand expression. Thus, a more detailed study of the molecular pathways involved in HO-1 induction needs to be conducted in a wider range of melanoma cell lines, wild type and BRAF mutated, in order to identify new targets to improve immune-recognition of melanoma cells. There may be other signalling pathways that can be modulated in BRAF mutated melanoma cells exposed to targeted therapies, and these need to be further investigated as they may be involved in HO-1 induction or cooperate with it in increasing cell resistance and in favouring immune-escape.

The experimental approach we used to study melanoma in normoxia or hypoxia can be further applied for an in depth analysis of the role of lowering oxygen tension in other cell lines, using both BRAF mutated and wild type BRAF cell lines. Similarly, the data obtained on the potential role of HO-1 induction in favouring angiogenesis need to be confirmed even though some results are already published by other authors. Further studies, using other mutated cell lines, are warrented to avoid cell-specific results. In summary, based on the present study, further research

is required to clarify the molecular pathway(s) linking HO-1 overexpression to the proangiogenic stimulus in conditioned MeOV-1 media, taking also into account other angiogenic factors closely related to HO-1 upregulation, such as CO and bilirubin and their potential role in modulating endothelial cells in a tumor microenvironment. Furthermore, such studies should be investigated not only under standard culture conditions (18kPa O_2) also under normoxia (5kPa O_2) and hypoxia (1kPa O_2) since different pathways may be affected under the different oxygen tensions.

7 REFERENCES

Agyeman, A. S., Chaerkady, R., Shaw, P. G., Davidson, N. E., Visvanathan, K., Pandey, A., & Kensler, T. W. (2012). Transcriptomic and proteomic profiling of KEAP1 disrupted and sulforaphane-treated human breast epithelial cells reveals common expression profiles. *Breast Cancer Research and Treatment*, *132*(1), 175–187. https://doi.org/10.1007/s10549-011-1536-9

Ahmed, S. M. U., Luo, L., Namani, A., Wang, X. J., & Tang, X. (2017). Nrf2 signaling pathway: Pivotal roles in inflammation. *Biochimica et Biophysica Acta - Molecular Basis of Disease*, *1863*(2), 585–597. https://doi.org/10.1016/j.bbadis.2016.11.005

Alam, J., Shibahara, S., & Smith, A. (1989). Transcriptional activation of the heme oxygenase gene by heme and cadmium in mouse hepatoma cells. *Journal of Biological Chemistry*, *264*(11), 6371–6375.

Alam, Jawed, & Cook, J. L. (2007). How many transcription factors does it take to turn on the heme oxygenase-1 gene? *American Journal of Respiratory Cell and Molecular Biology*, *36*(2), 166–174. https://doi.org/10.1165/rcmb.2006-0340TR

Albert, I., Hefti, M., & Luginbuehl, V. (2014). Physiological oxygen concentration alters glioma cell malignancy and responsiveness to photodynamic therapy in vitro. *Neurological Research*, *36*(11), 1001–1010. https://doi.org/10.1179/1743132814Y.0000000401

Albert, M. R., & Ostheimer, K. G. (2002). The evolution of current medical and popular attitudes toward ultraviolet light exposure: Part 1. *Journal of the American Academy of Dermatology*, *47*(6), 930–937. https://doi.org/10.1067/mjd.2002.127254

Arena, V., Pennacchia, I., Guerriero, G., & Mancuso, C. (2015). The heme oxygenase/biliverdin reductase system in skin cancers. In *Journal of biological regulators and homeostatic agents* (Vol. 29, Issue 1, pp. 259–264).

Arnold, J. N., Magiera, L., Kraman, M., & Fearon, D. T. (2014). Tumoral immune suppression by macrophages expressing fibroblast activation protein-α and heme oxygenase-1. *Cancer Immunology Research*, *2*(2), 121–126. https://doi.org/10.1158/2326-6066.CIR-13-0150

Atzori, M. G., Ceci, C., Ruffini, F., Trapani, M., Barbaccia, M. L., Tentori, L., D'Atri, S., Lacal, P. M., & Graziani, G. (2020). Role of VEGFR-1 in melanoma acquired resistance to the BRAF inhibitor vemurafenib. *Journal of Cellular and Molecular Medicine*, *24*(1), 465–475. https://doi.org/10.1111/jcmm.14755

Azimi, F., Scolyer, R. A., Rumcheva, P., Moncrieff, M., Murali, R., McCarthy, S. W., Saw, R. P., & Thompson, J. F. (2012). Tumor-infiltrating lymphocyte grade is an independent predictor of sentinel lymph node status and survival in patients with cutaneous melanoma. *Journal of Clinical Oncology*, *30*(21), 2678–2683. https://doi.org/10.1200/JCO.2011.37.8539

Balan, M., Mier Y Teran, E., Waaga-Gasser, A. M., Gasser, M., Choueiri, T. K., Freeman, G., & Pal, S. (2015). Novel roles of c-met in the survival of renal cancer cells through the regulation of HO-1 and PD-L1 expression. *Journal of Biological Chemistry*, *290*(13), 8110–8120. https://doi.org/10.1074/jbc.M114.612689

Balla, G., Jacob, H. S., Balla, J., Rosenberg, M., Nath, K., Apple, F., Eaton, J. W., & Vercellotti, G. M. (1992). Ferritin: A cytoprotective antioxidant strategem of endothelium. *Journal of Biological Chemistry*, *267*(25), 18148–18153.

Bancos, S., Baglole, C. J., Rahman, I., & R.P.Phipps. (2010). Induction of heme oxygenase-1 in normal and malignant B lymphocytes by 15-deoxy-Delta(12,14)-prostaglandin J(2) requires Nrf2. *Cell Immunol*, *626*(1), 18–27. https://doi.org/10.1038/jid.2014.371

Barbagallo, I., Giallongo, C., Volti, G. L., Distefano, A., Camiolo, G., Raffaele, M., Salerno, L., Pittalà, V., Sorrenti, V., Avola, R., Di Rosa, M., Vanella, L., Di Raimondo, F., & Tibullo, D. (2019). Heme Oxygenase Inhibition Sensitizes Neuroblastoma Cells to Carfilzomib. *Molecular Neurobiology*, *56*(2), 1451–1460. https://doi.org/10.1007/s12035-018-1133-6

Barbagallo, I., Parenti, R., Zappalà, A., Vanella, L., Tibullo, D., Pepe, F., Onni, T., & Li Volti, G. (2015). Combined inhibition of Hsp90 and heme oxygenase-1 induces apoptosis and endoplasmic reticulum stress in melanoma. *Acta Histochemica*, *117*(8), 705–711. https://doi.org/10.1016/j.acthis.2015.09.005

Barrera, L. N., Rushworth, S. A., Bowles, K. M., & MacEwan, D. J. (2012). Bortezomib induces heme oxygenase-1 expression in multiple myeloma. *Cell Cycle*, *11*(12), 2248–2252. https://doi.org/10.4161/cc.20343

Beazley-Long, N., Gaston, K., Harper, S. J., Orlando, A., & Bates, D. O. (2015). Novel mechanisms of resistance to vemurafenib in melanoma - V600E B-Raf reversion and switching VEGF-A splice isoform expression. *American Journal of Cancer Research*, *5*(1), 433–441.

Berberat, P. O., Dambrauskas, Z., Gulbinas, A., Giese, T., Giese, N., Künzli, B., Autschbach, F., Meuer, S., Büchler, M. W., & Friess, H. (2005). Inhibition of heme oxygenase-1 increases responsiveness of pancreatic cancer cells to anticancer treatment. *Clinical Cancer Research*, *11*(10), 3790–3798. https://doi.org/10.1158/1078-0432.CCR-04-2159

Bergers, G., & Benjamin, L. E. (2003). Tumorigenesis and the angiogenic switch. *Nature Reviews Cancer*, *3*(6), 401–410. https://doi.org/10.1038/nrc1093

Birrane, G., Li, H., Yang, S., Tachado, S. D., & Seng, S. (2013). Cigarette smoke induces nuclear translocation of heme oxygenase 1 (HO-1) in prostate cancer cells: Nuclear HO-1 promotes vascular endothelial growth factor secretion. *International Journal of Oncology*, *42*(6), 1919–1928. https://doi.org/10.3892/ijo.2013.1910

Biswas, S. K., Allavena, P., & Mantovani, A. (2013). Tumor-associated macrophages: Functional diversity, clinical significance, and open questions. *Seminars in Immunopathology*, *35*(5), 585–600. https://doi.org/10.1007/s00281-013-0367-7

Bollag, G., Hirth, P., Tsai, J., Zhang, J., Ibrahim, P. N., Cho, H., Spevak, W., Zhang, C., Zhang, Y., Habets, G., Burton, E. A., Wong, B., Tsang, G., West, B. L., Powell, B., Shellooe, R., Marimuthu, A., Nguyen, H., Zhang, K. Y. J., … Nolop, K. (2010). Clinical efficacy of a RAF inhibitor needs broad target blockade in BRAF-mutant melanoma. *Nature*, *467*(7315), 596–599. https://doi.org/10.1038/nature09454

Bollag, G., Tsai, J., Zhang, J., Zhang, C., Ibrahim, P., Nolop, K., & Hirth, P. (2012). Vemurafenib: The

first drug approved for BRAF-mutant cancer. *Nature Reviews Drug Discovery*, *11*(11), 873–886. https://doi.org/10.1038/nrd3847

Brenner, M., & Hearing, J. V. (2008). The protective role of melanin against UV. *Photochem Photobiology*, *84*(3), 539–549. https://doi.org/10.1111/j.1751-1097.2007.00226.x.The

Bronckaers, A., Gago, F., Balzarini, J., & Liekens, S. (2009). The dual role of thymidine phosphorylase in cancer development and chemotherapy. *Medicinal Research Reviews*, *29*(6), 903–953. https://doi.org/10.1002/med

Bryan, H. K., Olayanju, A., Goldring, C. E., & Park, B. K. (2013). The Nrf2 cell defence pathway: Keap1-dependent and -independent mechanisms of regulation. *Biochemical Pharmacology*, *85*(6), 705–717. https://doi.org/10.1016/j.bcp.2012.11.016

Bryceson, Y. T., March, M. E., Ljunggren, H.-G., & Long, E. O. (2006). Activation, co–activation, and co–stimulation of resting human NK cells. *Immunological Reviews*, *29*, 997–1003. https://doi.org/10.1016/j.biotechadv.2011.08.021.Secreted

Buhrmann, C., Kraehe, P., Lueders, C., Shayan, P., Goel, A., & Shakibaei, M. (2014). Curcumin suppresses crosstalk between colon cancer stem cells and stromal fibroblasts in the tumor microenvironment: Potential role of EMT. *PLoS ONE*, *9*(9). https://doi.org/10.1371/journal.pone.0107514

Bussolati, B., Ahmed, A., Pemberton, H., Landis, R. C., Di Carlo, F., Haskard, D. O., & Mason, J. C. (2004). Bifunctional role for VEGF-induced heme oxygenase-1 in vivo: Induction of angiogenesis and inhibition of leukocytic infiltration. *Blood*, *103*(3), 761–766. https://doi.org/10.1182/blood-2003-06-1974

Canning, P., Sorrell, F. J., & Bullock, A. N. (2015). Structural basis of Keap1 interactions with Nrf2. *Free Radical Biology and Medicine*, *88*(Part B), 101–107. https://doi.org/10.1016/j.freeradbiomed.2015.05.034

Cao, Z., Liao, Q., Su, M., Huang, K., Jin, J., & Cao, D. (2019). AKT and ERK dual inhibitors: The way forward? *Cancer Letters*, *459*(January), 30–40. https://doi.org/10.1016/j.canlet.2019.05.025

Chan, X. Y., Singh, A., Osman, N., & Piva, T. J. (2017). Role played by signalling pathways in overcoming BRAF inhibitor resistance in melanoma. In *International Journal of Molecular Sciences*. https://doi.org/10.3390/ijms18071527

Chang, T. C., Huang, C. J., Tam, K., Chen, S. F., Tan, K. T., Tsai, M. S., Lin, T. N., & Shyue, S. K. (2005). Stabilization of hypoxia-inducible factor-1α by prostacyclin under prolonged hypoxia via reducing reactive oxygen species level in endothelial cells. *Journal of Biological Chemistry*, *280*(44), 36567–36574. https://doi.org/10.1074/jbc.M504280200

Chao, C. Y., Lii, C. K., Hsu, Y. T., Lu, C. Y., Liu, K. L., Li, C. C., & Chen, H. W. (2013). Induction of heme oxygenase-1 and inhibition of TPA-induced matrix metalloproteinase-9 expression by andrographolide in MCF-7 human breast cancer cells. *Carcinogenesis*, *34*(8), 1843–1851. https://doi.org/10.1093/carcin/bgt131

Chapman, P. B., Hauschild, A., Robert, C., Haanen, J. B., Ascierto, P., Larkin, J., Dummer, R., Garbe, C., Testori, A., Maio, M., Hogg, D., Lorigan, P., Lebbe, C., Jouary, T., Schadendorf, D., Ribas, A., O'Day, S. J., Sosman, J. A., Kirkwood, J. M., … McArthur, G. A. (2011). Improved Survival with

Vemurafenib in Melanoma with BRAF V600E Mutation. *New England Journal of Medicine*, *364*(26), 2507–2516. https://doi.org/10.1056/nejmoa1103782

Chapple, S. J., Keeley, T. P., Mastronicola, D., Arno, M., Vizcay-Barrena, G., Fleck, R., Siow, R. C. M., & Mann, G. E. (2016). Bach1 differentially regulates distinct Nrf2-dependent genes in human venous and coronary artery endothelial cells adapted to physiological oxygen levels. *Free Radical Biology and Medicine*, *92*, 152–162. https://doi.org/https://doi.org/10.1016/j.freeradbiomed.2015.12.013

Chau, L. Y. (2015). Heme oxygenase-1: Emerging target of cancer therapy. *Journal of Biomedical Science*, *22*(1), 1–7. https://doi.org/10.1186/s12929-015-0128-0

Chauveau, C., Rémy, S., Royer, P. J., Hill, M., Tanguy-Royer, S., Hubert, F. X., Tesson, L., Brion, R., Beriou, G., Gregoire, M., Josien, R., Cuturi, M. C., & Anegon, I. (2005). Heme oxygenase-1 expression inhibits dendritic cell maturation and proinflammatory function but conserves IL-10 expression. *Blood*, *106*(5), 1694–1702. https://doi.org/10.1182/blood-2005-02-0494

Chen, W., Sun, Z., Wang, X., Jiang, T., Huang, Z., Fang, D., & Zhang, D. D. (2009). Direct interaction between Nrf2 and p21Cip1/WAF1 upregulates the Nrf2-mediated antioxidant response. *Molecular Cell*, *34*(6), 663–673. https://doi.org/10.1016/j.molcel.2009.04.029.Direct

Cheng, C. C., Guan, S. S., Yang, H. J., Chang, C. C., Luo, T. Y., Chang, J., & Ho, A. S. (2016). Blocking heme oxygenase-1 by zinc protoporphyrin reduces tumor hypoxia-mediated VEGF release and inhibits tumor angiogenesis as a potential therapeutic agent against colorectal cancer. *Journal of Biomedical Science*, *23*(1), 1–10. https://doi.org/10.1186/s12929-016-0219-6

Cheng, P. Y., Lee, Y. M., Shih, N. L., Chen, Y. C., & Yen, M. H. (2006). Heme oxygenase-1 contributes to the cytoprotection of alpha-lipoic acid via activation of p44/42 mitogen-activated protein kinase in vascular smooth muscle cells. *Free Radical Biology and Medicine*, *40*(8), 1313–1322. https://doi.org/10.1016/j.freeradbiomed.2005.11.024

Cho, W. C., Jour, G., & Aung, P. P. (2019). Role of angiogenesis in melanoma progression: Update on key angiogenic mechanisms and other associated components. *Seminars in Cancer Biology*, *59*(February), 175–186. https://doi.org/10.1016/j.semcancer.2019.06.015

Chorley, B. N., Campbell, M. R., Wang, X., Karaca, M., Sambandan, D., Bangura, F., Xue, P., Pi, J., Kleeberger, S. R., & Bell, D. A. (2012). Identification of novel NRF2-regulated genes by ChiP-Seq: Influence on retinoid X receptor alpha. *Nucleic Acids Research*, *40*(15), 7416–7429. https://doi.org/10.1093/nar/gks409

Chowdhry, S., Zhang, Y., McMahon, M., Sutherland, C., Cuadrado, A., & Hayes, J. D. (2013). Nrf2 is controlled by two distinct β-TrCP recognition motifs in its Neh6 domain, one of which can be modulated by GSK-3 activity. *Oncogene*, *32*(32), 3765–3781. https://doi.org/10.1038/onc.2012.388

Chowdhry, Sudhir, Zhang, Y., & Mcmahon, M. (2013). Nrf2 is controlled by two distinct β -TrCP recognition motifs in its Neh6 domain , one of which can be modulated by GSK-3 activity . *Oncogene*, *32*(32), 3765–3781. https://doi.org/10.1038/onc.2012.388.Nrf2

Comunanza, V., Corà, D., Orso, F., Consonni, F. M., Middonti, E., Di Nicolantonio, F., Buzdin, A., Sica, A., Medico, E., Sangiolo, D., Taverna, D., & Bussolino, F. (2017). VEGF blockade enhances the antitumor effect of BRAF V 600E inhibition . *EMBO Molecular Medicine*, *9*(2), 219–237.

https://doi.org/10.15252/emmm.201505774

Corazao-Rozas, P., Guerreschi, P., Jendoubi, M., André, F., Jonneaux, A., Scalbert, C., Garçon, G., Malet-Martino, M., Balayssac, S., Rocchi, S., Savina, A., Formstecher, P., Mortier, L., Kluza, J., & Marchetti, P. (2013). Mitochondrial oxidative stress is the achille's heel of melanoma cells resistant to Braf-mutant inhibitor. *Oncotarget*, *4*(11), 1986–1998. https://doi.org/10.18632/oncotarget.1420

Corrales, L., Matson, V., Flood, B., Spranger, S., & Gajewski, T. F. (2017). Innate immune signaling and regulation in cancer immunotherapy. *Cell Research*, *27*(1), 96–108. https://doi.org/10.1038/cr.2016.149

Crocetti, E., Mallone, S., Robsahm, T. E., Gavin, A., Agius, D., Ardanaz, E., Lopez, M. D. C., Innos, K., Minicozzi, P., Borgognoni, L., Pierannunzio, D., & Eisemann, N. (2015). Survival of patients with skin melanoma in Europe increases further: Results of the EUROCARE-5 study. *European Journal of Cancer*, *51*(15), 2179–2190. https://doi.org/10.1016/j.ejca.2015.07.039

Cui, R., Widlund, H. R., Feige, E., Lin, J. Y., Wilensky, D. L., Igras, V. E., D'Orazio, J., Fung, C. Y., Schanbacher, C. F., Granter, S. R., & Fisher, D. E. (2007). Central Role of p53 in the Suntan Response and Pathologic Hyperpigmentation. *Cell*, *128*(5), 853–864. https://doi.org/10.1016/j.cell.2006.12.045

Cullinan, S. B., Zhang, D., Hannink, M., Arvisais, E., Kaufman, R. J., & Diehl, J. A. (2003). Nrf2 Is a Direct PERK Substrate and Effector of PERK-Dependent Cell Survival. *Molecular and Cellular Biology*, *23*(20), 7198–7209. https://doi.org/10.1128/mcb.23.20.7198-7209.2003

Da Forno, P., Howard Pringle, J., Hutchinson, P., Osborn, J., Huang, Q., Potter, L., Hancox, R. A., Fletcher, A., & Saldanha, G. S. (2008). WNT5A expression increases during melanoma progression and correlates with outcome. *Clinical Cancer Research*, *14*(18), 5825–5832. https://doi.org/10.1158/1078-0432.CCR-07-5104

Dal-Cim, T., Molz, S., Egea, J., Parada, E., Romero, A., Budni, J., Martín De Saavedra, M. D., Barrio, L. Del, Tasca, C. I., & López, M. G. (2012). Guanosine protects human neuroblastoma SH-SY5Y cells against mitochondrial oxidative stress by inducing heme oxigenase-1 via PI3K/Akt/GSK-3β pathway. *Neurochemistry International*, *61*(3), 397–404. https://doi.org/10.1016/j.neuint.2012.05.021

Dennery, P. A. (2014). Signaling function of heme oxygenase proteins. *Antioxidants and Redox Signaling*, *20*(11), 1743–1753. https://doi.org/10.1089/ars.2013.5674

Dhakshinamoorthy, S., Jain, A. K., Bloom, D. A., & Jaiswal, A. K. (2005). Bach1 competes with Nrf2 leading to negative regulation of the antioxidant response element (ARE)-mediated NAD(P)H:quinone oxidoreductase 1 gene expression and induction in response to antioxidants. *Journal of Biological Chemistry*, *280*(17), 16891–16900. https://doi.org/10.1074/jbc.M500166200

Ding, Z. Y., Zou, X. L., & Wei, Y. Q. (2012). Cancer microenvironment and cancer vaccine. *Cancer Microenvironment*, *5*(3), 333–344. https://doi.org/10.1007/s12307-012-0107-x

Do, M. T., Kim, H. G., Khanal, T., Choi, J. H., Kim, D. H., Jeong, T. C., & Jeong, H. G. (2013). Metformin inhibits heme oxygenase-1 expression in cancer cells through inactivation of Raf-ERK-Nrf2 signaling and AMPK-independent pathways. *Toxicology and Applied Pharmacology*, *271*(2), 229–

238. https://doi.org/10.1016/j.taap.2013.05.010

Domingues, B., Lopes, J., Soares, P., & Populo, H. (2018). Melanoma treatment in review. *ImmunoTargets and Therapy*, *Volume 7*, 35–49. https://doi.org/10.2147/itt.s134842

Dulak, J., Józkowicz, A., Foresti, R., Kasza, A., Frick, M., Huk, I., Green, C. J., Pachinger, O., Weidinger, F., & Motterlini, R. (2002). Heme oxygenase activity modulates vascular endothelial growth factor synthesis in vascular smooth muscle cells. *Antioxidants and Redox Signaling*, *4*(2), 229–240. https://doi.org/10.1089/152308602753666280

El Alami, M., Viña-Almunia, J., Gambini, J., Mas-Bargues, C., Siow, R. C. M., Peñarrocha, M., Mann, G. E., Borrás, C., & Viña, J. (2014). Activation of p38, p21, and NRF-2 mediates decreased proliferation of human dental pulp stem cells cultured under 21% O2. *Stem Cell Reports*, *3*(4), 566–573. https://doi.org/10.1016/j.stemcr.2014.08.002

Emmett, M. S., Dewing, D., & Pritchard-Jones, R. O. (2011). Angiogenesis and melanoma - from basic science to clinical trials. *American Journal of Cancer Research*, *1*(7), 852–868. http://www.ncbi.nlm.nih.gov/pubmed/22016833%0Ahttp://www.pubmedcentral.nih.gov/articlerender.fcgi?artid=PMC3196284

Fang, M., Hutchinson, L., Deng, A., & Green, M. R. (2016). Common BRAF(V600E)-directed pathway mediates widespread epigenetic silencing in colorectal cancer and melanoma. *Proceedings of the National Academy of Sciences of the United States of America*, *113*(5), 1250–1255. https://doi.org/10.1073/pnas.1525619113

Fedorenko, I. V., Paraiso, K. H. T., & Smalley, K. S. M. (2011). Acquired and intrinsic BRAF inhibitor resistance in BRAF V600E mutant melanoma. *Biochemical Pharmacology*, *82*(3), 201–209. https://doi.org/10.1016/j.bcp.2011.05.015.Acquired

Ferrando, M., Gueron, G., Elguero, B., Giudice, J., Salles, A., Leskow, F. C., Jares-Erijman, E. A., Colombo, L., Meiss, R., Navone, N., De Siervi, A., & Vazquez, E. (2011). Heme oxygenase 1 (HO-1) challenges the angiogenic switch in prostate cancer. *Angiogenesis*, *14*(4), 467–479. https://doi.org/10.1007/s10456-011-9230-4

Fick, A. (1855). V. On liquid diffusion. *The London, Edinburgh, and Dublin Philosophical Magazine and Journal of Science*, *10*(63), 30–39. https://doi.org/10.1080/14786445508641925

Fidler, I. J. (1988). Macrophage therapy of cancer metastasis. *Ciba Foundation Symposium*, *141*, 211–222. https://doi.org/10.1002/9780470513736.ch12

Flick, A. (1855). Ueber Diffusion. *Annalen Der Physik*, *140*(1), 59–83. https://doi.org/10.1002/btpr.359

Foresti, R., Clark, J. E., Green, C. J., & Motterlini, R. (1997). Thiol compounds interact with nitric oxide in regulating heme oxygenase- 1 induction in endothelial cells: Involvement of superoxide and peroxynitrite anions. *Journal of Biological Chemistry*, *272*(29), 18411–18417. https://doi.org/10.1074/jbc.272.29.18411

Frazao, A., Colombo, M., Fourmentraux-Neves, E., Messaoudene, M., Rusakiewicz, S., Zitvogel, L., Vivier, E., Vély, F., Faure, F., Dréno, B., Benlalam, H., Bouquet, F., Savina, A., Pasmant, E., Toubert, A., Avril, M. F., & Caignard, A. (2017). Shifting the balance of activating and inhibitory natural killer receptor ligands on BRAFV600E melanoma lines with vemurafenib. *Cancer*

Immunology Research, *5*(7), 582–593. https://doi.org/10.1158/2326-6066.CIR-16-0380

Furfaro, A. L., Piras, S., Domenicotti, C., Fenoglio, D., De Luigi, A., Salmona, M., Moretta, L., Marinari, U. M., Pronzato, M. A., Traverso, N., & Nitti, M. (2016). Role of Nrf2, HO-1 and GSH in neuroblastoma cell resistance to bortezomib. *PLoS ONE*, *11*(3), 1–17. https://doi.org/10.1371/journal.pone.0152465

Furfaro, A. L., Traverso, N., Domenicotti, C., Piras, S., Moretta, L., Marinari, U. M., Pronzato, M. A., & Nitti, M. (2016). The Nrf2/HO-1 Axis in Cancer Cell Growth and Chemoresistance. *Oxidative Medicine and Cellular Longevity*, *2016*(Table 1). https://doi.org/10.1155/2016/1958174

Furfaro, Anna L., Ottonello, S., Loi, G., Cossu, I., Piras, S., Spagnolo, F., Queirolo, P., Marinari, U. M., Moretta, L., Pronzato, M. A., Mingari, M. C., Pietra, G., & Nitti, M. (2020). HO-1 downregulation favors BRAFV600 melanoma cell death induced by Vemurafenib/PLX4032 and increases NK recognition. *International Journal of Cancer*, *146*(7), 1950–1962. https://doi.org/10.1002/ijc.32611

Furfaro, Anna Lisa, MacAy, J. R. Z., Marengo, B., Nitti, M., Parodi, A., Fenoglio, D., Marinari, U. M., Pronzato, M. A., Domenicotti, C., & Traverso, N. (2012). Resistance of neuroblastoma GI-ME-N cell line to glutathione depletion involves Nrf2 and heme oxygenase-1. *Free Radical Biology and Medicine*, *52*(2), 488–496. https://doi.org/10.1016/j.freeradbiomed.2011.11.007

Furfaro, Anna Lisa, Piras, S., Passalacqua, M., Domenicotti, C., Parodi, A., Fenoglio, D., Pronzato, M. A., Marinari, U. M., Moretta, L., Traverso, N., & Nitti, M. (2014). HO-1 up-regulation: A key point in high-risk neuroblastoma resistance to bortezomib. *Biochimica et Biophysica Acta - Molecular Basis of Disease*, *1842*(4), 613–622. https://doi.org/10.1016/j.bbadis.2013.12.008

Gan, L., Johnson, D. A., & Johnson, J. A. (2010). Keap1-Nrf2 activation in the presence and absence of DJ-1. *European Journal of Neuroscience*, *31*(6), 967–977. https://doi.org/10.1111/j.1460-9568.2010.07138.x

Garbe, C., & Eigentler, T. K. (2018). Small Molecules in Oncology. *Small Molecules in Oncology*. *Recent Results in Cancer Research*, *201*, 77–89. https://doi.org/10.1007/978-3-642-54490-3

Garibyan, L., & Fisher, D. E. (2010). How sunlight causes melanoma. *Current Oncology Reports*, *12*(5), 319–326. https://doi.org/10.1007/s11912-010-0119-y

Gollnick, S. O., Owczarczak, B., & Maier, P. (2006). Photodynamic therapy and anti-tumor immunity. *Lasers in Surgery and Medicine*, *38*(5), 509–515. https://doi.org/10.1002/lsm.20362

Gómez-Lomelí, P., Bravo-Cuellar, A., Hernández-Flores, G., Jave-Suárez, L. F., Aguilar-Lemarroy, A., Lerma-Díaz, J. M., Domínguez-Rodríguez, J. R., Sánchez-Reyes, K., & Ortiz-Lazareno, P. C. (2014). Increase of IFN-γ and TNF-α production in CD107a + NK-92 cells co-cultured with cervical cancer cell lines pre-treated with the HO-1 inhibitor. *Cancer Cell International*, *14*(1), 1–13. https://doi.org/10.1186/s12935-014-0100-1

Gozzelino, R., Jeney, V., & Soares, M. P. (2010). Mechanisms of Cell Protection by Heme Oxygenase-1. *Annual Review of Pharmacology and Toxicology*, *50*(1), 323–354. https://doi.org/10.1146/annurev.pharmtox.010909.105600

Graziani, G., Tentori, L., & Navarra, P. (2012). Ipilimumab: A novel immunostimulatory monoclonal antibody for the treatment of cancer. *Pharmacological Research*, *65*(1), 9–22.

https://doi.org/10.1016/j.phrs.2011.09.002

Grochot-Przeczek, A., Dulak, J., & Jozkowicz, A. (2012). Haem oxygenase-1: Non-canonical roles in physiology and pathology. *Clinical Science*, *122*(3), 93–103. https://doi.org/10.1042/CS20110147

Grochot-Przeczek, A., Lach, R., Mis, J., Skrzypek, K., Gozdecka, M., Sroczynska, P., Dubiel, M., Rutkowski, A., Kozakowska, M., Zagorska, A., Walczynski, J., Was, H., Kotlinowski, J., Drukala, J., Kurowski, K., Kieda, C., Herault, Y., Dulak, J., & Jozkowicz, A. (2009). Heme oxygenase-1 accelerates cutaneous wound healing in mice. *PLoS ONE*, *4*(6). https://doi.org/10.1371/journal.pone.0005803

Haga, Y., Tempero, M. A., Kay, D., & Zetterman, R. K. (1996). Intracellular accumulation of unconjugated bilirubin inhibits phytohemagglutinin-induced proliferation and interleukin-2 production of human lymphocytes. *Digestive Diseases and Sciences*, *41*(7), 1468–1474. https://doi.org/10.1007/BF02088574

Hall, A., Meyle, K. D., Lange, M. K., Klima, M., Sanderhoff, M., Dahl, C., Abildgaard, C., Thorup, K., Moghimi, S. M., Jensen, P. B., Bartek, J., Guldberg, P., & Christensen, C. (2013). Dysfunctional oxidative phosphorylation makes malignant melanoma cells addicted to glycolysis driven by the V600EBRAF oncogene. *Oncotarget*, *4*(4), 584–599. https://doi.org/10.18632/oncotarget.965

Hanada, N., Takahata, T., Zhou, Q., Ye, X., Sun, R., Itoh, J., Ishiguro, A., Kijima, H., Mimura, J., Itoh, K., Fukuda, S., & Saijo, Y. (2012). Methylation of the KEAP1 gene promoter region in human colorectal cancer. *BMC Cancer*, *12*, 1–11. https://doi.org/10.1186/1471-2407-12-66

Hayes, J. D., & Dinkova-Kostova, A. T. (2014). The Nrf2 regulatory network provides an interface between redox and intermediary metabolism. *Trends in Biochemical Sciences*, *39*(4), 199–218. https://doi.org/10.1016/j.tibs.2014.02.002

Hayes, J. D., & McMahon, M. (2009). NRF2 and KEAP1 mutations: permanent activation of an adaptive response in cancer. *Trends in Biochemical Sciences*, *34*(4), 176–188. https://doi.org/10.1016/j.tibs.2008.12.008

He, M., Nitti, M., Piras, S., Furfaro, A. L., Traverso, N., Pronzato, M. A., & Mann, G. E. (2015). Heme oxygenase-1-derived bilirubin protects endothelial cells against high glucose-induced damage. *Free Radical Biology and Medicine*, *89*, 91–98. https://doi.org/10.1016/j.freeradbiomed.2015.07.151

Henry, W. (1803). Experiments on the quantity of gases absorbed by water, at different temperatures, and under different pressures. *Royal Society*, *93*, 29–43. https://doi.org/10.11164/jjsps.8.3_292

Higgins, L. G., & Hayes, J. D. (2011). Mechanisms of induction of cytosolic and microsomal glutathione transferase (GST) genes by xenobiotics and pro-inflammatory agents. *Drug Metabolism Reviews*, *43*(2), 92–137. https://doi.org/10.3109/03602532.2011.567391

Hill, M., Pereira, V., Chauveau, C., Zagani, R., Remy, S., Tesson, L., Mazal, D., Ubillos, L., Brion, R., Ashgar, K., Mashreghi, M. F., Kotsch, K., Moffett, J., Doebis, C., Seifert, M., Boczkowski, J., Osinaga, E., & Anegon, I. (2005). Heme oxygenase-1 inhibits rat and human breast cancer cell proliferation: mutual cross inhibition with indoleamine 2,3-dioxygenase. *The FASEB Journal*, *19*(14), 1957–1968. https://doi.org/10.1096/fj.05-3875com

Hinshaw, D. C., & Shevde, L. A. (2019). The tumor microenvironment innately modulates cancer

progression. *Cancer Research*, *79*(18), 4557–4567. https://doi.org/10.1158/0008-5472.CAN-18-3962

Hirotsu, Y., Katsuoka, F., Funayama, R., Nagashima, T., Nishida, Y., Nakayama, K., Douglas Engel, J., & Yamamoto, M. (2012). Nrf2-MafG heterodimers contribute globally to antioxidant and metabolic networks. *Nucleic Acids Research*, *40*(20), 10228–10239. https://doi.org/10.1093/nar/gks827

Holland, R., & Fishbein, J. C. (2010). Chemistry of the cysteine sensors in kelch-like ECH-associated protein 1. *Antioxidants and Redox Signaling*, *13*(11), 1749–1761. https://doi.org/10.1089/ars.2010.3273

Holmquist-Mengelbier, L., Fredlund, E., Löfstedt, T., Noguera, R., Navarro, S., Nilsson, H., Pietras, A., Vallon-Christersson, J., Borg, Å., Gradin, K., Poellinger, L., & Påhlman, S. (2006). Recruitment of HIF-1α and HIF-2α to common target genes is differentially regulated in neuroblastoma: HIF-2α promotes an aggressive phenotype. *Cancer Cell*, *10*(5), 413–423. https://doi.org/10.1016/j.ccr.2006.08.026

Ichimura, Y., Waguri, S., Sou, Y. shin, Kageyama, S., Hasegawa, J., Ishimura, R., Saito, T., Yang, Y., Kouno, T., Fukutomi, T., Hoshii, T., Hirao, A., Takagi, K., Mizushima, T., Motohashi, H., Lee, M. S., Yoshimori, T., Tanaka, K., Yamamoto, M., & Komatsu, M. (2013). Phosphorylation of p62 Activates the Keap1-Nrf2 Pathway during Selective Autophagy. *Molecular Cell*, *51*(5), 618–631. https://doi.org/10.1016/j.molcel.2013.08.003

Imai, K., Matsuyama, S., Miyake, S., Suga, K., & Nakachi, K. (2000). Natural cytotoxic activity of peripheral-blood lymphocytes and cancer incidence: An 11-year follow-up study of a general population. *Lancet*, *356*(9244), 1795–1799. https://doi.org/10.1016/S0140-6736(00)03231-1

International Agency for Research on Cancer. (2013). *Estimated cancer incidence, mortality, and prevalence worldwide in 2012*. GLOBOCAN. http://globocan.iarc.fr

Itoh, K., Igarashi, K., Hayashi, N., Nishizawa, M., & Yamamoto, M. (1995). Cloning and characterization of a novel erythroid cell-derived CNC family transcription factor heterodimerizing with the small Maf family proteins. *Molecular and Cellular Biology*, *15*(8), 4184–4193. https://doi.org/10.1128/mcb.15.8.4184

Ivanov, V. N., & Hei, T. K. (2011). Regulation of apoptosis in human melanoma and neuroblastoma cells by statins, sodium arsenite and TRAIL: A role of combined treatment versus monotherapy. *Apoptosis*, *16*(12), 1268–1284. https://doi.org/10.1007/s10495-011-0649-2

Jain, A., Lamark, T., Sjøttem, E., Larsen, K. B., Awuh, J. A., Øvervatn, A., McMahon, M., Hayes, J. D., & Johansen, T. (2010). p62/SQSTM1 is a target gene for transcription factor NRF2 and creates a positive feedback loop by inducing antioxidant response element-driven gene transcription. *Journal of Biological Chemistry*, *285*(29), 22576–22591. https://doi.org/10.1074/jbc.M110.118976

Jaramillo, M. C., & Zhang, D. D. (2013). The emerging role of the Nrf2-Keap1 signaling pathway in cancer. *Genes and Development*, *27*(20), 2179–2191. https://doi.org/10.1101/gad.225680.113

Jayakumar, S., Kunwar, A., Sandur, S. K., Pandey, B. N., & Chaubey, R. C. (2014). Differential response of DU145 and PC3 prostate cancer cells to ionizing radiation: Role of reactive oxygen species, GSH and Nrf2 in radiosensitivity. *Biochimica et Biophysica Acta - General Subjects*, *1840*(1), 485–494.

https://doi.org/10.1016/j.bbagen.2013.10.006

Jeong, Y., Hoang, N. T., Lovejoy, A., Stehr, H., Aaron, M., Gentles, A. J., Kong, W., Truong, D., Martin, S., Heiser, D., Zhou, L., Say, C., Carter, J. N., Hiniker, S. M., Jr, B. W. L., West, R. B., Beachy, P., & Alizadeh, A. A. (2018). *Role of KEAP1/NRF2 and TP53 mutations in lung squamous cell carcinoma development and radiotherapy response prediction*. *7*(1), 86–101. https://doi.org/10.1158/2159-8290.CD-16-0127.Role

Johnson, D. B., & Puzanov, I. (2015). Treatment of NRAS-Mutant Melanoma. *Current Treatment Options in Oncology*, *16*(4). https://doi.org/10.1007/s11864-015-0330-z

Jözkowicz, A., Huk, I., Nigisch, A., Weigel, G., Dietrich, W., Motterlini, R., & Dulak, J. (2003). Heme oxygenase and angiogenic activity of endothelial cells: Stimulation by carbon monoxide and inhibition by tin protoporphyrin-IX. *Antioxidants and Redox Signaling*, *5*(2), 155–162. https://doi.org/10.1089/152308603764816514

Jozkowicz, A., Was, H., & Dulak, J. (2007). Europe PMC Funders Group Heme Oxygenase-1 in Tumors : Is It a False Friend? *Antioxid Redox Signal.*, *9*(12), 2099–2117. https://doi.org/10.1089/ars.2007.1659.Heme

Katoh, Y., Iida, K., Kang, M. Il, Kobayashi, A., Mizukami, M., Tong, K. I., McMahon, M., Hayes, J. D., Itoh, K., & Yamamoto, M. (2005). Evolutionary conserved N-terminal domain of Nrf2 is essential for the Keap1-mediated degradation of the protein by proteasome. *Archives of Biochemistry and Biophysics*, *433*(2), 342–350. https://doi.org/10.1016/j.abb.2004.10.012

Katoh, Y., Itoh, K., Yoshida, E., Miyagishi, M., Fukamizu, A., & Yamamoto, M. (2001). Two domains of Nrf2 cooperatively bind CBP, a CREB binding protein, and synergistically activate transcription. *Genes to Cells*, *6*(10), 857–868. https://doi.org/10.1046/j.1365-2443.2001.00469.x

Ke, Q., & Costa, M. (2006). *Hypoxia-Inducible Factor-1 (HIF-1)*. *70*(5), 1469–1480. https://doi.org/10.1124/mol.106.027029.ABBREVIATIONS

Keeley, T. P., & Mann, G. E. (2019). Defining physiological normoxia for improved translation of cell physiology to animal models and humans. *Physiological Reviews*, *99*(1), 161–234. https://doi.org/10.1152/physrev.00041.2017

Keyse, S. M., & Tyrrell, R. M. (1989). Heme oxygenase is the major 32-kDa stress protein induced in human skin fibroblasts by UVA radiation, hydrogen peroxide, and sodium arsenite. *Proceedings of the National Academy of Sciences of the United States of America*, *86*(1), 99–103. https://doi.org/10.1073/pnas.86.1.99

Kim, J. H., Yu, S., Chen, J. D., & Kong, A. N. (2013). The nuclear cofactor RAC3/AIB1/SRC-3 enhances Nrf2 signaling by interacting with transactivation domains. *Oncogene*, *32*(4), 514–527. https://doi.org/10.1038/onc.2012.59

Kiraz, Y., Baran, Y., & Nalbant, A. (2015). T cells in tumor microenvironment. *Tumor Biology*, *37*(1), 39–45. https://doi.org/10.1007/s13277-015-4241-1

Kiuru, M., & Busam, K. J. (2017). The NF1 gene in tumor syndromes and melanoma. *Laboratory Investigation*, *97*(2), 146–157. https://doi.org/10.1038/labinvest.2016.142

Kobayashi, A., Kang, M.-I., Watai, Y., Tong, K. I., Shibata, T., Uchida, K., & Yamamoto, M. (2006).

Oxidative and Electrophilic Stresses Activate Nrf2 through Inhibition of Ubiquitination Activity of Keap1. *Molecular and Cellular Biology*, *26*(1), 221–229. https://doi.org/10.1128/mcb.26.1.221-229.2006

Kobayashi, M., Li, L., Iwamoto, N., Nakajima-Takagi, Y., Kaneko, H., Nakayama, Y., Eguchi, M., Wada, Y., Kumagai, Y., & Yamamoto, M. (2009). The Antioxidant Defense System Keap1-Nrf2 Comprises a Multiple Sensing Mechanism for Responding to a Wide Range of Chemical Compounds. *Molecular and Cellular Biology*, *29*(2), 493–502. https://doi.org/10.1128/mcb.01080-08

Kobayashi, Makoto, Itoh, K., Suzuki, T., Osanai, H., Nishikawa, K., Katoh, Y., Takagi, Y., & Yamamoto, M. (2002). Identification of the interactive interface and phylogenic conservation of the Nrf2-Keap1 system. *Genes to Cells*, *7*(8), 807–820. https://doi.org/10.1046/j.1365-2443.2002.00561.x

Komatsu, M., Kurokawa, H., Waguri, S., Taguchi, K., Kobayashi, A., Ichimura, Y., Sou, Y. S., Ueno, I., Sakamoto, A., Tong, K. I., Kim, M., Nishito, Y., Iemura, S. I., Natsume, T., Ueno, T., Kominami, E., Motohashi, H., Tanaka, K., & Yamamoto, M. (2010). The selective autophagy substrate p62 activates the stress responsive transcription factor Nrf2 through inactivation of Keap1. *Nature Cell Biology*, *12*(3), 213–223. https://doi.org/10.1038/ncb2021

Kornev, A. P., Taylor, S. S., Jolla, L., & Jolla, L. (2016). *Dynamics driven allostery in protein kinases*. *40*(11), 628–647. https://doi.org/10.1016/j.tibs.2015.09.002.Dynamics

Kumar, A., Dailey, L. A., Swedrowska, M., Siow, R., Mann, G. E., Vizcay-Barrena, G., Arno, M., Mudway, I. S., & Forbes, B. (2016). Quantifying the magnitude of the oxygen artefact inherent in culturing airway cells under atmospheric oxygen versus physiological levels. *FEBS Letters*, *590*(2), 258–269. https://doi.org/10.1002/1873-3468.12026

Kumar, S. M., Yu, H., Edwards, R., Chen, L., Kazianis, S., Brafford, P., Acs, G., Herlyn, M., & Xu, X. (2007). Mutant V600E BRAF increases hypoxia inducible factor-1α expression in melanoma. *Cancer Research*, *67*(7), 3177–3184. https://doi.org/10.1158/0008-5472.CAN-06-3312

Kuphal, S., Winklmeier, A., Warnecke, C., & Bosserhoff, A. K. (2010). Constitutive HIF-1 activity in malignant melanoma. *European Journal of Cancer*, *46*(6), 1159–1169. https://doi.org/10.1016/j.ejca.2010.01.031

Laemmli, U. K. (1970). 227680a0. *Nature*, *227*, 680–685.

Lakshmikanth, T., Burke, S., Ali, T. H., Kimpfler, S., Ursini, F., Ruggeri, L., Capanni, M., Umansky, V., Paschen, A., Sucker, A., Pende, D., Groh, V., Biassoni, R., Höglund, P., Kato, M., Shibuya, K., Schadendorf, D., Anichini, A., Ferrone, S., … Colucci, F. (2009). Sfdphojujpo Boe Mztjt Pg Ivnbo Boe Npvtf Nfmbopnb Dfmm Mjoft Jo Wjusp Boe Jo Wjwp. *Journal of Clinical Investigation*, *119*(5), 1251–1263. https://doi.org/10.1172/JCI36022DS1

Lau, A., Wang, X.-J., Zhao, F., Villeneuve, N. F., Wu, T., Jiang, T., Sun, Z., White, E., & Zhang, D. D. (2010). A Noncanonical Mechanism of Nrf2 Activation by Autophagy Deficiency: Direct Interaction between Keap1 and p62. *Molecular and Cellular Biology*, *30*(13), 3275–3285. https://doi.org/10.1128/mcb.00248-10

Lavrovsky, Y., Schwartzman, M. L., Levere, R. D., Kappas, A., & Abraham, N. G. (1994). Identification of binding sites for transcription factors NF-κB and AP-2 in the promoter region of the human heme

oxygenase 1 gene. *Proceedings of the National Academy of Sciences of the United States of America*, *91*(13), 5987–5991. https://doi.org/10.1073/pnas.91.13.5987

Lee, S., Lim, M. J., Kim, M. H., Yu, C. H., Yun, Y. S., Ahn, J., & Song, J. Y. (2012). An effective strategy for increasing the radiosensitivity of Human lung Cancer cells by blocking Nrf2-dependent antioxidant responses. *Free Radical Biology and Medicine*, *53*(4), 807–816. https://doi.org/10.1016/j.freeradbiomed.2012.05.038

Lehraiki, A., Cerezo, M., Rouaud, F., Abbe, P., Allegra, M., Kluza, J., Marchetti, P., Imbert, V., Cheli, Y., Bertolotto, C., Ballotti, R., & Rocchi, S. (2015). Increased CD271 expression by the NF-kB pathway promotes melanoma cell survival and drives acquired resistance to BRAF inhibitor vemurafenib. *Cell Discovery*, *1*, 1–13. https://doi.org/10.1038/celldisc.2015.30

Levenberg, S., Rouwkema, J., Macdonald, M., Garfein, E. S., Kohane, D. S., Darland, D. C., Marini, R., Van Blitterswijk, C. A., Mulligan, R. C., D'Amore, P. A., & Langer, R. (2005). Engineering vascularized skeletal muscle tissue. *Nature Biotechnology*, *23*(7), 879–884. https://doi.org/10.1038/nbt1109

Li, K., Ouyang, L., He, M., Luo, M., Cai, W., Tu, Y., Pi, R., & Liu, A. (2017). IDH1 R132H mutation regulates glioma chemosensitivity through Nrf2 pathway. *Oncotarget*, *8*(17), 28865–28879. https://doi.org/10.18632/oncotarget.15868

Lim, J. H., Luo, C., Vazquez, F., & Puigserver, P. (2014). Targeting mitochondrial oxidative metabolism in melanoma causes metabolic compensation through glucose and glutamine utilization. *Cancer Research*, *74*(13), 3535–3545. https://doi.org/10.1158/0008-5472.CAN-13-2893-T

Lin, H. H., Chiang, M. T., Chang, P. C., & Chau, L. Y. (2015). Myeloid heme oxygenase-1 promotes metastatic tumor colonization in mice. *Cancer Science*, *106*(3), 299–306. https://doi.org/10.1111/cas.12604

Lin, Q., Weis, S., Yang, G., Weng, Y. H., Helston, R., Rish, K., Smith, A., Bordner, J., Polte, T., Gaunitz, F., & Dennery, P. A. (2007). Heme oxygenase-1 protein localizes to the nucleus and activates transcription factors important in oxidative stress. *Journal of Biological Chemistry*, *282*(28), 20621–20633. https://doi.org/10.1074/jbc.M607954200

Liu, L., Wu, Y., Bian, C., Nisar, M. F., Wang, M., Hu, X., Diao, Q., Nian, W., Wang, E., Xu, W., & Zhong, J. L. (2019). Heme oxygenase 1 facilitates cell proliferation via the B-Raf-ERK signaling pathway in melanoma. *Cell Communication and Signaling*, *17*(1), 1–12. https://doi.org/10.1186/s12964-018-0313-3

Loboda, A., Damulewicz, M., Pyza, E., Jozkowicz, A., & Dulak, J. (2016). Role of Nrf2/HO-1 system in development, oxidative stress response and diseases: an evolutionarily conserved mechanism. *Cellular and Molecular Life Sciences*, *73*(17), 3221–3247. https://doi.org/10.1007/s00018-016-2223-0

Loboda, A., Jazwa, A., Grochot-Przeczek, A., Rutkowski, A. J., Cisowski, J., Agarwal, A., Jozkowicz, A., & Dulak, J. (2008). Heme oxygenase-1 and the vascular bed: From molecular mechanisms to therapeutic opportunities. *Antioxidants and Redox Signaling*, *10*(10), 1767–1812. https://doi.org/10.1089/ars.2008.2043

Loboda, A., Jozkowicz, A., & Dulak, J. (2015). HO-1/CO system in tumor growth, angiogenesis and metabolism - Targeting HO-1 as an anti-tumor therapy. *Vascular Pharmacology*, *74*, 11–22. https://doi.org/10.1016/j.vph.2015.09.004

Lochhead, P., Kuchiba, A., Imamura, Y., Liao, X., Yamauchi, M., Nishihara, R., Qian, Z. R., Morikawa, T., Shen, J., Meyerhardt, J. A., Fuchs, C. S., & Ogino, S. (2013). Microsatellite instability and braf mutation testing in colorectal cancer prognostication. *Journal of the National Cancer Institute*, *105*(15), 1151–1156. https://doi.org/10.1093/jnci/djt173

López-Cobo, S., Pieper, N., Campos-Silva, C., García-Cuesta, E. M., Reyburn, H. T., Paschen, A., & Valés-Gómez, M. (2018). Impaired NK cell recognition of vemurafenib-treated melanoma cells is overcome by simultaneous application of histone deacetylase inhibitors. *OncoImmunology*, *7*(2). https://doi.org/10.1080/2162402X.2017.1392426

Luebker, S. A., & Koepsell, S. A. (2019). Diverse mechanisms of BRAF inhibitor resistance in melanoma identified in clinical and preclinical studies. *Frontiers in Oncology*, *9*(MAR), 1–8. https://doi.org/10.3389/fonc.2019.00268

Ma, D., Fang, Q., Wang, P., Gao, R., Wu, W., Lu, T., Cao, L., Hu, X., & Wang, J. (2015). Induction of Heme Oxygenase-1 by Na+-H+ exchanger 1 protein plays a crucial role in Imatinib-resistant chronic myeloid leukemia cells. *Journal of Biological Chemistry*, *290*(20), 12558–12571. https://doi.org/10.1074/jbc.M114.626960

Ma, J., Wang, H., Guo, S., Yi, X., Zhao, T., Liu, Y., Shi, Q., Gao, T., Li, C., & Guo, W. (2020). A20 promotes melanoma progression via the activation of Akt pathway. *Cell Death and Disease*, *11*(9). https://doi.org/10.1038/s41419-020-03001-y

MacKie, R. M., Hauschild, A., & Eggermont, A. M. M. (2009). Epidemiology of invasive cutaneous melanoma. *Annals of Oncology*, *20*(SUPPL. 4), 1–7. https://doi.org/10.1093/annonc/mdp252

Macleod, A. K., Mcmahon, M., Plummer, S. M., Higgins, L. G., Penning, T. M., Igarashi, K., & Hayes, J. D. (2009). Characterization of the cancer chemopreventive NRF2-dependent gene battery in human keratinocytes: Demonstration that the KEAP1-NRF2 pathway, and not the BACH1-NRF2 pathway, controls cytoprotection against electrophiles as well as redox-cycling compounds. *Carcinogenesis*, *30*(9), 1571–1580. https://doi.org/10.1093/carcin/bgp176

Mahabeleshwar, G. H., & Byzova, T. V. (2007). Angiogenesis in Melanoma. *Seminars in Oncology*, *34*(6), 555–565. https://doi.org/10.1053/j.seminoncol.2007.09.009

Mahmoud, S. M. A., Paish, E. C., Powe, D. G., Macmillan, R. D., Grainge, M. J., Lee, A. H. S., Ellis, I. O., & Green, A. R. (2011). Tumor-infiltrating CD8+ lymphocytes predict clinical outcome in breast cancer. *Journal of Clinical Oncology*, *29*(15), 1949–1955. https://doi.org/10.1200/JCO.2010.30.5037

Maines, M. D. (1988). Heme Oxygenase: function, multiplicity, regulatory mechanisms, and clinical applications. *Federation of America Societies For Experimental Biology*, *2*(10), 2557–2568. https://doi.org/10.1096/fasebj.2.10.3290025

Maines, M. D., Trakshel, G. M., & Kutty, R. K. (1986). Characterization of two constitutive forms of rat liver microsomal heme oxygenase. Only one molecular species of the enzyme is inducible. *Journal*

of Biological Chemistry, *261*(1), 411–419.

Malhotra, D., Portales-Casamar, E., Singh, A., Srivastava, S., Arenillas, D., Happel, C., Shyr, C., Wakabayashi, N., Kensler, T. W., Wasserman, W. W., & Biswal, S. (2010). Global mapping of binding sites for Nrf2 identifies novel targets in cell survival response through chip-seq profiling and network analysis. *Nucleic Acids Research*, *38*(17), 5718–5734. https://doi.org/10.1093/nar/gkq212

Mallia, A. K., Frovenzano, M. D., Fujimoto, E. K., Olson, B. J., Klenk, D. C., & Company, P. C. (1985). *1-S2.0-0003269785904427-Main.Pdf*. *85*, 76–85. https://doi.org/10.1016/0003-2697(85)90442-7

Mancuso, C. (2017). Bilirubin and brain: A pharmacological approach. In *Neuropharmacology* (Vol. 118). Elsevier Ltd. https://doi.org/10.1016/j.neuropharm.2017.03.013

Maniotis, A. J., Folberg, R., Hess, A., Seftor, E. A., Gardner, L. M. G., Pe'er, J., Trent, J. M., Meltzer, P. S., & Hendrix, M. J. C. (1999). Vascular channel formation by human melanoma cells in vivo and in vitro: Vasculogenic mimicry. *American Journal of Pathology*, *155*(3), 739–752. https://doi.org/10.1016/S0002-9440(10)65173-5

Mao, Y., Keller, E. T., Garfield, D. H., Shen, K., & Wang, J. (2013). Stromal cells in tumor microenvironment and breast cancer. *Cancer and Metastasis Reviews*, *32*(1–2), 303–315. https://doi.org/10.1007/s10555-012-9415-3

Martin, M. J., Hayward, R., Viros, A., & Marais, R. (2012). Metformin accelerates the growth of BRAFV600E -driven melanoma by upregulating VEGF-A. *Cancer Discovery*, *2*(4), 344–355. https://doi.org/10.1158/2159-8290.CD-11-0280

Martin, S., Prise, K. M., & Hill, M. A. (2019). Tumor oxygenation and cancer therapy—then and now. *British Journal of Radiology*, *92*(1093).

McArthur, G. A., Chapman, P. B., Robert, C., Larkin, J., & Haanen, J. B. (2014). *Safety and efficacy of vemurafenib in BRAFV600E and BRAFV600K mutation-positive melanoma (BRIM-3): extended follow-up of a phase 3, randomised, open-label study*. *15*(3), 323–332. https://doi.org/10.1126/science.1249098.Sleep

McBean, G. J., Aslan, M., Griffiths, H. R., & Torrão, R. C. (2015). Thiol redox homeostasis in neurodegenerative disease. *Redox Biology*, *5*, 186–194. https://doi.org/10.1016/j.redox.2015.04.004

McMahon, M., Itoh, K., Yamamoto, M., & Hayes, J. D. (2003). Keap1-dependent proteasomal degradation of transcription factor Nrf2 contributes to the negative regulation of antioxidant response element-driven gene expression. *Journal of Biological Chemistry*, *278*(24), 21592–21600. https://doi.org/10.1074/jbc.M300931200

McMahon, M., Lamont, D. J., Beattie, K. A., & Hayes, J. D. (2010). Keap1 perceives stress via three sensors for the endogenous signaling molecules nitric oxide, zinc, and alkenals. *Proceedings of the National Academy of Sciences of the United States of America*, *107*(44), 18838–18843. https://doi.org/10.1073/pnas.1007387107

McMahon, M., Thomas, N., Itoh, K., Yamamoto, M., & Hayes, J. D. (2004). Redox-regulated turnover of Nrf2 is determined by at least two separate protein domains, the redox-sensitive Neh2 degron and the redox-insensitive Neh6 degron. *Journal of Biological Chemistry*, *279*(30), 31556–31567. https://doi.org/10.1074/jbc.M403061200

McMahon, M., Thomas, N., Itoh, K., Yamamoto, M., & Hayes, J. D. (2006). Dimerization of substrate adaptors can facilitate Cullin-mediated ubiquitylation of proteins by a 'tethering' mechanism: A two-site interaction model for the Nrf2-Keap1 complex. *Journal of Biological Chemistry*, *281*(34), 24756–24768. https://doi.org/10.1074/jbc.M601119200

Menegon, S., Columbano, A., & Giordano, S. (2016). The Dual Roles of NRF2 in Cancer. *Trends in Molecular Medicine*, *22*(7), 578–593. https://doi.org/10.1016/j.molmed.2016.05.002

Menon, D. R., Das, S., Krepler, C., Vultur, A., Rinner, B., Schauer, S., Kashofer, K., Wagner, K., Zhang, G., Bonyadi Rad, E., Haass, N. K., Soyer, H. P., Gabrielli, B., Somasundaram, R., Hoefler, G., Herlyn, M., & Schaider, H. (2015). A stress-induced early innate response causes multidrug tolerance in melanoma. *Oncogene*, *34*(34), 4448–4459. https://doi.org/10.1038/onc.2014.372

Mimura, I., & Nangaku, M. (2010). The suffocating kidney: tubulointerstitial hypoxia in end-stage renal disease. *Nature Reviews Nephrology*, *6*(11), 667–678. https://doi.org/10.1038/nrneph.2010.124

Mitsuishi, Y., Motohashi, H., & Yamamoto, M. (2012). The Keap1–Nrf2 system in cancers: stress response and anabolic metabolism. *Frontiers in Oncology*, *2*(December), 1–13. https://doi.org/10.3389/fonc.2012.00200

Miyake, M., Fujimoto, K., Anai, S., Ohnishi, S., Kuwada, M., Nakai, Y., Inoue, T., Matsumura, Y., Tomioka, A., Ikeda, T., Tanaka, N., & Hirao, Y. (2011). Heme oxygenase-1 promotes angiogenesis in urothelial carcinoma of the urinary bladder. *Oncology Reports*, *25*(3), 653–660. https://doi.org/10.3892/or.2010.1125

Moi, P., Chan, K., Asunis, I., Cao, A., & Kan, Y. W. (1994). Isolation of NF-E2-related factor 2 (Nrf2), a NF-E2-like basic leucine zipper transcriptional activator that binds to the tandem NF-E2/AP1 repeat of the β-globin locus control region. *Proceedings of the National Academy of Sciences of the United States of America*, *91*(21), 9926–9930. https://doi.org/10.1073/pnas.91.21.9926

Mondragon-Teran, P., Lye, G. J., & Veraitch, F. S. (2009). Lowering oxygen tension enhances the differentiation of mouse embryonic stem cells into neuronal cells. *Biotechnology Progress*, *25*(5), 1480–1488. https://doi.org/10.1002/btpr.248

Moon, E. J., & Giaccia, A. (2015). Dual roles of NRF2 in tumor prevention and progression: Possible implications in cancer treatment. *Free Radical Biology and Medicine*, *79*, 292–299. https://doi.org/10.1016/j.freeradbiomed.2014.11.009

Moretta, A., Marcenaro, E., Sivori, S., Della Chiesa, M., Vitale, M., & Moretta, L. (2005). Early liaisons between cells of the innate immune system in inflamed peripheral tissues. *Trends in Immunology*, *26*(12), 668–675. https://doi.org/10.1016/j.it.2005.09.008

Mosmann, T. (1983). Rapid colorimetric assay for cellular growth and survival: Application to proliferation and cytotoxicity assays. *Journal of Immunological Methods*, *65*(1–2), 55–63. https://doi.org/10.1016/0022-1759(83)90303-4

Motohashi, H., & Yamamoto, M. (2004). Nrf2-Keap1 defines a physiologically important stress response mechanism. *Trends in Molecular Medicine*, *10*(11), 549–557. https://doi.org/10.1016/j.molmed.2004.09.003

Muliaditan, T., Opzoomer, J. W., Caron, J., Okesola, M., Kosti, P., Lall, S., Van Hemelrijck, M., Dazzi,

F., Tutt, A., Grigoriadis, A., Gillett, C. E., Madden, S. F., Burchell, J. M., Kordasti, S., Diebold, S. S., Spicer, J. F., & Arnold, J. N. (2018). Repurposing tin mesoporphyrin as an immune checkpoint inhibitor shows therapeutic efficacy in preclinical models of cancer. *Clinical Cancer Research*, *24*(7), 1617–1628. https://doi.org/10.1158/1078-0432.CCR-17-2587

Muñoz-Couselo, E., Adelantado, E. Z., Ortiz, C., García, J. S., & Perez-Garcia, J. (2017). NRAS-mutant melanoma: Current challenges and future prospect. *OncoTargets and Therapy*, *10*, 3941–3947. https://doi.org/10.2147/OTT.S117121

Muscarella, L. A., Parrella, P., D'Alessandro, V., la Torre, A., Barbano, R., Fontana, A., Tancredi, A., Guarnieri, V., Balsamo, T., Coco, M., Copetti, M., Pellegrini, F., de Bonis, P., Bisceglia, M., Scaramuzzi, G., Maiello, E., Valori, V. M., Merla, G., Vendemiale, G., & Fazio, V. M. (2011). Frequent epigenetics inactivation of KEAP1 gene in non-small cell lung cancer. *Epigenetics*, *6*(6), 710–719. https://doi.org/10.4161/epi.6.6.15773

Na, H. K., & Surh, Y. J. (2014). Oncogenic potential of Nrf2 and its principal target protein heme oxygenase-1. *Free Radical Biology and Medicine*, *67*, 353–365. https://doi.org/10.1016/j.freeradbiomed.2013.10.819

Naito, Y., Takagi, T., & Higashimura, Y. (2014). Heme oxygenase-1 and anti-inflammatory M2 macrophages. *Archives of Biochemistry and Biophysics*, *564*(September), 83–88. https://doi.org/10.1016/j.abb.2014.09.005

Nazarian, R., Shi, H., Wang, Q., Kong, X., Koya, R. C., Lee, H., Chen, Z., Lee, M.-K., Attar, N., Sazegar, H., Chodon, T., Nelson, S. F., McArthur, G., Sosman, J. A., Ribas, A., & Lo, R. S. (2011). Melanomas acquire resistance to B-RAF(V600E) inhibition by RTK or N-RAS upregulation. *Bone*, *23*(1), 1–7. https://doi.org/10.1161/CIRCULATIONAHA.110.956839

Nioi, P., & Nguyen, T. (2007). A mutation of Keap1 found in breast cancer impairs its ability to repress Nrf2 activity. *Biochemical and Biophysical Research Communications*, *362*(4), 816–821. https://doi.org/10.1016/j.bbrc.2007.08.051

Nitti, M., Furfaro, A. L., & Mann, G. E. (2020). Heme Oxygenase Dependent Bilirubin Generation in Vascular Cells: A Role in Preventing Endothelial Dysfunction in Local Tissue Microenvironment? *Frontiers in Physiology*, *11*(January), 1–20. https://doi.org/10.3389/fphys.2020.00023

Nitti, M., Piras, S., Marinari, U. M., Moretta, L., Pronzato, M. A., & Furfaro, A. L. (2017). HO-1 induction in cancer progression: A matter of cell adaptation. *Antioxidants*, *6*(2), 1–20. https://doi.org/10.3390/antiox6020029

Nuhn, P., Künzli, B. M., Hennig, R., Mitkus, T., Ramanauskas, T., Nobiling, R., Meuer, S. C., Friess, H., & Berberat, P. O. (2009). Heme oxygenase-1 and its metabolites affect pancreatic tumor growth in vivo. *Molecular Cancer*, *8*, 1–10. https://doi.org/10.1186/1476-4598-8-37

Ogawa, K., Sun, J., Taketani, S., Nakajima, O., Nishitani, C., Sassa, S., Hayashi, N., Yamamoto, M., Shibahara, S., Fujita, H., & Igarashi, K. (2001). Heme mediates derepression of Maf recognition element through direct binding to transcription repressor Bach1. *EMBO Journal*, *20*(11), 2835–2843. https://doi.org/10.1093/emboj/20.11.2835

Osburn, W. O., & Kensler, T. W. (2008). Nrf2 signaling: An adaptive response pathway for protection

against environmental toxic insults. *Mutation Research - Reviews in Mutation Research*, *659*(1–2), 31–39. https://doi.org/10.1016/j.mrrev.2007.11.006

Osrodek, M., Hartman, M. L., & Czyz, M. (2019). Physiologically Relevant Oxygen Concentration (6 % O 2) as an Important Component of the Microenvironment Impacting Melanoma Phenotype and Melanoma Response to Targeted Therapeutics In Vitro. *International Journal of Molecular Sciences*, *20*(4203). https://doi.org/10.3390/ijms20174203

Paek, J., Lo, J. Y., Narasimhan, S. D., Nguyen, T. N., Glover-Cutter, K., Robida-Stubbs, S., Suzuki, T., Yamamoto, M., Blackwell, T. K., & Curran, S. P. (2012). Mitochondrial SKN-1/Nrf mediates a conserved starvation response. *Cell Metabolism*, *16*(4), 526–537. https://doi.org/10.1016/j.cmet.2012.09.007

Pagès, F., Galon, J., Dieu-Nosjean, M. C., Tartour, E., Sautès-Fridman, C., & Fridman, W. H. (2010). Immune infiltration in human tumors: A prognostic factor that should not be ignored. *Oncogene*, *29*(8), 1093–1102. https://doi.org/10.1038/onc.2009.416

Paladino, S., Conte, A., Caggiano, R., Pierantoni, G. M., & Faraonio, R. (2018). Nrf2 pathway in age-related neurological disorders: Insights into MicroRNAs. *Cellular Physiology and Biochemistry*, *47*(5), 1951–1976. https://doi.org/10.1159/000491465

Pan, J. H., Zhou, H., Zhu, S. Bin, Huang, J. L., Zhao, X. X., Ding, H., & Pan, Y. L. (2018). Development of small-molecule therapeutics and strategies for targeting RAF kinase in BRAF-mutant colorectal cancer. *Cancer Management and Research*, *10*, 2289–2301. https://doi.org/10.2147/CMAR.S170105

Pietra, G., Manzini, C., Rivara, S., Vitale, M., Cantoni, C., Petretto, A., Balsamo, M., Conte, R., Benelli, R., Minghelli, S., Solari, N., Gualco, M., Queirolo, P., Moretta, L., & Mingari, M. C. (2012). Melanoma cells inhibit natural killer cell function by modulating the expression of activating receptors and cytolytic activity. *Cancer Research*, *72*(6), 1407–1415. https://doi.org/10.1158/0008-5472.CAN-11-2544

Pietra, G., Manzini, C., Vitale, M., Balsamo, M., Ognio, E., Boitano, M., Queirolo, P., Moretta, L., & Mingari, M. C. (2009). Natural killer cells kill human melanoma cells with characteristics of cancer stem cells. *International Immunology*, *21*(7), 793–801. https://doi.org/10.1093/intimm/dxp047

Pimstone, N. R., Engel, P., Tenhunen, R., Seitz, P. T., Marver, H. S., & Schmid, R. (1971). Inducible heme oxygenase in the kidney: a model for the homeostatic control of hemoglobin catabolism. *The Journal of Clinical Investigation*, *50*(10), 2042–2050. https://doi.org/10.1172/JCI106697

Pinder, A. G., & James, P. E. (2009). When does low oxygen become hypoxia? Implications for nitrite reduction. *Circulation Research*, *104*(3), 25–26. https://doi.org/10.1161/CIRCRESAHA.108.191569

Piras, S., Furfaro, A. L., Brondolo, L., Passalacqua, M., Marinari, U. M., Pronzato, M. A., & Nitti, M. (2017). Differentiation impairs Bach1 dependent HO-1 activation and increases sensitivity to oxidative stress in SH-SY5Y neuroblastoma cells. *Scientific Reports*, *7*(1), 1–12. https://doi.org/10.1038/s41598-017-08095-7

Pucciarelli, D., Lengger, N., Takacova, M., Csaderova, L., Bartosova, M., Breiteneder, H., Pastorekova,

S., & Hafner, C. (2015). Anti-chondroitin sulfate proteoglycan 4-specific antibodies modify the effects of vemurafenib on melanoma cells differentially in normoxia and hypoxia. *International Journal of Oncology*, *47*(1), 81–90. https://doi.org/10.3892/ijo.2015.3010

Qian, B., & J. W. Pollard. (2010). Macrophage diversity enhances tumor progression and metastasis. *Cell*, *141*(1), 1477–1490. https://doi.org/10.1161/CIRCRESAHA.116.303790.The

Rada, P., Rojo, A. I., Chowdhry, S., McMahon, M., Hayes, J. D., & Cuadrado, A. (2011). SCF/ -TrCP Promotes Glycogen Synthase Kinase 3-Dependent Degradation of the Nrf2 Transcription Factor in a Keap1-Independent Manner. *Molecular and Cellular Biology*, *31*(6), 1121–1133. https://doi.org/10.1128/mcb.01204-10

Rafique, I., Kirkwood, J. M., & Tarhini, A. A. (2015). Immune Checkpoint Blockade and Interferon-α in Melanoma. *Semin Oncology*, *42*(3), 436–447. https://doi.org/10.1016/j.physbeh.2017.03.040

Raghunath, A., Sundarraj, K., Nagarajan, R., Arfuso, F., Bian, J., Kumar, A. P., Sethi, G., & Perumal, E. (2018). Antioxidant response elements: Discovery, classes, regulation and potential applications. *Redox Biology*, *17*(April), 297–314. https://doi.org/10.1016/j.redox.2018.05.002

Ramesh, R., Munshi, A., & Panda, S. K. (1992). Polymerase chain reaction. *The National Medical Journal of India*, *5*(3), 115–119.

Rastrelli, M., Tropea, S., Rossi, C., & Alaibac, M. (2014). Melanoma: Epidemiology, Risk Factors, Pathogenesis, Diagnosis and Classification. *In Vivo (Athens, Greece)*, *28*(6), 1005–10012. http://www.ncbi.nlm.nih.gov/pubmed/25398793

Ratcliffe, P. J., O'Rourke, J. F., Maxwell, P. H., & Pugh, C. W. (1998). Oxygen sensing, hypoxia-inducible factor-1 and the regulation of mammalian gene expression. *Journal of Experimental Biology*, *201*(8), 1153–1162.

Reddy, B. Y., Miller, D. M., & Tsao, H. (2017). Somatic driver mutations in melanoma. *Cancer*, *123*, 2104–2117. https://doi.org/10.1002/cncr.30593

Rigel, D. S. (2010). Epidemiology of Melanoma. *Seminars in Cutaneous Medicine and Surgery*, *29*(4), 204–209. https://doi.org/10.1016/j.sder.2010.10.005

Roberts, D. L. ., A.V.ANSTEY, .BARLOW, R. J., N.H.COXà, BISHOP, J. A. N., P.G.CORRIE, J.EVANS, M.E.GORE, P.N.HALL, & N.KIRKHAM. (2002). UK guidelines for the management of cutaneous melanoma. *British Journal of Plastic Surgery*, *146*, 7–17. https://doi.org/10.1054/bjps.2002.3944

Rojo de la Vega, M., Chapman, E., & Zhang, D. D. (2018). NRF2 and the Hallmarks of Cancer. *Cancer Cell*, *34*(1), 21–43. https://doi.org/10.1016/j.ccell.2018.03.022

Romano, P., Manniello, A., Aresu, O., Armento, M., Cesaro, M., & Parodi, B. (2009). Cell Line Data Base: Structure and recent improvements towards molecular authentication of human cell lines. *Nucleic Acids Research*, *37*(SUPPL. 1), 925–932. https://doi.org/10.1093/nar/gkn730

Rushmore, T. H., Morton, M. R., & Pickett, C. B. (1991). The Antioxidant Responsive Element. *The Journal of Biological Chemistry*, *266*(18), 11632–11639. http://www.jbc.org/content/266/18/11632.full.pdf

Ryter, S. W., & Choi, A. M. K. (2016). Targeting Heme Oxygenase-1/Carbon Monoxide for Therapeutic

Modulation of Inflammation. *Transl Res*, *167*(1), 7–34. https://doi.org/10.1016/j.trsl.2015.06.011.Targeting

Schadendorf, D., van Akkooi, A. C. J., Berking, C., Griewank, K. G., Gutzmer, R., Hauschild, A., Stang, A., Roesch, A., & Ugurel, S. (2018). Melanoma. *The Lancet*, *392*(10151), 971–984. https://doi.org/10.1016/S0140-6736(18)31559-9

Schillingmann, D., Riese, S., Vijayan, V., Tischer-Zimmermann, S., Schmetzer, H., Maecker-Kolhoff, B., Blasczyk, R., Immenschuh, S., & Eiz-Vesper, B. (2019). Inhibition of Heme Oxygenase-1 Activity Enhances Wilms Tumor-1-Specific T-Cell Responses in Cancer Immunotherapy. *International Journal of Molecular Sciences*, *20*(3), 482. https://doi.org/10.3390/ijms20030482

Schreck, R., & Rapp, U. R. (2006). Raf kinases: Oncogenesis and drug discovery. *International Journal of Cancer*, *119*(10), 2261–2271. https://doi.org/10.1002/ijc.22144

Schwartz, H. P., Haberman, B. E., & Ruddy, R. M. (2011). Hyperbilirubinemia: Current guidelines and emerging therapies. *Pediatric Emergency Care*, *27*(9), 884–889. https://doi.org/10.1097/PEC.0b013e31822c9b4c

Semenza, G. L. (2014). Oxygen Sensing, Hypoxia-Inducible Factors, and Disease Pathophysiology. *Annual Review of Pathology: Mechanisms of Disease*, *9*(1), 47–71. https://doi.org/10.1146/annurev-pathol-012513-104720

Seo, G. S., Jiang, W. Y., Chi, J. H., Jin, H., Park, W. C., Sohn, D. H., Park, P. H., & Lee, S. H. (2015). Heme oxygenase-1 promotes tumor progression and metastasis of colorectal carcinoma cells by inhibiting antitumor immunity. *Oncotarget*, *6*(23), 19792–19806. https://doi.org/10.18632/oncotarget.4075

Shain, A. H., & Bastian, B. C. (2016). From melanocytes to melanomas. *Nature Reviews Cancer*, *16*(6), 345–358. https://doi.org/10.1038/nrc.2016.37

Shang, F. tai, Hui, L. liang, An, X. sheng, Zhang, X. cheng, Guo, S. guang, & Kui, Z. (2015). ZnPPIX inhibits peritoneal metastasis of gastric cancer via its antiangiogenic activity. *Biomedicine and Pharmacotherapy*, *71*, 240–246. https://doi.org/10.1016/j.biopha.2015.03.005

Shen, H., Yang, Y., Xia, S., Rao, B., Zhang, J., & Wang, J. (2014). Blockage of Nrf2 suppresses the migration and invasion of esophageal squamous cell carcinoma cells in hypoxic microenvironment. *Diseases of the Esophagus*, *27*(7), 685–692. https://doi.org/10.1111/dote.12124

Shi, J., Yu, J., Zhang, Y., Wu, L., Dong, S., Wu, L., Wu, L., Du, S., Zhang, Y., & Ma, D. (2019). PI3K/Akt pathway-mediated HO-1 induction regulates mitochondrial quality control and attenuates endotoxin-induced acute lung injury. *Laboratory Investigation*, *99*(12), 1795–1809. https://doi.org/10.1038/s41374-019-0286-x

Shibata, T., Ohta, T., Tong, K. I., Kokubu, A., Odogawa, R., Tsuta, K., Asamura, H., Yamamoto, M., & Hirohashi, S. (2008). Cancer related mutations in NRF2 impair its recognition by Keap1-Cul3 E3 ligase and promote malignancy. *Proceedings of the National Academy of Sciences of the United States of America*, *105*(36), 13568–13573. https://doi.org/10.1073/pnas.0806268105

Shibata, T., Saito, S., Kokubu, A., Suzuki, T., Yamamoto, M., & Hirohashi, S. (2010). Global downstream pathway analysis reveals a dependence of oncogenic NF-E2 - Related factor 2 mutation on the mTOR

growth signaling pathway. *Cancer Research*, *70*(22), 9095–9105. https://doi.org/10.1158/0008-5472.CAN-10-0384

Siegel, R. L., Miller, K. D., & Jemal, A. (2017). Cancer statistics, 2017. *CA: A Cancer Journal for Clinicians*, *67*(1), 7–30. https://doi.org/10.3322/caac.21387

Speyer, C. L., Hachem, A. H., Assi, A. A., Johnson, J. S., DeVries, J. A., & Gorski, D. H. (2014). Metabotropic glutamate receptor-1 as a novel target for the antiangiogenic treatment of breast cancer. *PLoS ONE*, *9*(3). https://doi.org/10.1371/journal.pone.0088830

Stacy, D., Ely, K., Massion, P., WG, Y., Hallahan, D., Sekhar, K., & Freeman, M. (2006). INCREASED EXPRESSION OF NUCLEAR FACTOR E2 p45-RELATED FACTOR 2 (NRF2) IN HEAD AND NECK SQUAMOUS CELL CARCINOMAS. *Head and Neck*, 813–818. https://doi.org/10.1002/HED

Stocker, R., Yamamoto, Y., McDonagh, A. F., Glazer, A. N., & Ames, B. N. (1987). Bilirubin is an antioxidant of possible physiological importance. *Science*, *235*(4792), 1043–1046. https://doi.org/10.1126/science.3029864

Stones, C. J., Kim, J. E., Joseph, W. R., Leung, E., Marshall, E. S., Finlay, G. J., Shelling, A. N., & Baguley, B. C. (2013). Comparison of responses of human melanoma cell lines to MEK and BRAF inhibitors. *Frontiers in Genetics*, *4*(MAY), 1–6. https://doi.org/10.3389/fgene.2013.00066

Strojan, P. (2010). Role of radiotherapy in melanoma management. *Radiology and Oncology*, *44*(1), 1–12. https://doi.org/10.2478/v10019-010-0008-x

Sundararaghavan, V. L., Binepal, S., Stec, D. E., Sindhwani, P., & Jr, T. D. H. (2018). Bilirubin, a new therapeutic for kidney transplant? *Transplant Rec2*, *32*(4), 234–240. https://doi.org/10.1016/j.trre.2018.06.003.Bilirubin

Taguchi, K., Fujikawa, N., Komatsu, M., Ishii, T., Unno, M., Akaike, T., Motohashi, H., & Yamamoto, M. (2012). Keap1 degradation by autophagy for the maintenance of redox homeostasis. *Proceedings of the National Academy of Sciences of the United States of America*, *109*(34), 13561–13566. https://doi.org/10.1073/pnas.1121572109

Taguchi, K., Motohashi, H., & Yamamoto, M. (2011). Molecular mechanisms of the Keap1-Nrf2 pathway in stress response and cancer evolution. *Genes to Cells*, *16*(2), 123–140. https://doi.org/10.1111/j.1365-2443.2010.01473.x

Taira, T., Saito, Y., Niki, T., Iguchi-Ariga, S. M. M., Takahashi, K., & Ariga, H. (2004). DJ-1 has a role in antioxidative stress to prevent cell death. *EMBO Reports*, *5*(2), 213–218. https://doi.org/10.1038/sj.embor.7400074

Takaya, K., Suzuki, T., Motohashi, H., Onodera, K., Satomi, S., Kensler, T. W., & Yamamoto, M. (2012). Validation of the multiple sensor mechanism of the Keap1-Nrf2 system. *Free Radical Biology and Medicine*, *53*(4), 817–827. https://doi.org/10.1016/j.freeradbiomed.2012.06.023

Taube, J. M., Galon, J., Sholl, L. M., Rodig, S. J., Cottrell, T. R., Giraldo, N. A., Baras, A. S., Patel, S. S., Anders, R. A., & David, L. (2018). *Implications of the tumor immune microenvironment for staging and therapeutics*. *31*(2), 214–234. https://doi.org/10.1038/modpathol.2017.156.Implications

Tebay et al. (2016). Pathways Through Which It Attenuates Degenerative Disease. *Free Radic Biol Med*,

88(0 0), 108–146. https://doi.org/10.1016/j.freeradbiomed.2015.06.021.Mechanisms

Tenhunen, R., Marver, H., Pimstone, N. R., Träger, W. F., Cooper, D. Y., & Schmid, R. (1972). Enzymatic Degradation of Heme. Oxygenative Cleavage Requiring Cytochrome P-450. *Biochemistry*, *11*(9), 1716–1720. https://doi.org/10.1021/bi00759a029

Tenhunen, R., Marver, H. S., & Schmid, R. (1968). The enzymatic conversion of heme to bilirubin by microsomal heme oxygenase. *Proceedings of the National Academy of Sciences of the United States of America*, *61*(2), 748–755. https://doi.org/10.1073/pnas.61.2.748

Tenhunen, Raimo, Marven, H. S., & Schmid, R. (1969). Microsomal Heme Oxygenase. Characterization of the enzyme. *The Journal of Biological Chemistry*, *244*(23), 6388–6394.

Terry, C. M., Clikeman, J. A., Hoidal, J. R., & Callahan, K. S. (1998). Effect of tumor necrosis factor-a and interleukin-la on heme oxygenase-1 expression in human endothelial cells. *American Journal of Physiology*, *274*(3 PART 2), 883–891.

The Cancer Genome Atlas Network. (2015). *Genomic classification of cutaneous melanoma.*

Tibullo, D., Barbagallo, I., Giallongo, C., La Cava, P., Parrinello, N., Vanella, L., Stagno, F., A. Palumbo, G., Li Volti, G., & Di Raimondo, F. (2013). Nuclear Translocation of Heme Oxygenase-1 Confers Resistance to Imatinib in Chronic Myeloid Leukemia Cells. *Current Pharmaceutical Design*, *19*(15), 2765–2770. https://doi.org/10.2174/1381612811319150012

Tong, K. I., Katoh, Y., Kusunoki, H., Itoh, K., Tanaka, T., & Yamamoto, M. (2006). Keap1 Recruits Neh2 through Binding to ETGE and DLG Motifs: Characterization of the Two-Site Molecular Recognition Model. *Molecular and Cellular Biology*, *26*(8), 2887–2900. https://doi.org/10.1128/mcb.26.8.2887-2900.2006

Torres-Collado, A. X., Knott, J., & Jazirehi, A. R. (2018). Reversal of resistance in targeted therapy of metastatic melanoma: Lessons learned from vemurafenib (BRAFV600E-specific inhibitor). *Cancers*, *10*(6). https://doi.org/10.3390/cancers10060157

Traverso, N., Ricciarelli, R., Nitti, M., Marengo, B., Furfaro, A. L., Pronzato, M. A., Marinari, U. M., & Domenicotti, C. (2013). Role of glutathione in cancer progression and chemoresistance. *Oxidative Medicine and Cellular Longevity*, *2013*. https://doi.org/10.1155/2013/972913

Trinh, V. A., & Hagen, B. (2013). Ipilimumab for advanced melanoma: A pharmacologic perspective. *Journal of Oncology Pharmacy Practice*, *19*(3), 195–201. https://doi.org/10.1177/1078155212459100

Tsai, J., Lee, J. T., Wang, W., Zhang, J., Cho, H., Mamo, S., Bremer, R., Gillette, S., Kong, J., Haass, N. K., Sproesser, K., Li, L., Smalley, K. S. M., Fong, D., Zhu, Y. L., Marimuthu, A., Nguyen, H., Lam, B., Liu, J., … Bollag, G. (2008). Discovery of a selective inhibitor of oncogenic B-Raf kinase with potent antimelanoma activity. *Proceedings of the National Academy of Sciences of the United States of America*, *105*(8), 3041–3046. https://doi.org/10.1073/pnas.0711741105

Tsai, M. T., & Tarng, D. C. (2019). Beyond a measure of liver function—bilirubin acts as a potential cardiovascular protector in chronic kidney disease patients. *International Journal of Molecular Sciences*, *20*(1), 1–19. https://doi.org/10.3390/ijms20010117

Valaes, T., Petmezaki, S., Henschke, C., Drummond, G. S., & Kappas, A. (1994). Control of jaundice in

preterm newborns by an inhibitor of bilirubin production: studies with tin-mesoporphyrin. *Pediatrics*, *93*(1), 1–11.

van der Wijst, M. G. P., Brown, R., & Rots, M. G. (2014). Nrf2, the master redox switch: The Achilles' heel of ovarian cancer? *Biochimica et Biophysica Acta - Reviews on Cancer*, *1846*(2), 494–509. https://doi.org/10.1016/j.bbcan.2014.09.004

Vaupel, P., Höckel, M., & Mayer, A. (2007). Detection and characterization of tumor hypoxia using pO2 histography. *Antioxidants and Redox Signaling*, *9*(8), 1221–1235. https://doi.org/10.1089/ars.2007.1628

Villanueva, J., Vultur, A., & Herlyn, M. (2013). Future Treatment Options. *Cancer Research*, *71*(23), 7137–7140. https://doi.org/10.1158/0008-5472.CAN-11-1243.Resistance

Vivier, E., Raulet, D. H., Moretta, A., Caligiuri, M. A., Zitvogel, L., Lanier, L. L., Yokoyama, W. M., & Ugolini, S. (2011). Innate or adaptive immunity? The example of natural killer cells. Science. 2011;331(6013):44–9. *Science*, *331*(6013), 44–49. https://doi.org/10.1126/science.1198687.Innate

Vu, K., Weksler, B., Romero, I., Couraud, P. O., & Gelli, A. (2009). Immortalized human brain endothelial cell line HCMEC/D3 as a model of the blood-brain barrier facilitates in vitro studies of central nervous system infection by cryptococcus neoformans. *Eukaryotic Cell*, *8*(11), 1803–1807. https://doi.org/10.1128/EC.00240-09

Wagle, N., Emery, C., Berger, M. F., Davis, M. J., Sawyer, A., Pochanard, P., Kehoe, S. M., Johannessen, C. M., MacConaill, L. E., Hahn, W. C., Meyerson, M., & Garraway, L. A. (2011). Dissecting therapeutic resistance to RAF inhibition in melanoma by tumor genomic profiling. *Journal of Clinical Oncology*, *29*(22), 3085–3096. https://doi.org/10.1200/JCO.2010.33.2312

Wallace, M. R., Marchunk, D. A., Andersen, L. B., Letcher, R., Odeh, H. M., Saulino, A. M., Fountain, J. W., Brereton, A., Nicholson, J., Mitcheli, A. L., Brownstein, B. H., & Collins, F. S. (1990). Type I neurofibrimatosis Gene: Identification of a Large Transcript in Three NF1 Patients. *Science*, *249*(4965), 181–186. https://doi.org/10.1136/jmg.25.8.573-a

Wang, A. X., & Qi, X. Y. (2013). Targeting RAS/RAF/MEK/ERK signaling in metastatic melanoma. *IUBMB Life*, *65*(9), 748–758. https://doi.org/10.1002/iub.1193

Wang, H., Liu, K., Geng, M., Gao, P., Wu, X., Hai, Y., Li, Y., Li, Y., Luo, L., Hayes, J. D., Wang, X. J., & Tang, X. (2013). RXRα inhibits the NRF2-ARE signaling pathway through a direct interaction with the Neh7 domain of NRF2. *Cancer Research*, *73*(10), 3097–3108. https://doi.org/10.1158/0008-5472.CAN-12-3386

Wang, J., Zhang, M., Zhang, L., Cai, H., Zhou, S., Zhang, J., & Wang, Y. (2010). Correlation of Nrf2, HO-1, and MRP3 in gallbladder cancer and their relationships to clinicopathologic features and survival. *Journal of Surgical Research*, *164*(1), e99–e105. https://doi.org/10.1016/j.jss.2010.05.058

Wang, X. J., Sun, Z., Villeneuve, N. F., Zhang, S., Zhao, F., Li, Y., Chen, W., Yi, X., Zheng, W., Wondrak, G. T., Wong, P. K., & Zhang, D. D. (2008). Nrf2 enhances resistance of cancer cells to chemotherapeutic drugs, the dark side of Nrf2. *Carcinogenesis*, *29*(6), 1235–1243. https://doi.org/10.1093/carcin/bgn095

Warren, B. A., & Shubik, P. (1966). The growth of the blood supply to melanoma transplants in the hamster

cheek pouch. *Laboratory Investigation; a Journal of Technical Methods and Pathology*, *15*(2), 464—478. http://europepmc.org/abstract/MED/5932611

Was, H., Cichon, T., Smolarczyk, R., Rudnicka, D., Stopa, M., Chevalier, C., Leger, J. J., Lackowska, B., Grochot, A., Bojkowska, K., Ratajska, A., Kieda, C., Szala, S., Dulak, J., & Jozkowicz, A. (2006). Overexpression of heme oxygenase-1 in murine melanoma: Increased proliferation and viability of tumor cells, decreased survival of mice. *American Journal of Pathology*, *169*(6), 2181–2198. https://doi.org/10.2353/ajpath.2006.051365

Weinberg, F., & Chandel, N. S. (2009). Reactive oxygen species-dependent signaling regulates cancer. *Cellular and Molecular Life Sciences*, *66*(23), 3663–3673. https://doi.org/10.1007/s00018-009-0099-y

Weinmann, M., Jendrossek, V., Güner, D., Goecke, B., & Belka, C. (2004). Cyclic exposure to hypoxia and reoxygenation selects for tumor cells with defects in mitochondrial apoptotic pathways. *The FASEB Journal*, *18*(15), 1906–1908. https://doi.org/10.1096/fj.04-1918fje

Weksler, B., Romero, I. A., & Couraud, P. O. (2013). The hCMEC/D3 cell line as a model of the human blood brain barrier. *Fluids and Barriers of the CNS*, *10*(1), 1–10. https://doi.org/10.1186/2045-8118-10-16

Whiteman, D. C., Green, A. C., & Olsen, C. M. (2016). The Growing Burden of Invasive Melanoma: Projections of Incidence Rates and Numbers of New Cases in Six Susceptible Populations through 2031. *Journal of Investigative Dermatology*, *136*(6), 1161–1171. https://doi.org/10.1016/j.jid.2016.01.035

Widmer, D. S., Hoek, K. S., Cheng, P. F., Eichhoff, O. M., Biedermann, T., Raaijmakers, M. I. G., Hemmi, S., Dummer, R., & Levesque, M. P. (2013). Hypoxia contributes to melanoma heterogeneity by triggering HIF1α-dependent phenotype switching. *Journal of Investigative Dermatology*, *133*(10), 2436–2443. https://doi.org/10.1038/jid.2013.115

Woo, S. R., Corrales, L., & Gajewski, T. F. (2015). Innate immune recognition of cancer. *Annual Review of Immunology*, *33*(January), 445–474. https://doi.org/10.1146/annurev-immunol-032414-112043

Wu, X., Tao, Y., Hou, J., Meng, X., & Shi, J. (2012). Valproic acid upregulates NKG2D ligand expression through an ERK-dependent mechanism and potentially enhances NK cell-mediated lysis of myeloma. *Neoplasia (United States)*, *14*(12), 1178–1189. https://doi.org/10.1593/neo.121236

Yamamoto, M., Kensler, T. W., & Motohashi, H. (2018). The KEAP1-NRF2 system: A thiol-based sensor-effector apparatus for maintaining redox homeostasis. *Physiological Reviews*, *98*(3), 1169–1203. https://doi.org/10.1152/physrev.00023.2017

Yong, S. B., Kim, J., Chung, J. Y., Ra, S., kim, S. S., & Kim, Y. H. (2020). Heme Oxygenase 1-Targeted Hybrid Nanoparticle for Chemo- and Immuno-Combination Therapy in Acute Myelogenous Leukemia. *Advanced Science*, *7*(13). https://doi.org/10.1002/advs.202000487

Yoshida, T., BIRO, P., COHEN, T., MÜLLER, R. M., & SHIBAHARA, S. (1988). Human heme oxygenase cDNA and induction of its mRNA by hemin. *European Journal of Biochemistry*, *171*(3), 457–461. https://doi.org/10.1111/j.1432-1033.1988.tb13811.x

Yoshida, T., & Kikuchi, G. (1977). Heme oxygenase purified to apparent homogeneity from pig spleen

microsomes. *Journal of Biochemistry*, *81*(1), 265–268. https://doi.org/10.1093/oxfordjournals.jbchem.a131445

Yoshinaga, T., Sassa, S., & Kappas, A. (1982). The oxidative degradation of heme c by the microsomal heme oxygenase system. *Journal of Biological Chemistry*, *257*(13), 7803–7807.

Young, C. (2009). Solar ultraviolet radiation and skin cancer. *Occupational Medicine*, *59*(2), 82–88. https://doi.org/10.1093/occmed/kqn170

Zelboraf. (2016). *[summary of product characteristics] Welwyn Garden City: Roche Registration Limited*.

Zgheib, E., Limonciel, A., Jiang, X., Wilmes, A., Wink, S., Van De Water, B., Kopp-Schneider, A., Bois, F. Y., & Jennings, P. (2018). Investigation of Nrf2, AhR and ATF4 activation in toxicogenomic databases. *Frontiers in Genetics*, *9*(OCT). https://doi.org/10.3389/fgene.2018.00429

Zhang, D. D., Lo, S., Cross, J. V, Templeton, D. J., & Hannink, M. (2004). *Pippan96_fat.pdf*. *24*(24), 10941–10953. https://doi.org/10.1128/MCB.24.24.10941

Zhang, W., Heinzmann, D., & Grippo, J. F. (2017). Clinical Pharmacokinetics of Vemurafenib. *Clinical Pharmacokinetics*, *56*(9), 1033–1043. https://doi.org/10.1007/s40262-017-0523-7

Zhong, Y., Zhang, F., Sun, Z., Zhou, W., Li, Z. Y., You, Q. D., Guo, Q. L., & Hu, R. (2013). Drug resistance associates with activation of Nrf2 in MCF-7/DOX cells, and wogonin reverses it by down-regulating Nrf2-mediated cellular defense response. *Molecular Carcinogenesis*, *52*(10), 824–834. https://doi.org/10.1002/mc.21921

Zhou, B. P., Deng, J., Xia, W., Xu, J., Li, Y. M., Gunduz, M., & Hung, M. C. (2004). Dual regulation of Snail by GSK-3β-mediated phosphorylation in control of epithelial-mesenchymal transition. *Nature Cell Biology*, *6*(10), 931–940. https://doi.org/10.1038/ncb1173

8 APPENDIXES

Appendix 1: Composition of RPMI 1640 medium for MeOV-1 cell line	
Amino Acids	**Concentration (mg/L)**
Glycine	10.0
L-Arginine	200.0
L-Asparagine	50.0
L-Aspartic acid	20.0
L-Cystine 2HCl	65.0
L-Glutamic Acid	20.0
L-Histidine	15.0
L-Hydroxyproline	20.0
L-Isoleucine	50.0
L-Leucine	50.0
L-Lysine hydrochloride	40.0
L-Methionine	15.0
L-Phenylalanine	15.0
L-Proline	20.0
L-Serine	30.0
L-Threonine	20.0
L-Tryptophan	5.0
L-Tyrosine disodium salt	29.0
L-Valine	20.0
Vitamins	**Concentration (mg/L)**
Biotin	0.2
Choline chloride	3.0
D-Calcium pantothenate	0.25
Folic Acid	1.0
Niacinamide	1.0
Para-Aminobenzoic Acid	1.0
Pyridoxine hydrochloride	1.0
Riboflavin	0.2
Thiamine hydrochloride	1.0
Vitamin B12	0.005

i-Inositol	35
Inorganic Salts	
Calcium nitrate (Ca(NO3)2 4H2O)	100
Magnesium Sulfate (MgSO4-7H2O)	100
Potassium Chloride (KCl)	400
Sodium Bicarbonate (NaHCO3)	2000
Sodium Chloride (NaCl)	6000
Sodium Phosphate dibasic (Na2HPO4-7H2O)	1512
Other Components	**Molecular Weight**
D-Glucose (Dextrose)	2000
Glutathione (reduced)	1
Phenol Red	5

Appendix 2: Composition of DMEM medium for endothelium cell lines	
Inorganoc Salts	**Concentration (mg/L)**
$CaCl_2$	265
$Fe(NO_3)3 \cdot 9H_2O$	0.1
$MgSO_4$	97.67
KCl	400
$NaHCO_3$	3700
NaCl	6400
$NaH\ 2PO_4$	109
Amino Acids	
L-arginine • HCl	840
L-cystine • 2HCl	626
L-Glutamine	---
Glycine	30
L-Histinine • HCl • H_2O	420
L-isoleucine	105
L-leucine	105
L-lysine • HCl	146
L-methionine	30
L-Phenylalanine	66
L-serine	42
L-Threonine	95
L-Tryptophan	16

L-Tyrosine • 2Na • $2H_2O$	120.37
L-valine	94
Vitamins	
Choline Chloride	4
Folic Acid	4
Myo-inositol	7.2
Niacinamide	4
D-pantothenic Acid • ½ Ca	4
Pyridoxine • HCl	4.04
Riboflavin	0.4
Thiamine • HCl	4
Other	
D-glucose	1000
Hepes	---
ADD	
L-glutamine	584

Appendix 3: Composition of 4x tris-SDS pH 8.8		
Component	**Concentration**	
Tris base	1.5 M	pH 8.8
SDS	0.4%	

Appendix 4: Composition of 4x tris-SDS pH 6.8		
Component	**Concentration**	
Trizma base	0.5 M	pH 6.8
SDS	0.4 %	

Appendix 5: Staking gel for SDS-PAGE	
Component	**Concentration**
4x Tris-SDS pH 6.8	Tris-base 125 mM SDS 0.1%
30% Acrylamide	4%
Ammonium persulfate (APS)	0.05%
Tetramethylethylenediamide (TEMED)	0.08%

Appendix 6: Resolving gel for SDS-PAGE	
Component	**Concentration**
4x Tris-SDS pH 8.8	Tris-base 375 mM SDS 0.1%
30% Acrylamide	10% or 8%
Ammonium persulfate (APS)	0.04%
Tetramethylethylenediamide (TEMED)	0.08%

Appendix 7: SDS-PAGE electrophoresis Buffer (Cambridge Reagents)	
Component	**Concentration**
Tris base	25 mM
Glycine	192 mM
SDS	1%

Appendix 8: Transfer buffer	
Component	**Concentration**
Tris Base	25 mM
Glycine	192 mM
Methanol	20%

Appendix 9: Phosphatase Buffered Saline (PBS) with 0.1% Tween (1 litre)	
Component	Concentration
10x PBS tablets (OXOID, BR0014C)	1x
TWEEN® (Sigma, P5927-500)	0.1%

Appendix 10: Tris Buffered Saline (TBS) with 0.1% Tween (1 litre)	
Component	**Concentration**
Tris-base	20 mM
NaCl	137 mM
HCl (1M)	--
TWEEN® (Sigma, P5927-500)	0.1%
Adjust pH to 7.5	

Appendix 11: List of primary antibodies for immunoblotting and IF					
Antibody	**Manufacturer**	**Product ID**	**Dilution**	**Host species**	**Molecular Weight (kDa)**
HO-1	BD	Ab610713	1:500	mouse	32
HO-1	Origene		1:2000	rabbit	32
HIF-1a	AbCAM	Ab179483	1:1000	rabbit	95-105
ERK tot	Cell signalling	91025	1:1000	rabbit	42-44
Phospho-ERK	Cell signalling		1:1000	rabbit	42-44
Bach1	Bethyl Lab	A303-057A	1:4000	rabbit	
b-actin	Sigma	A1978	1:10000	mouse	42
Actin	Sigma		1:10000	mouse	42
Nrf2	Santa cruz	Sc-365949 C-20	1:100 (IF)	rabbit	---

Appendix 12: List of secondary antibodies for immunoblotting and IF			
Antibody	**Manufacturer**	**Product ID**	**Dilution**
Anti-Rabbit	Amersham	NA934V	1:10000
Anti-Mouse	Amersham	NA9310V	1:10000
ALEXAfluor antibody 488	Thermo Fisher		1:500

Appendix 13: Primers for PCR for MeOV-1			
Primer name	**Amplicon**	**Forward 5 → 3**	**Reverse 5 → 3**
HMOX1	284 bp	gtc caa cat cca gct ctt tga gg	gac aaa gtt cat ggc cct ggg a
B7H6	143 bp	gac ctg gag cca ttg tgt ct	aag ctg gac tgt tcc ctg tg
ULBP3	209 bp	gcc tcg cga ttc ttc cgt	ctg ctc ttc tag gtg acc c
Nrf2	500 bp	cct gag tta cag tgt ctt aa	act gag tgt tct ggt gat g
GCLC	206 bp	atg gag gtg caa tta aca gac	act gca ttg cca cct ttg ca
GCLM	408 bp	cca gat gtc ttg gaa tgc	tgc agt caa atc tgg tgg
NQO1	516 bp	cac tga tcg tac tgg ctc a	gca gaa tgc cac tct gaa t
VEGFA	221 bp	ggg cag aat cat cac gaa gt	tgg tga tgt tgg act cct ca
18S	296 bp	ggg gcc cga agc gtt tac t	ggt cgg aac tac gac ggt atc

Appendix 15: Ripa Buffer	
Component	**Concentration**
Deoxycholic acid (Serva, DE)	2%
NaCl	150mM
Tris HCl	50mM
Sodium Dodecyl Sulphate	0.1%
Igepal NP40 (Sigma, UK)	1%

Appendix 17: Ripa Buffer + Inhibitors	
Component	**Concentration**
Complete™, Mini, EDTA-free Protease Inhibitor Cocktail (Roche, DE)	1x
Phosphatase Inhibitor Cocktail 3 (Sigma, UK)	1%
PMSF (Sigma, UK)	1mM